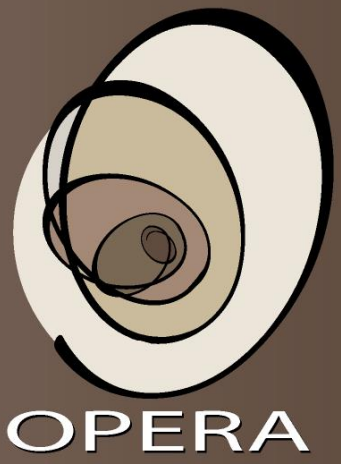

Geological and geohydrological characterization of the Boom Clay and its overburden

OPERA-PU-TNO411

Radioactive substances and ionizing radiation are used in medicine, industry, agriculture, research, education and electricity production. This generates radioactive waste. In the Netherlands, this waste is collected, treated and stored by COVRA (Centrale Organisatie Voor Radioactief Afval). After interim storage for a period of at least 100 years radioactive waste is intended for disposal. There is a world-wide scientific and technical consensus that geological disposal represents the safest long-term option for radioactive waste.
Geological disposal is emplacement of radioactive waste in deep underground formations. The goal of geological disposal is long-term isolation of radioactive waste from our living environment in order to avoid exposure of future generations to ionising radiation from the waste. OPERA (OnderzoeksProgramma Eindberging Radioactief Afval) is the Dutch research programme on geological disposal of radioactive waste.
Within OPERA, researchers of different organisations in different areas of expertise will cooperate on the initial, conditional Safety Cases for the host rocks Boom Clay and Zechstein rock salt. As the radioactive waste disposal process in the Netherlands is at an early, conceptual phase and the previous research programme has ended more than a decade ago, in OPERA a first preliminary or initial safety case will be developed to structure the research necessary for the eventual development of a repository in the Netherlands. The safety case is conditional since only the long-term safety of a generic repository will be assessed. OPERA is financed by the Dutch Ministry of Economic Affairs, Agriculture and Innovation and the public limited liability company Electriciteits-Produktiemaatschappij Zuid-Nederland (EPZ) and coordinated by COVRA. Further details on OPERA and its outcomes can be accessed at www.covra.nl.

This report has been reviewed by:
N. Vandenberghe (KU Leuven, Belgium)
M.D.C. De Craen (SCK·CEN, Belgium)
J. Grupa (NRG, Netherlands)

OPERA-PU-TNO411
Title: Geological and geohydrological characterization of the Boom Clay and its overburden
Authors: G.-J. Vis & J.M. Verweij
Date of publication: March 2014
Keywords: Rupel Clay Member, depth, thickness, lithology, permeability

Contents

Summary

This desk-study presents the geological and geohydrological characteristics of a clay layer in the Dutch subsurface (Boom Clay, officially Rupel Clay Member). New depth and thickness maps show that the Rupel Clay Member is present in nearly the whole Dutch subsurface, up to a depth of ~1500 m. The thickness varies around a mean of 65 m. In the proposed disposal concept for OPERA, the repository depth is 500 meter with a clay thickness of 100 meter. Therefore for this study, a clay layer deeper than 400 m and thicker than 100 m has been selected. In the Netherlands three locations have been identified: Roer Valley Graben (Noord Brabant), Zuiderzee Low (Gelderland) and North Netherlands (Friesland). The Rupel Clay Member is not a homogeneous clay; both vertical and lateral grain-size trends are present. The calculated permeability of the clay is lowest in the north of the Netherlands and higher and more variable in the south and southeast and it generally decreases with increasing depth. The Roer Valley Graben is the only focus area where fresh groundwater flow extends to a depth of more than 400 m and may reach the Rupel Clay Member. Faults are known to cut through the clay layer, but are still poorly understood in the focus areas. A series of knowledge gaps has been identified, such as the mismatch of lithostratigraphic nomenclature between the Netherlands and neighbouring countries, measured geo(hydro)logical properties of the Rupel Clay Member and deposits above and below it in the focus areas, fault locations and properties, and groundwater flow measurements in the clay.

Samenvatting

Deze bureaustudie presenteert de geologische en geohydrologische eigenschappen van een kleilaag in de Nederlandse ondergrond (Boomse Klei, officieel Rupel Klei Laagpakket). Nieuwe diepte- en diktekaarten laten zien dat het Rupel Klei Laagpakket in vrijwel de hele Nederlandse ondergrond aanwezig is tot een diepte van ~1500 m. De dikte varieert rond een gemiddelde van 65 m. In het voorgestelde eindbergingsconcept voor OPERA is de eindbergingsdiepte 500 meter en de kleidikte 100 meter. Daarom zijn voor deze studie gebieden met een diepte groter dan 400 m en een dikte groter dan 100 m geselecteerd. In Nederland voldoen drie focusgebieden hieraan: Roerdalslenk (Brabant), Zuiderzee Diep (Gelderland) en Noord Nederland (Friesland). Het Rupel Klei Laagpakket bestaat niet uit homogene klei; zowel verticale als laterale korrelgroottetrends zijn waarneembaar. De berekende permeabiliteit van de klei is het laagst in noord Nederland en hoger en meer variabel in het zuiden en zuidoosten. De permeabiliteit neemt over het algemeen af met de diepte. De Roerdalslenk is het enige focusgebied waar zoete grondwaterstroming tot dieptes van meer dan 400 m reikt en het Rupel Klei Laagpakket kan bereiken. Er lopen breuken door de kleilaag heen, maar daarvan is weinig bekend in de focusgebieden. Een aantal lacunes in kennis is herkend, zoals de problematische correlatie van de Nederlandse lithostratigrafische nomenclatuur met die van de buurlanden, het gebrek aan gemeten geo(hydro)logische eigenschappen van het Rupel Klei Laagpakket en de afzettingen erboven en eronder in de focusgebieden, de ligging van breuken en de breukeigenschappen en de afwezigheid van grondwaterstromingsmetingen in de kleilaag.

1. Introduction

1.1. Background

The total amount of low-, medium- and high-level radioactive waste produced annually in the Netherlands measures about 1000 m^3. This material is collected, treated and stored by the "Centrale Organisatie Voor Radioactief Afval" (COVRA). The storage facility at COVRA does not provide a long-term permanent solution. Due to the generally long-term radioactivity of medium- and high-level radioactive waste (hundred thousands of years), measures need to be taken to safely dispose of the material in the future. Therefore COVRA has erected the five-year research programme "OnderzoeksProgramma Eindberging Radioactief Afval" (Dutch research programme on geological disposal of radioactive waste, OPERA, 2011-2015). This programme is designed to study safe long-term geological disposal of radioactive waste in the Netherlands. The OPERA programme consists of an evaluation of existing safety and feasibility studies: the **Safety Case**. The evaluation is supposed to be performed with respect to new insights and developments.

Previous research programmes coordinated by TNO have identified the possibility of disposal of radioactive waste in rock salt and clay layers in the Dutch subsurface. These programmes were the OPLA research programme (OPLAnd, On Land, 1974-1993) and the CORA research programme (Commissie Opberging Radioactief Afval, Committee on Disposal of Radioactive Waste, 1996-2001). The latter of these encompassed research on a clay layer known as the Boom Clay, as an alternative to disposal in rock salt. This clay layer is present in the subsurface of nearly the complete onshore part of the Netherlands. Further, it is present in the shallow subsurface of Belgium where it crops out along the southern fringes (Figure 1-1). In Belgium extensive research of the Boom Clay has been performed and an underground test facility is present in this layer near the town of Mol (based on Van de Vate, 2012).

1.2. Objectives

The present study is the execution of research described in Task 4.1.1 of the OPERA Research Plan and—despite the presence of other potentially suitable clay layers in the Dutch subsurface such as the Asse and Ieper Members—focusses on the Boom Clay, or Rupel Clay Member which is part of the Rupel Formation (Van Adrichem Boogaert and Kouwe, 1993). Important safety-relevant characteristics of this clay are homogeneity, self-sealing capacity, low hydraulic conductivity and a high fixation capacity for radionuclides and other contaminants potentially released from the repository (Smith et al., 2009). As part of the Safety Case a collection of arguments supporting or rejecting long-term safety of a repository for low-, medium- and high-level radioactive waste needs to be collected. The geological and geohydrological characterization of the Boom Clay and its overburden primarily contribute to the safety functions *'isolation'* and *'delay and attenuation of the releases'* (Smith et al., 2009). The aim of the present study is to strengthen the current geo(hydro)logical knowledge of the Boom Clay in the Netherlands, by combining data and knowledge from earlier CORA studies with data and knowledge which has been acquired and interpreted since then.

1.3. Realization

Geological disposal is the emplacement of radioactive waste in geological formations; in the Netherlands this disposal is required to be retrievable (Tweede Kamer, 1993). The goal of geological disposal is isolation of radioactive waste from the biosphere to avoid exposure of future generations to ionising radiation emitted by the waste. The isolation is provided by the host-rock or geological formation in which the waste is stored and should—amongst other safety arguments—last until the radioactivity has decayed to natural levels (like those of uranium ore).

This study considers geological and geohydrological aspects contributing to long-term safety for geological disposal in the Boom Clay.

Figure 1-1. Location of the study area and Dutch provinces, used boreholes for grain-size analyses and the onshore distribution of the Rupel Clay Member (= Boom Clay). Along the southern margin of the Rupel Clay Member in Belgium, it locally crops out.

Clay layers suited for radioactive-waste disposal preferably have the following properties contributing to isolation (Boisson, 2005):

- Low permeability and low hydraulic gradients;
- Tendency for plastic deformation and self-sealing of fractures;
- Chemical buffering capacity;
- Geochemical characteristics favouring low solubility of radionuclides;
- High capacity to retard the migration of radionuclides towards the accessible environment (biosphere), e.g. through sorption capacity and due to a diffusion-dominated transport.

Of these, the first property is discussed in this report. With respect to low permeability and/or hydraulic conductivity, the host-rock preferably is a homogeneous fine-grained sediment with a high clay content. In this way transport of radionuclides through the host-rock is limited as much as possible. Further, the host-rock should be thick enough to perform the required task of isolation, and it should be buried deep enough to be out of reach of future geologic developments such as glaciations, groundwater flow etc. (OPERA Task 4.1.2 focusses on the future evolution). The integrity of the host-rock should be high, which means that no or limited disturbances or discontinuities such as faults, fractures, salt domes, concretions and boreholes are present to prevent groundwater flow through the host-rock.

Based on a desk-study, we will provide a generic description of the present geological and geohydrological characteristics of the host-rock (Boom Clay) and the enclosing rock (above and below). Based on relevant literature references, existing map data, additional well data and recent seismic interpretations the present-day regional-scale geometry (depth and thickness) and the hydrostratigraphical overburden of the Boom Clay is updated. Based on that we will focus on those areas with a thickness of more than 100 m and a depth of the top of more than 400 m in line with the research proposal. In the discussion section the geometry, distribution and overburden of the focus areas are discussed. We also provide an inventory of features affecting the integrity of the clay layer. This is followed by a discussion of the geohydrology of the focus areas.

1.4.Data quality and limitations of the work

As stated above, this study provides a generic description of present geological and geohydrological characteristics. This implies that it does not provide a detailed full re-evaluation of the Boom Clay and its overburden. Although new data and insights have been utilized for a rough update of pre-existing data, no new sedimentological and stratigraphical interpretation of well data have been performed. The lithological and geohydrological characterization of the Boom Clay are based on large-scale assumptions and low-density datasets. In the middle and north of the Netherlands very limited data are available to enable a detailed study.

In this overview study we update previous studies performed in the framework of radioactive-waste disposal. Due to time restrictions we have adopted an approach using existing datasets (NITG-TNO, 2004; Kombrink et al., 2012), which themselves are new with respect to the latest Boom Clay study. The latest study was the CAR Fase I report (Bremmer et al., 1997), which has merely digitized maps from an earlier RGD report (De Mulder et al., 1984).

The results presented here reflect a greatly increased dataset and improved knowledge and technical possibilities which have been gathered over the last 30 years. As such the new results are timely. Nonetheless the new results should be handled with care, since no new stratigraphic interpretation of boreholes has been performed. We also did not interpret the Boom Clay on seismic data. Faults that were used have been interpreted for the Geological Atlas (NITG-TNO, 2004), which is based on interpreted seismic data (mainly 2D) and well data. They are known to be of limited reliability, especially in the Zuiderzee Low region in the middle of the country. The presented conceptual lithofacies

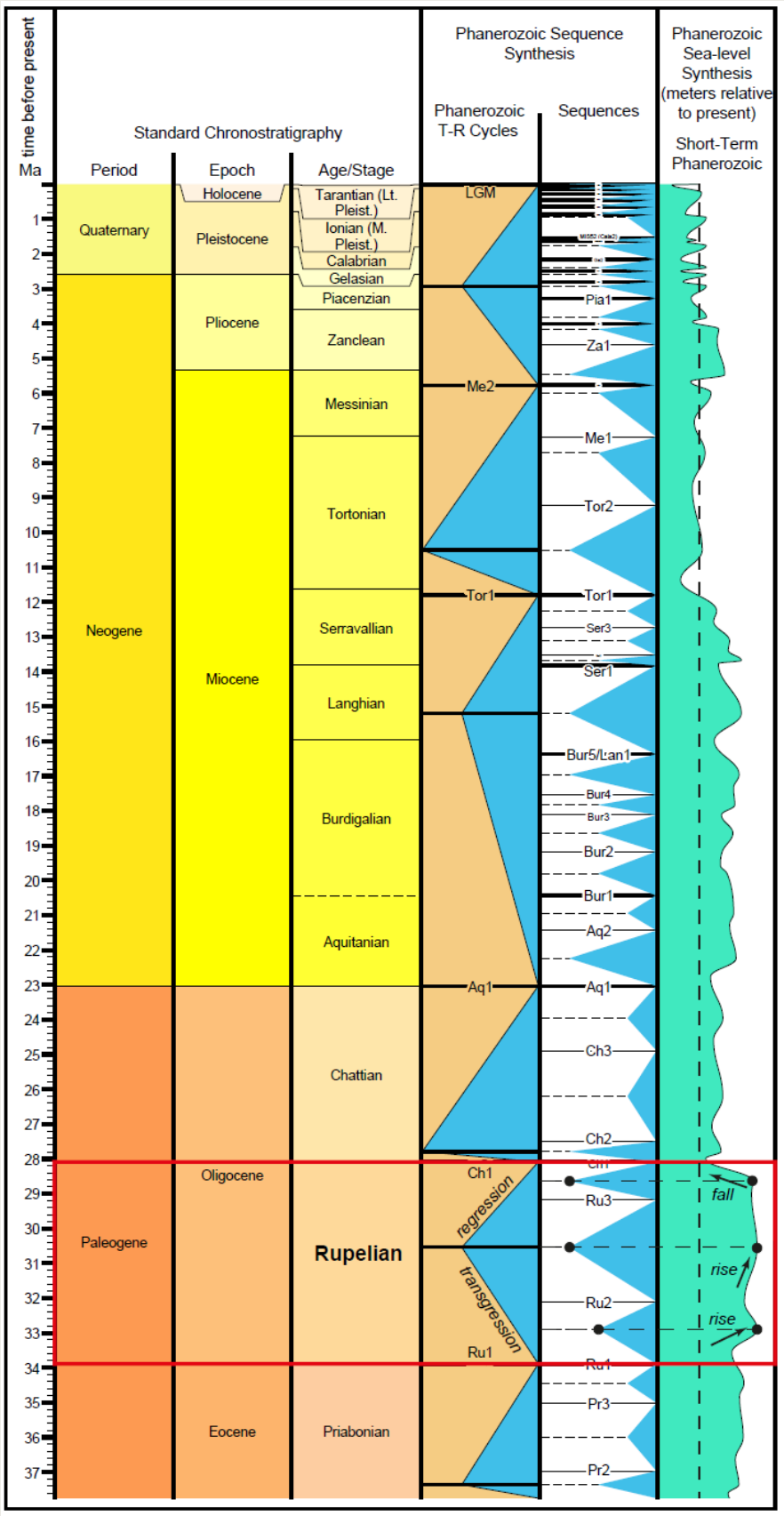

Figure 1-2. Chronostratigraphy, global sedimentary sequences and sea-level curves (Gradstein et al., 2012 and references therein). Made with Time Scale Creator software.

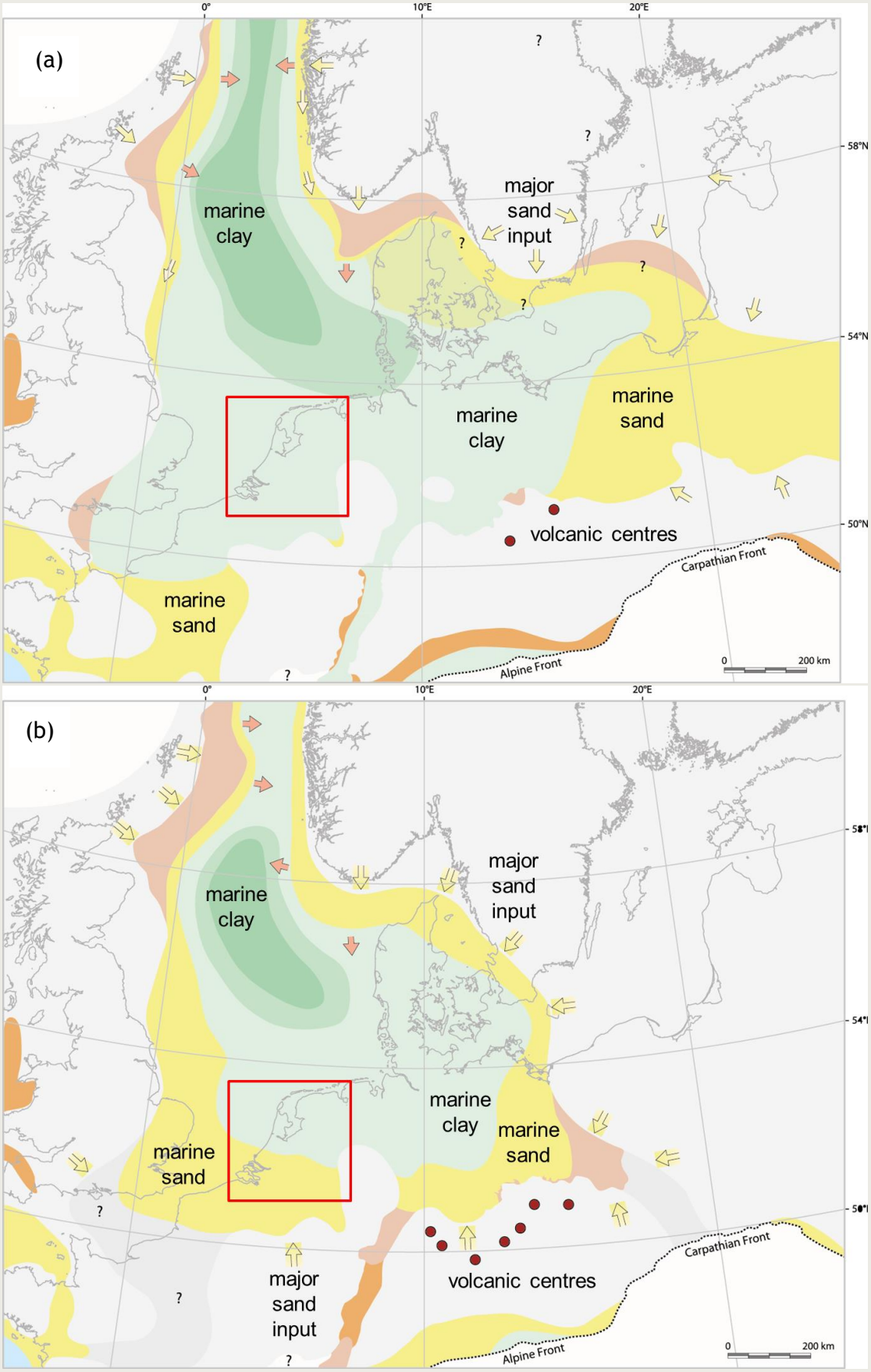

Figure 1-3. a) Rupelian palaeogeography; b) Chattian palaeogeography (modified after Knox et al., 2010).

model is based on a limited number of wells with grain-size data and therefore should be merely taken as a broad geologic setting.

1.5.What is the Boom Clay?

The Boom Clay is basically a marine clay, which means that it was deposited as a seafloor sediment. The Boom Clay is part of the Rupel Formation (see below) which was deposited during the geologic Rupelian stage between 33.9 and 28.1 million years ago (Figure 1-2). The beginning of the Rupelian stage coincides with the beginning of the Oligocene epoch, which corresponds with a major climate change from a greenhouse world during the preceding Eocene to a glaciated world during the Oligocene (Abels et al., 2006; Lear et al., 2000). The glaciated world was characterised by continental ice growth on the south pole, which resulted in a decreased global ocean-water volume and global sea-level fluctuations (Lear et al., 2000).

In the Boom Clay in Belgium, regionally correlatable lithologic alternations between silt and clay have been identified. The metre-scale sequences reflect sea-level fluctuations which affect local water depth and wave base, resulting in changing sorting intensities and lithological variation (Vandenberghe, 1978; Van Echelpoel and Weedon, 1990; Vandenberghe et al. 1997, 2001). The rhythmic lithological variations are considered to reflect astronomical control (Van Echelpoel and Weedon, 1990; Vandenberghe et al., 2001; Abels et al., 2006).

The deposits of the Rupel Formation were formed in the southern part of the North Sea Basin of which the London-Brabant Massif (which includes the present-day Ardennes) was the southern limit (Figure 1-3). The coastline of the sea was roughly oriented east-west and located in Belgium. Towards the north the sea was deeper, possibly up to 500 m depth (De Lang and Ebbing, 2003).

1.5.1. Rupel Formation (NMRFC)

The formation is named after the river Rupel in Belgium. The main part consists of heavy, dark brown-grey clays. Towards both base and top, the clays grade, rather abruptly, into sands along the southern basin margin. In the Netherlands the formation consists of three members from base to top (Figure 1-4): Vessem Member (NMRFS), Rupel Clay Member (NMRFC) and Steensel Member (NMRFT). The Rupel Clay Member is more or less equivalent with the unofficial name Boom Clay. The Boom Formation of the Belgian nomenclature Marechal and Laga (1988) more or less equals the Dutch Rupel Clay Member of the Rupel Formation (Welkenhuysen and De Ceukelaire, 2009).

The Rupel Clay Member consists of clays that become more silty towards base and top. The member is pyrite-rich, contains hardly any glauconite and calcium carbonate tends to be concentrated in the septaria layers. Besides a general trend of higher silt contents towards top and base, detailed studies in the Boom Clay in Belgium have shown that silt and clay layers alternate at a decimetre to metre scale (Vandenberghe, 1978). Moreover, the organic-matter content is highly variable and distinct bituminous layers are present. Large intervals are practically devoid of calcareous microfossils. In areas relatively close to the basin margin in the south and east of the Netherlands, the clay can be subdivided into three parts. The lower part of the clay is silty and has a blue-grey colour. Higher in the succession a great number of bituminous bands is intercalated and the colour of the clay changes to dark green-grey, dark-brown or even black. The dark clays, which stand out on gamma-ray logs, are overlain by green-grey to green clays that are more marly and slightly more silty (Van Adrichem Boogaert and Kouwe, 1993).
The Rupel Clay Member is thought to have been thicker than at present. Erosion has removed the top or—locally—the complete package. The greater original thickness has caused over-consolidation, making the clay quite hard. Observations of the Rupel Clay Member in the Netherlands and Belgium at shallow locations have identified fractures or slicken sides (De Lang and Ebbing, 2003; Dehandschutter et al., 2004, 2005).

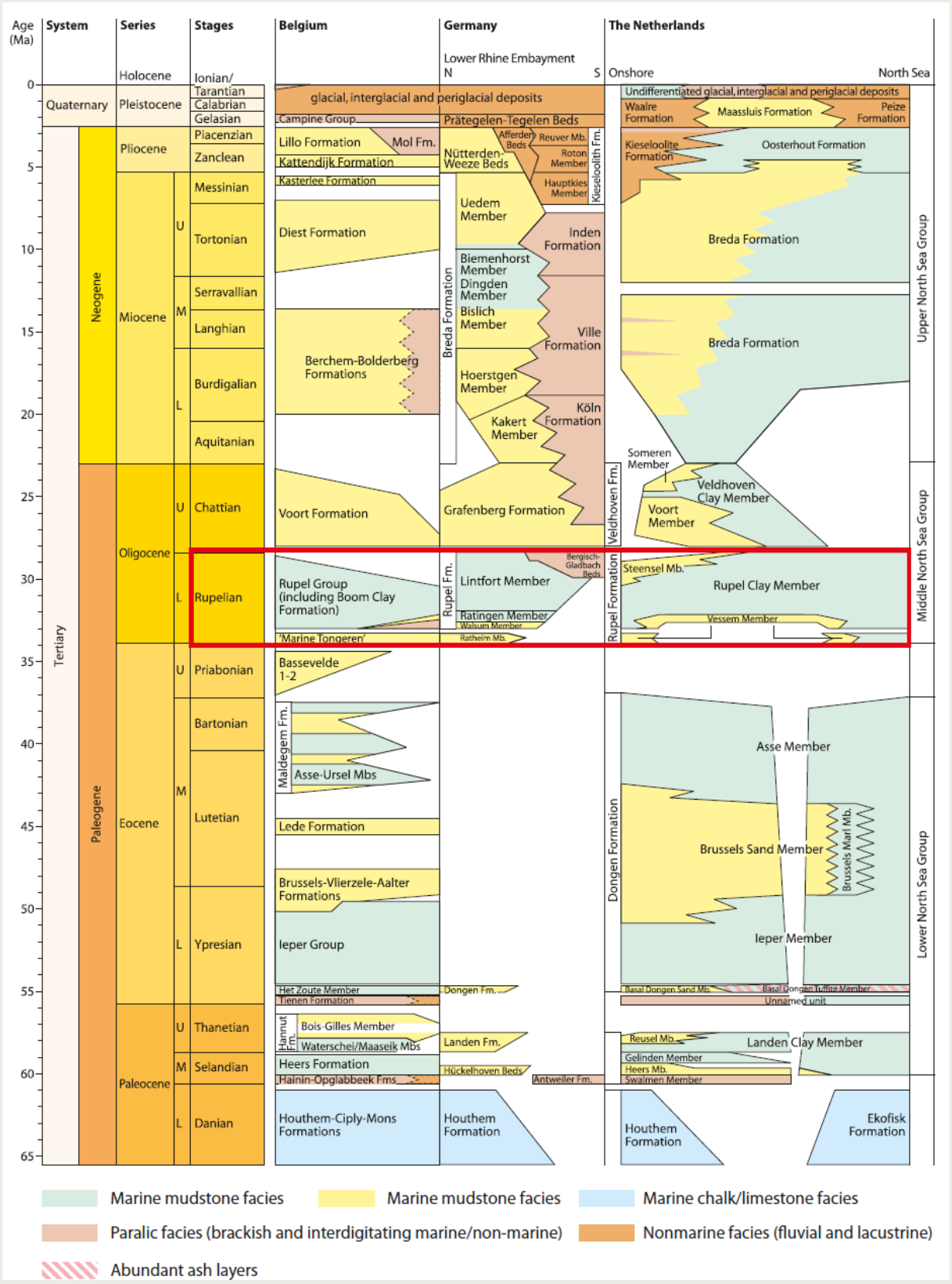

Figure 1-4. Tectonostratigraphy of the Cenozoic, comparing Belgium, Germany and the Netherlands (modified after Knox et al., 2010).

1.5.2. Underlying and overlying deposits

The lower boundary of the Rupel Clay Member conformably overlies the sandy Vessem Member which is variable in thickness but present in nearly the whole onshore part of the Netherlands (Figure 1-5). The Vessem Member includes several coarsening-upwards units that developed locally below the main transgressive surface. The member corresponds in the southern Netherlands with the sandy members of the Belgian Zelzate Formation and the Bilzen Formation (including the Berg Member) Marechal and Laga (1988). In the eastern Netherlands it can be correlated with the Ratum Member of Van den Bosch (1975). Over the major part of the Netherlands onshore area, the Vessem Member is developed as a simple transgressive unit consisting of silty to clayey sands with a low glauconite content; flint pebbles or phosphorite nodules commonly occur at the base. This is the equivalent of the Berg sands in Belgium (the Berg Member of the Bilzen Formation in Maréchal and Laga (1988). It is also time-equivalent with the base of the Boom Clay (Belsele-Waas Member) in the Antwerp Campine area in Belgium. Calcareous fossils are generally absent. In a basin setting, the Vessem Member becomes a more heterogeneous unit. In the Voorne Trough and the Zuiderzee Low and locally in the eastern part of the Netherlands, only the topmost part is a thin transgressive sand layer. There, the member consists largely of stacked coarsening-upwards units. The sands of these units have a relatively high glauconite content and contain no pebbles. Autochthonous phosphorite nodules occur in some areas. The sands and the intercalated clays have a low carbonate content or are devoid of calcium carbonate (Van Adrichem Boogaert and Kouwe, 1993). Over most of the area the Vessem Member is a transgressive shallow-marine sand. In southern Limburg a clay layer is intercalated. Basinward of this clay, the presence of a coastal barrier facies is inferred. The coarsening-upward sequences below the main transgressive surface represent shallow-marine sands prograding onto middle- to outer-neritic clays. The base itself is presumed to be a transgressive, shallow-marine sand (Van Adrichem Boogaert and Kouwe, 1993).

In Zeeuws-Vlaanderen the Rupel Clay Member overlies the Zelzate Member (Tongeren Formation), which consists of alternating sand and clay layers. In Limburg, the Rupel Clay Member unconformably overlies the locally occurring Tongeren and Dongen Formations.

In the southeast of the Netherlands, the Rupel Clay Member is conformably overlain by the sandy Steensel Member (Figure 1-6). This member has been created to accommodate the uppermost, sandy part of the Rupel Formation as found near the southeastern margin of the basin. In neighbouring countries sands occur in overall similar stratigraphic positions. In Belgium, the lithostratigraphic equivalent has been named Eigenbilzen Formation Maréchal and Laga (1988). The Steensel Member consists of an alternation of clays and silty clays with thin sand layers, grading upwards into fine-grained sands with a high glauconite content. The depositional environment was near-coastal (Van Adrichem Boogaert and Kouwe, 1993).

Further north (basinward), the sandy Steensel Member is absent and the similary sand-dominated Voort Member overlies the Rupel Clay Member. In the rest of the country the member is covered by the Veldhoven Clay Member and the Breda Formation, which is generally clay-dominated in the north and contains sandy intercalations in the south. In Zeeuws-Vlaanderen the Rupel Clay Formation is located at shallow depths, because of which it is covered with Quaternary deposits. Where Early Miocene erosion occurred, an unconformable contact exists with the overlying Breda Formation, which consists of glauconitic sands and clays.

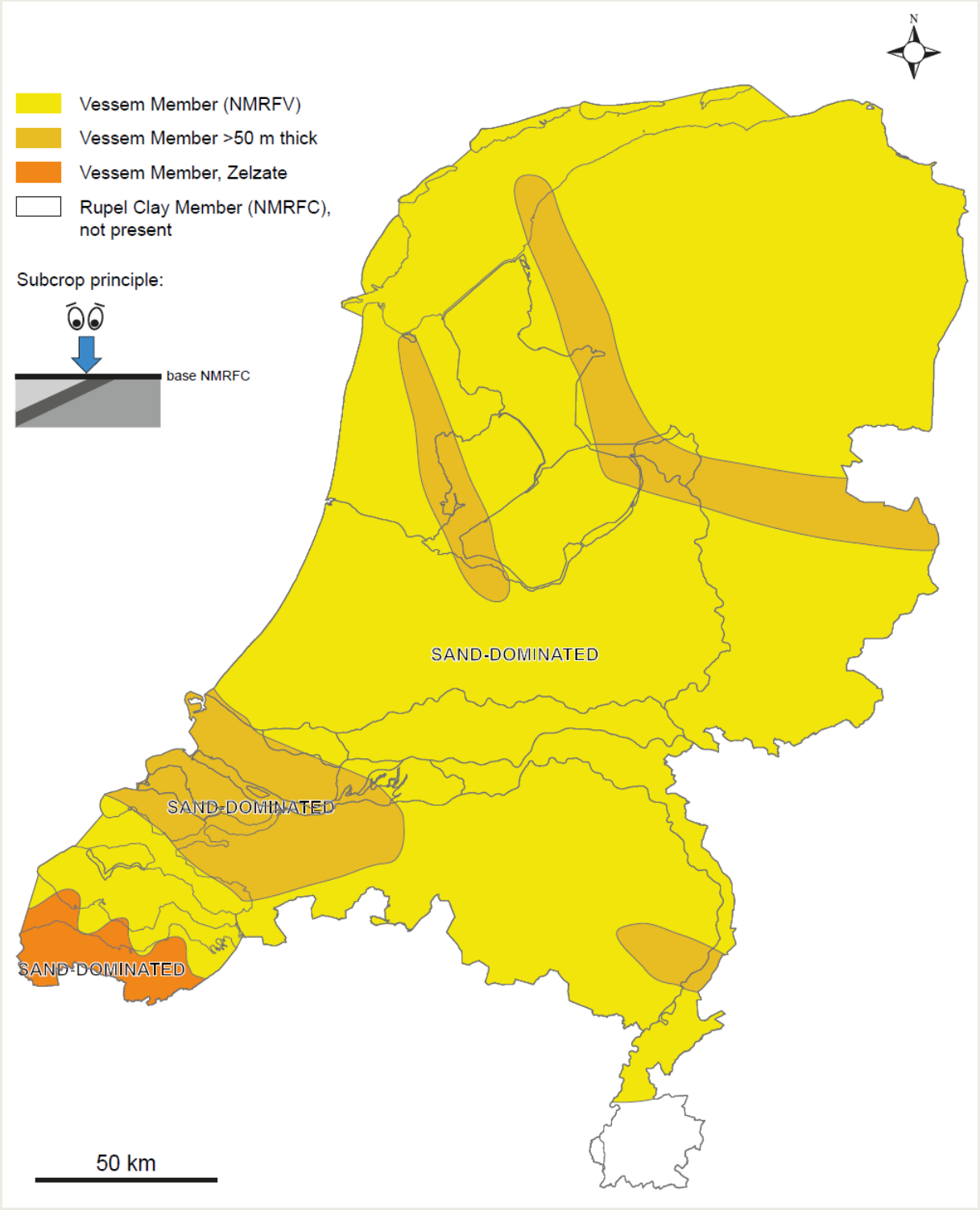

Figure 1-5. Schematic subcrop map of the Rupel Clay Member. The map shows the deposits on which the base of the member rests.

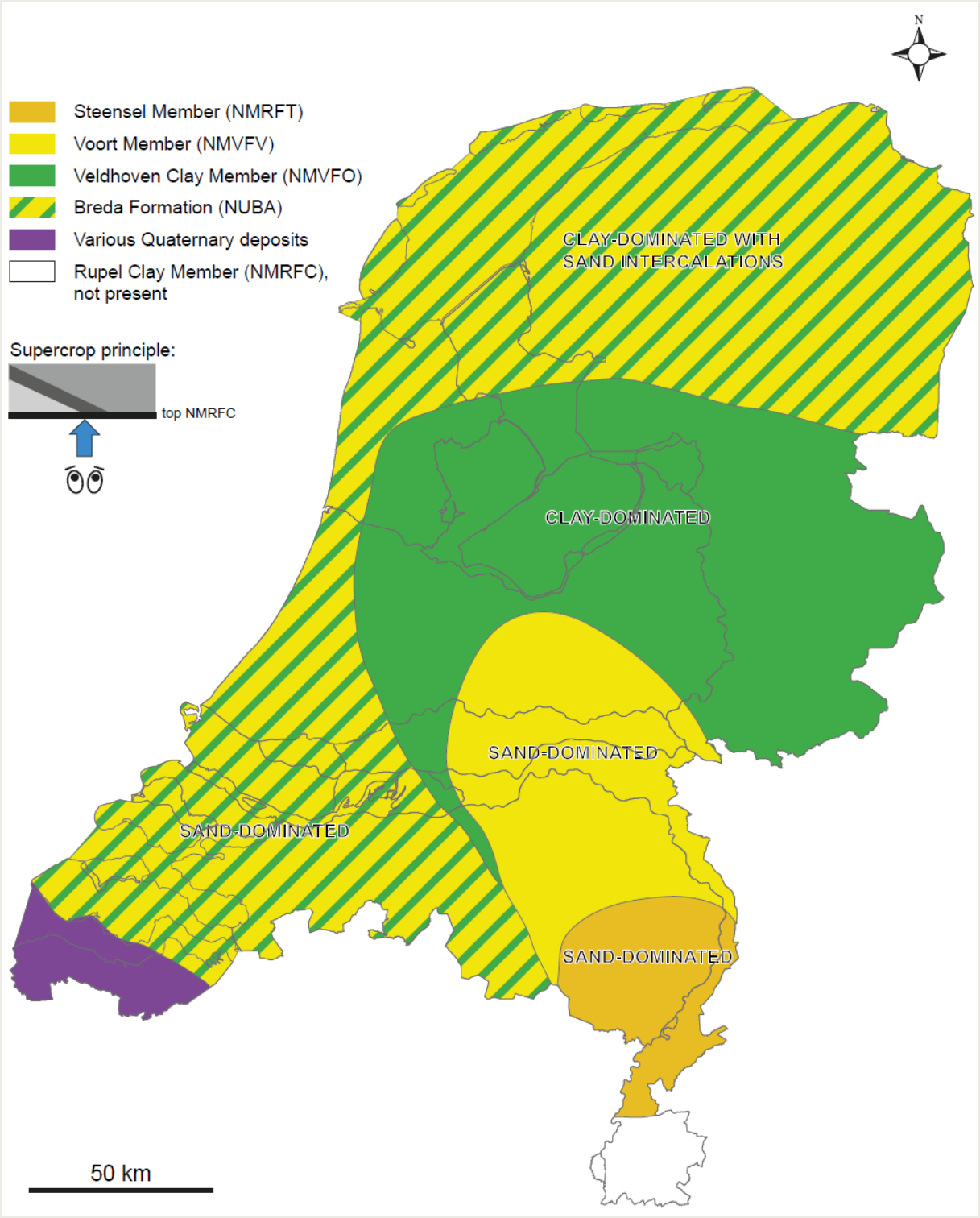

Figure 1-6. Schematic supercrop map of the Rupel Clay Member. The map shows the deposits overlying the top of the member.

2. Methods and assumptions

2.1. Rupel Clay Member maps

Three maps of the Rupel Clay Member have been constructed using the most recent publicly available data. The map-making procedure and used data are described below. All grids have a resolution of 250x250 m.

2.1.1. Depth maps

The depth maps of the top and the base of the Rupel Clay Member have been constructed based on a combination of existing, but recently updated data (NITG-TNO, 2004; Kombrink et al., 2012), which is based on interpreted seismic data (2D and 3D) and well data. The seismically interpreted base of the nearly nationwide present Breda Formation (base Upper North Sea Group) forms the basis for the maps (Figure 2-1). In parts of the country this formation directly overlies the Rupel Clay Member (Figure 1-6), and therefore in those regions the base of the Breda Formation equals the top of the Rupel Clay Member.

In some regions the Veldhoven Formation and the Steensel Member lie between the base of the Breda Formation and the top of the Rupel Clay Member. Because the Steensel Member is at most 28 m thick and only present in nine wells in the north of Limburg, no correction for this member was made. The thickness of the member lies within the vertical error range of the seismic data.

The Veldhoven Formation is up to ~200 m thick and present in 168 wells (oil, gas and groundwater). A correction was made to account for the thickness of this unit. This was achieved by subtracting the along-hole thickness of the formation from the base of the Breda Formation. The thickness is based on interpretation in boreholes as registered in the TNO-DINO database. Since in these relatively shallow-lying deposits the boreholes are still oriented vertically, the along-hole thickness is assumed to be equal to the true-vertical thickness.

The depth of the base of the Rupel Clay Member has been constructed by subtracting its along-hole thickness in 498 boreholes as registered in the TNO-DINO database (Appendix 1), from the above-described surface representing the top of the member (Figure 2-1). For this mainly oil and gas wells were used, because most groundwater wells do no penetrate the base of the member since it is buried too deep. On the southern and eastern fringes of its distribution, the member does reach depths shallow enough for groundwater wells to penetrate it. Here the detailed information from those boreholes was used to fine-tune the base of the grid in a later quality-control step (Section 2.1.3). This is mainly in the regions Zeeuws-Vlaanderen, Noord-Limburg and near Winterswijk.

The maps were made following the aforementioned procedure. Subsequently wells penetrating top and/or base of the member were used to verify and correct the obtained top and base grids. The difference between the depth in the obtained grids and the depth in the wells is the so-called residual. This residual is a measure for the reliability of the approach. The well data were used to correct the grids, to make the grids fit the top and base of the Rupel Clay Member at well locations (Section 2.1.3).

After the correction step, an existing dataset in the northeast of the country was used to improve the depth of the top map. For a study of the stability of benchmarks in Groningen, Cenozoic strata have been seismically interpreted using a 3D regional survey. The horizons were calibrated on data such as well logs, cuttings, and biostratigraphy (Duin, 1995). The interpreted area roughly covers the province of Groningen. We used the base Breda Formation grid to update our top Rupel Clay Member grid in that area, since it is considered of greater accuracy than the calculated top.

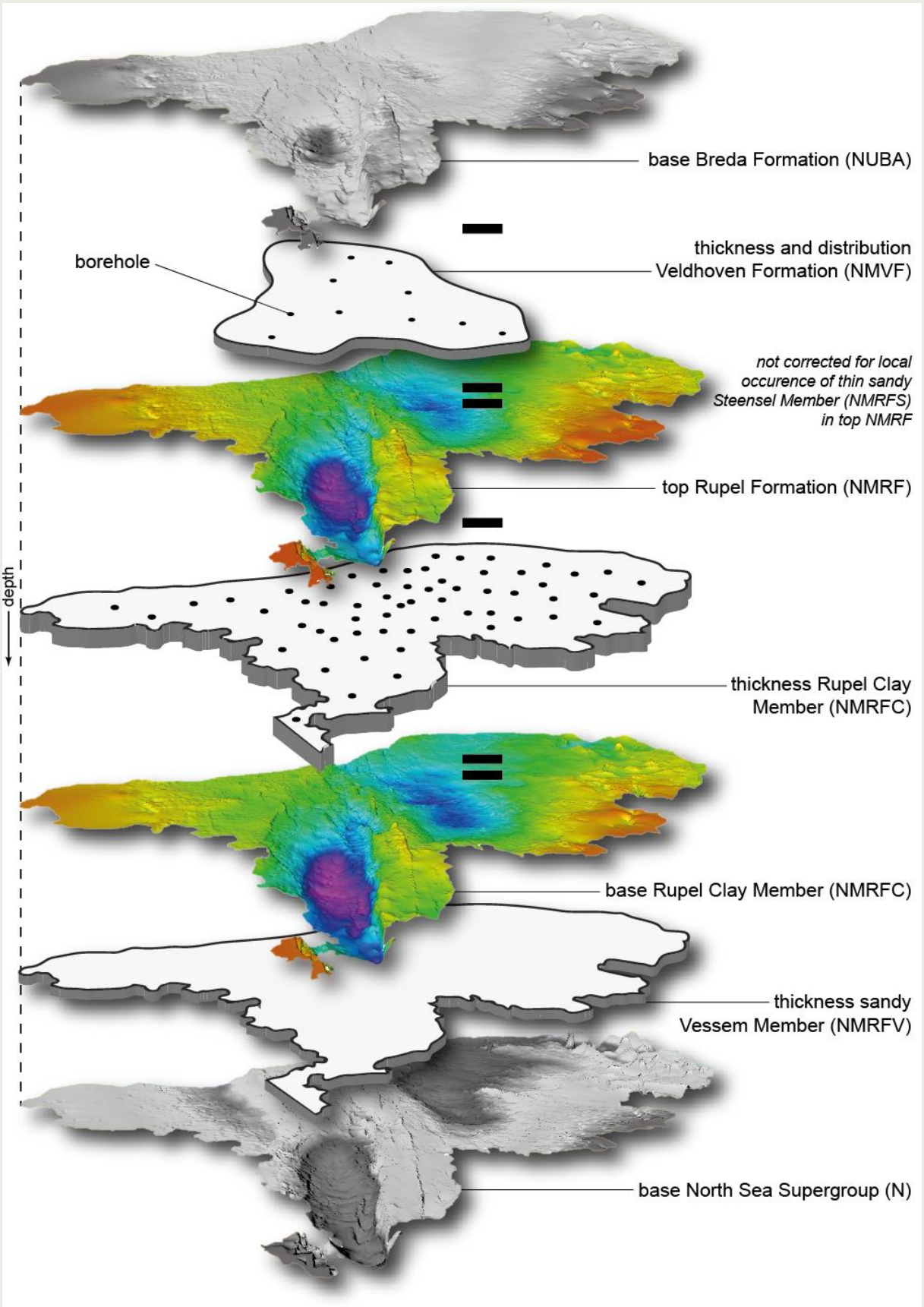

Figure 2-1. Map-making procedure for the top and base of the Rupel Clay Member (in colour). See tekst for explanation.

To get an impression whether the grids as calculated for the Dutch subsurface, fit with the Belgian subsurface, we used the depth map of the base of the Formatie van Boom and the identified faults (DOV, 2004). The top of the Formatie van Boom was simply calculated by assuming it lies 150 m above the base.

2.1.2. Thickness map

The thickness map was made by simply subtracting the grid of the base of the Rupel Clay Member from its top grid. This resulted in a grid showing the main depocentres and areas of erosion of the member in the Dutch subsurface. The thickness grid shows large areas with an unknown thickness or absence in the province of Zeeland because shallow boreholes have often not penetrated the base of the Rupel Clay Member. Interpolation of the base of the member is therefore not reliable and subtracting base from top therefore results in an erroneously thin or absent sediment layer.

2.1.3. Map accuracy and quality control

The source-map for the maps presented here is the regionally mapped base of the Breda Formation which equals the base Upper North Sea Group surface (Duin et al., 2006). This surface was mapped using mostly 2D seismic lines; 3D seismic surveys were at that time only available for the northeast of the country and for the West Netherlands Basin (Duin et al., 2006). The seismic interpretations were converted from the time-domain to the depth-domain using the VELMOD-1 velocity model (Van Dalfsen et al., 2006). Recently the more accurate VELMOD-2 velocity model has become publicly available (www.nlog.nl), but this was not used for the current study due to time-constraints. The stratigraphic information of boreholes was used to constrain the seismic interpretation.

The accuracy of the presented maps relies on the following items:

- Regional seismic interpretation of the base of the Upper North Sea Group surface and faults using 2D and 3D seismic data;
- Time-to-depth conversion;
- Stratigraphic interpretation of boreholes from well logs, cuttings and cores:
    - Interpretation of base Upper North Sea Group
    - Interpretation of the Veldhoven Formation
    - Interpretation of the Rupel Clay Member

Well point data identifying the Rupel Clay Member have been used to adjust the calculated top (822 points) and base grids (1047 points). The amount of adjustment that was necessary (residual) is a measure for the accuracy of the map-making procedure. The residual maps (Figure 2-2 and Figure 2-3) for top and base of the member show that the utilized methodology obtained reasonable results on a regional scale. Only on some locations the mismatch between the grid and the well data reaches up to 200 m in depth. A mismatch of up to 200 m is large, and probably results from incorrect stratigraphic interpretation in wells. These interpretations need to be reconsidered in a future study to improve the quality of the depth and thickness grids.

The corrections made for the top of the Rupel Clay Member occur distributed over the country (Figure 2-2). The residuals of the base of the member show most corrections in the southwest of the country (Figure 2-3). This is due to the fact that the seismically interpreted base of the Breda Formation (base Upper North Sea Group) is known to be inaccurate here due to absence of seismic data. For this study it is not a problem due to the limited thickness and depth of the member here.

It is noteworthy to say that especially in the area underneath the provinces of Flevoland and Noord-Holland, the seismic data quality did not allow accurate mapping of faults. Only 2D seismic lines were present while the geologic structure here is complex with many small faults. Although the grids appear to show little faults here, it is to be expected that many more faults are present.

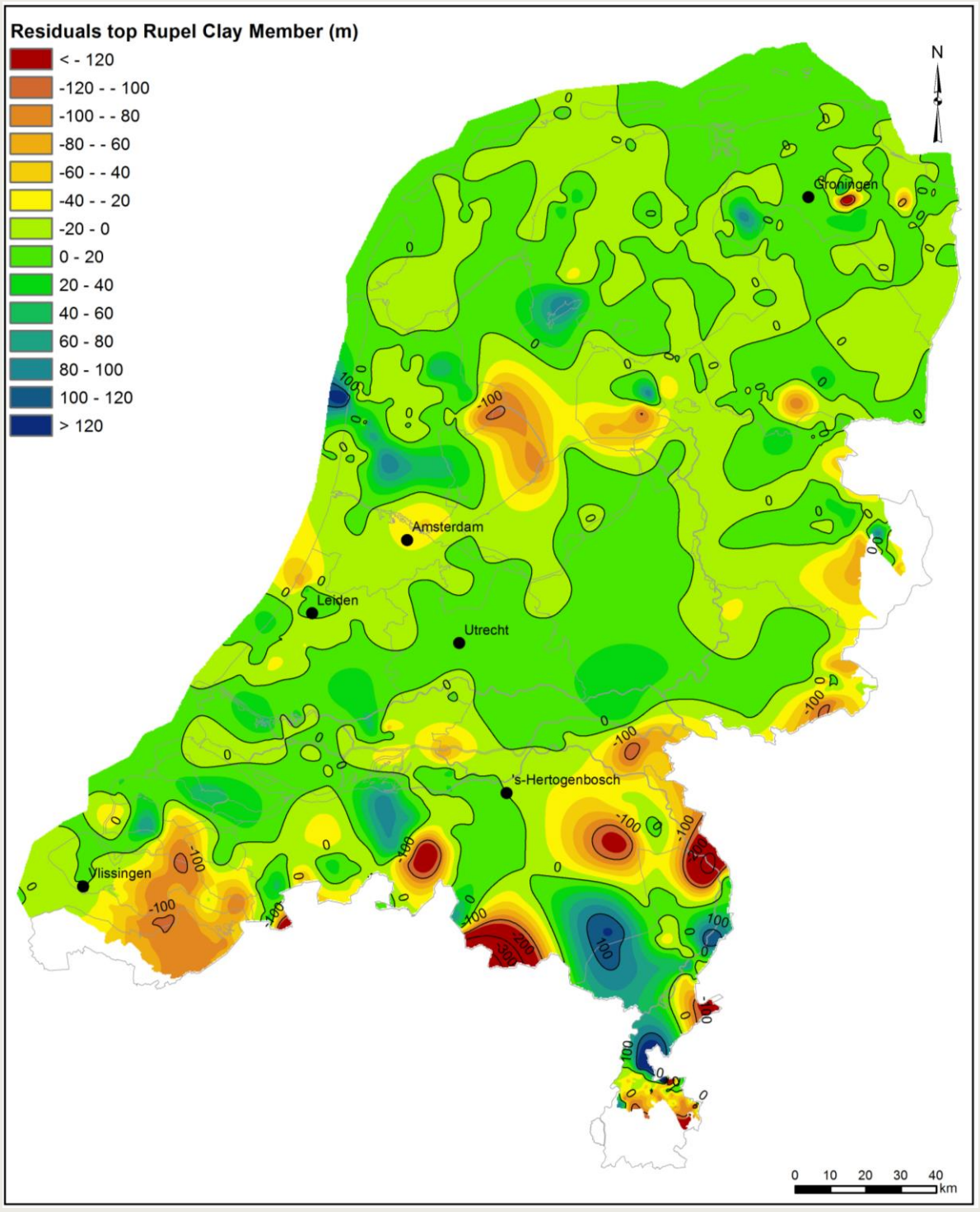

Figure 2-2. Corrections made for the top of the Rupel Clay Member. Well-point data (822 points) identifying the Rupel Clay Member have been used to adjust the calculated (Figure 2-1) top grid. The values on the map show the amount of correction that was needed in metres.

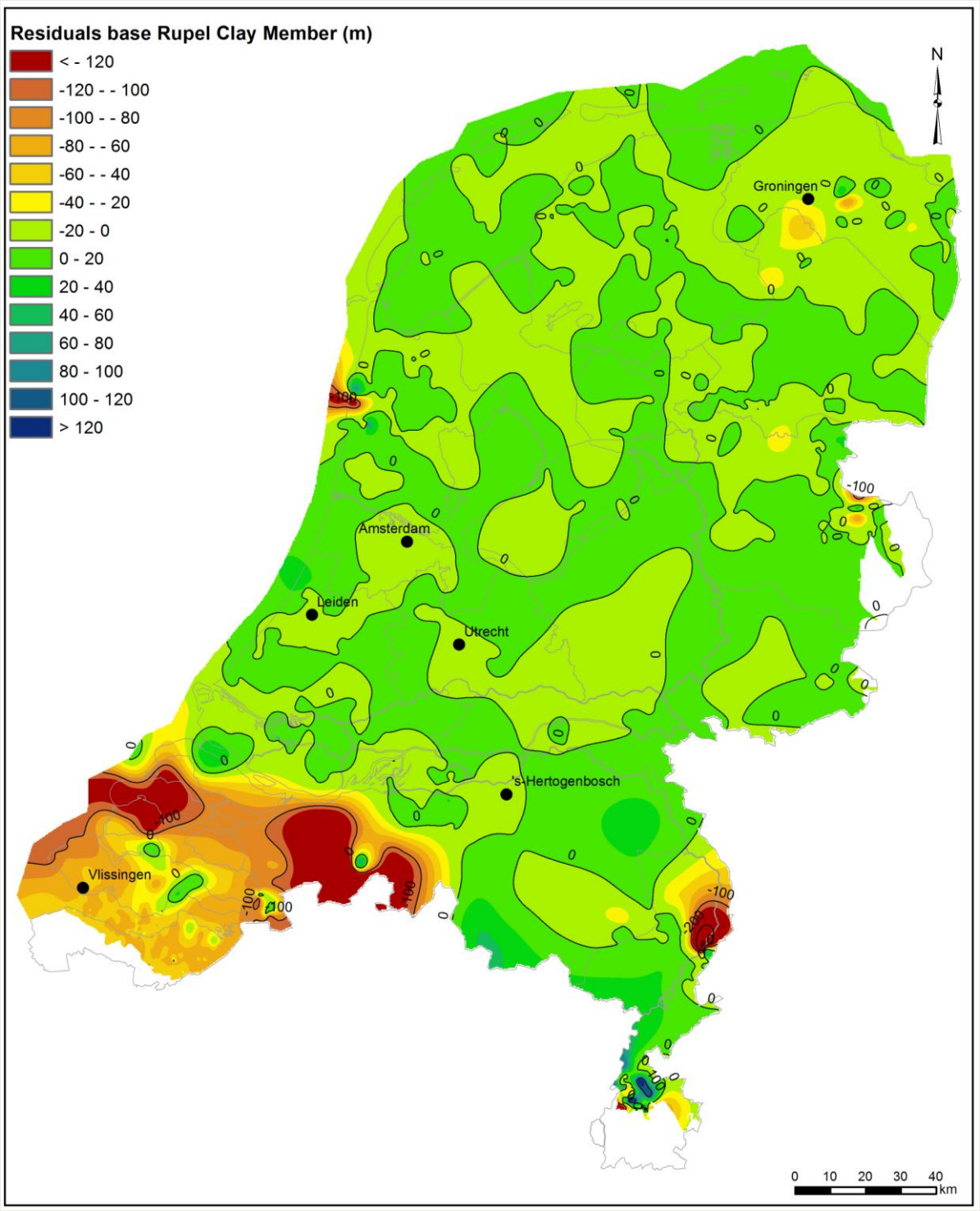

Figure 2-3. Corrections made for the base of the Rupel Clay Member. Well-point data (1047 points) identifying the Rupel Clay Member have been used to adjust the calculated (Figure 2-1) base grid. The values on the map show the amount of correction that was needed in metres.

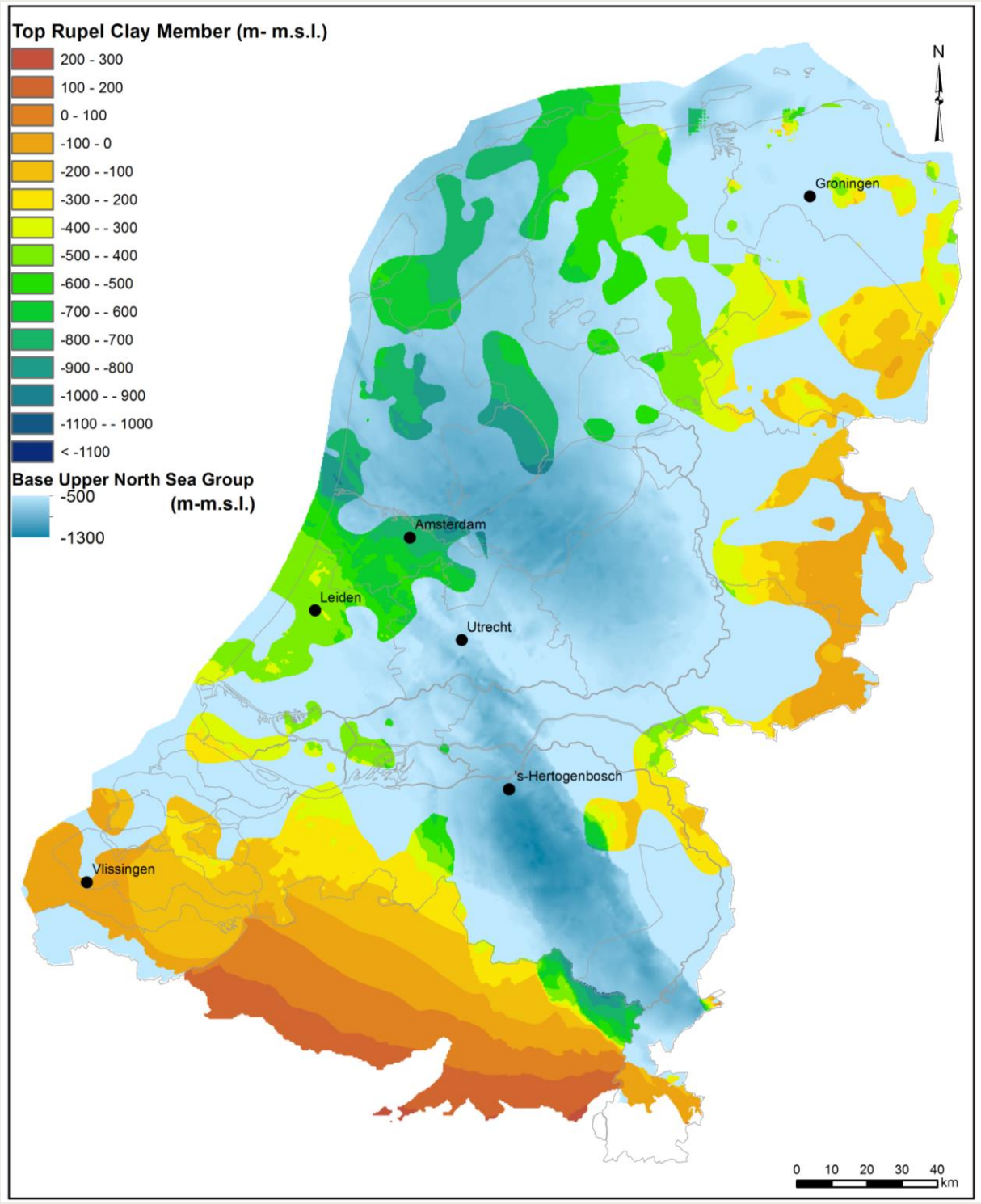

Figure 2-4. The blue grid represents the seismically mapped base of the Upper North Sea Group. The multi-colour grid represents the top of the calculated Rupel Clay Member, which lies stratigraphically below the Upper North Sea Group. Where the multi-colour Rupel grid appears, it lies above the blue North Sea grid (in the Netherlands), which is incorrect. A correction for this has been made in those cases.

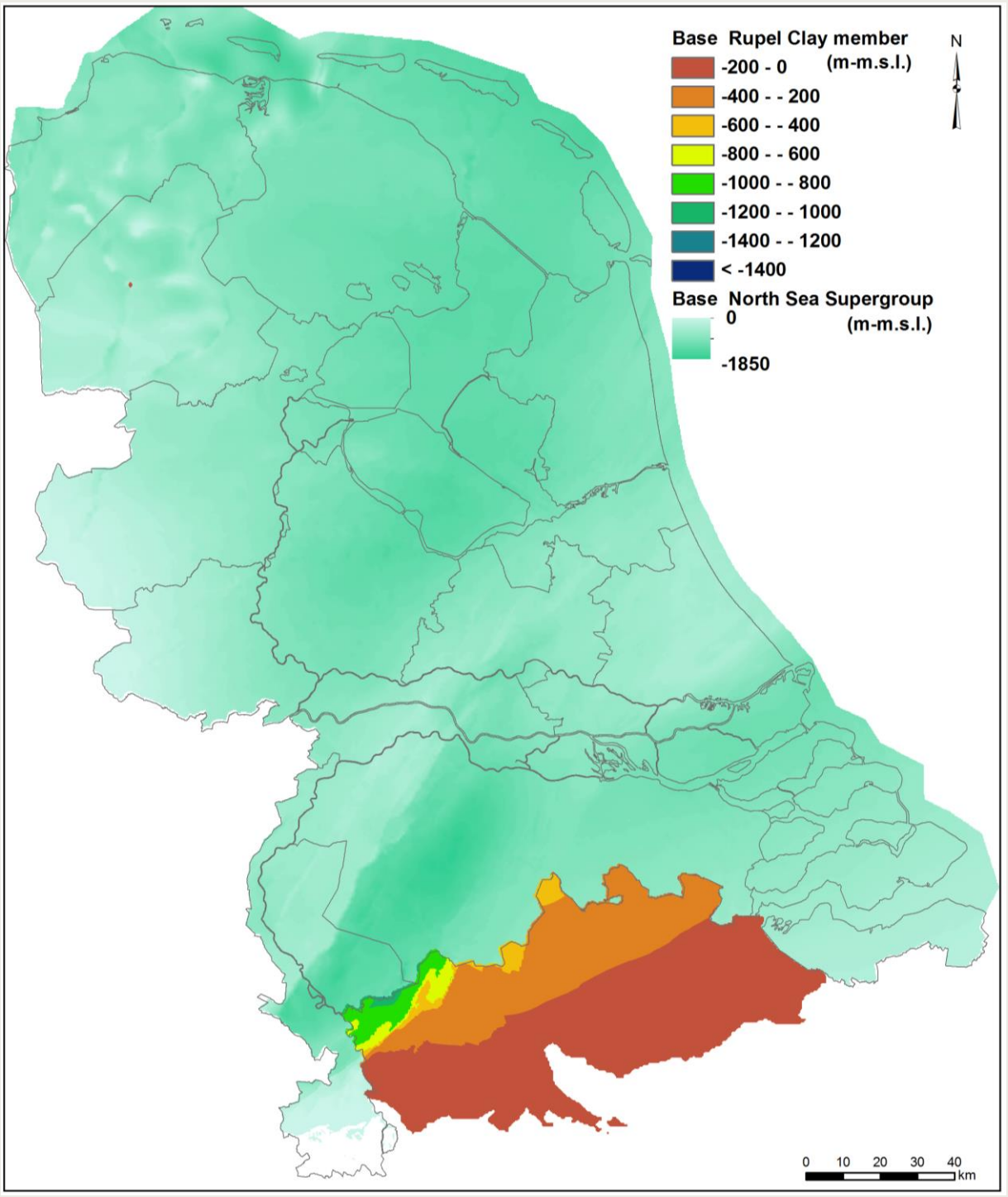

Figure 2-5. The Netherlands seen from below. The green grid represents the seismically mapped base of the North Sea Supergroup. The multi-colour grid represents the base of the calculated Rupel Clay Member, which lies stratigraphically above the base of the North Sea Supergroup. Where the multi-colour Rupel grid appears, it lies below the green North Sea grid (in the Netherlands), which is incorrect. A correction for this has been made in those cases.

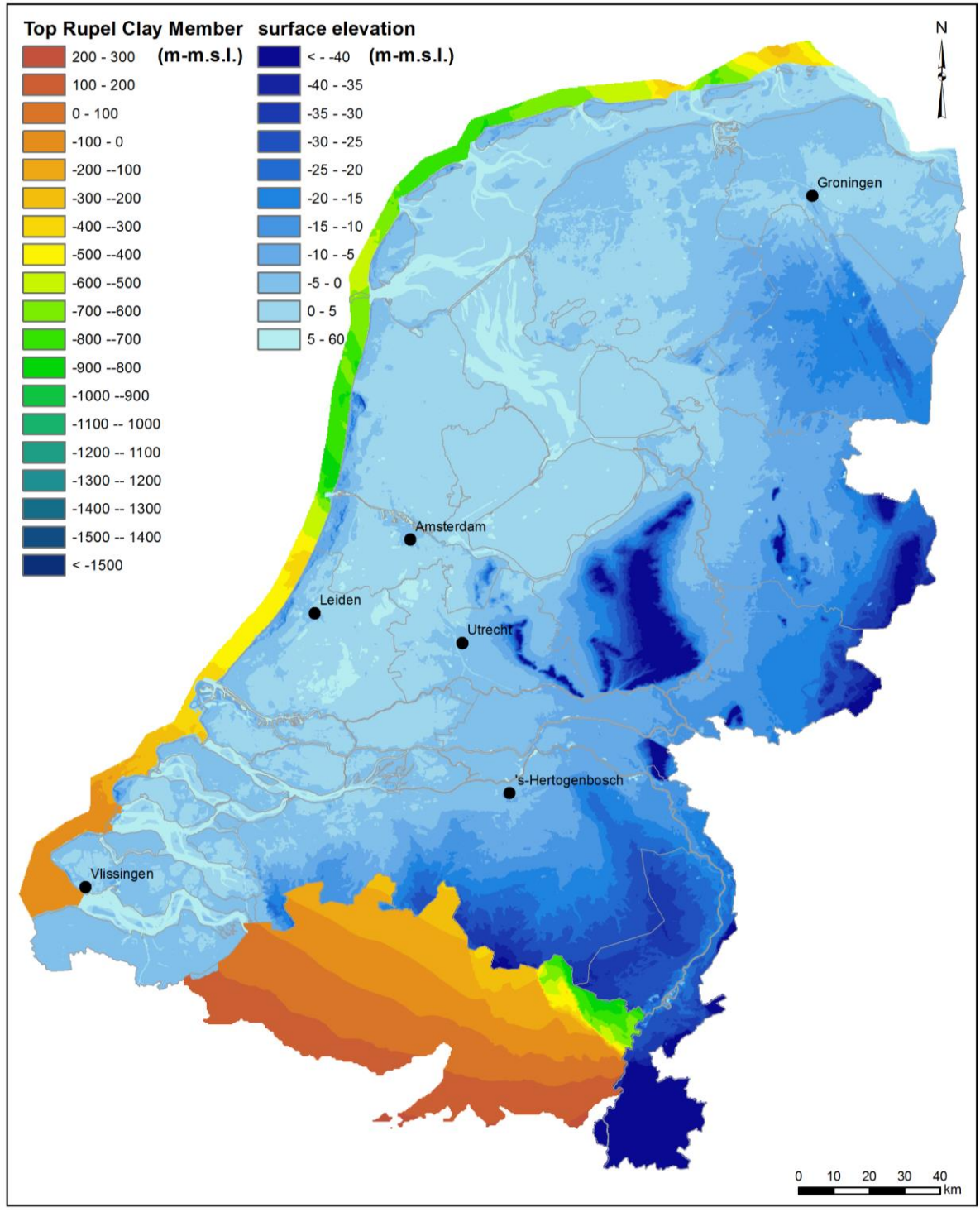

Figure 2-6. The blue grid represents the present-day land surface elevation based on AHN data. The multi-colour grid represents the top of the calculated Rupel Clay Member, which lies below the land surface. Where the multi-colour Rupel grid appears (locally), it lies above the blue North Sea grid (in the Netherlands), which is incorrect. A correction for this has been made in those cases.

Another way to check the quality of the grids is verifying whether the top and base of the Rupel Clay Member cross overlying and underlying stratigraphic horizons or the land surface. The top Rupel Clay Member grid does intersect with the base of the overlying Breda Formation grid at some locations (Figure 2-4). However, the base Rupel Clay Member grid hardly intersects with the underlying base North Sea Super Group grid (Figure 2-5). Because of uncertainties in the base Breda Formation and base North Sea Super Group grids, we decided not to correct the Rupel Clay member grids in these cases. The top Rupel Clay Member grid also intersects with the land surface at some small places (Figure 2-6). Because of the high accuracy of the AHN, this was corrected by setting the top Rupel Clay Member grid to be equal to the land surface where it occurs above it.

When comparing the Dutch Rupel Clay Member top and base with the Formatie van Boom top and base in Belgium, it appears difficult to match these two grids well. The difficulty to match the two grids primarily reflects differences in stratigraphic definitions and nomenclature across the Dutch-Belgian border. To solve this an integrated cross-border stratigraphy needs to be established. Other reasons explaining the mismatch are the different technical approaches to produce the grids in both countries. Despite the mismatch, the grids show similar geometrical characteristics.

2.2.Grain-size data

2.2.1. Grain-size analyses

Grain size was measured by Qmineral bvba in Belgium (www.qmineral.com) in samples taken from 16 boreholes spread across the country (Figure 1-1). Selection criteria were a thickness of more than 100 m and a depth of more than 400 m for the top of the Rupel Clay Member. The following description is taken from their final report on the analysed samples, which is in Dutch.

To disconnect individual grains, the cement that binds them was removed. Carbonate cement and Fe-oxides and hydroxides and organic compounds were dissolved. Carbonates were removed using 1.5N HCl, iron was removed by reduction of Fe3+ using oxalic acid and an Al plate. Organic matter was removed using H_2O_2.

After the removal of cements, the samples were shaken during one night using a shaking table. After that, they were given an ultrasonic treatment for one minute. The samples were split in equally sized sub-samples using a Rotary Cone Sample Divider.

Laser diffraction

One-fifth of a prepared sample was used for grain-size analyses using laser diffraction (low-angle laser light scattering, or LALLS). This sample was subdivided into ten equally sized samples using a Rotary Cone Sample Divider. Subdivision was necessary to be able to replicate measurements and to gradually increase the sample size to generate a suitable suspension for measurement. Samples were measured using a Malvern Mastersizer S Long Bed. At least two separate measurements were done, of which the average was calculated.

From sample 9 in borehole B58G0192 (287,8 m depth), only the fraction <2 mm was analysed because a large part of the sample consisted of flat flint stone pebbles.

Sedigraph

Three-fifth of a prepared sample was used for grain size analyses using a Sedigraph (X-ray measurements). This method has been specifically developed for fine-grained clay-rich sediments and is usually not used for sandy sediments. For technical reasons only grains smaller than 250 µm can be analysed using this machine. The fraction smaller than 250 µm was centrifuged and dried. Afterwards, water was added to obtain a suspension with a suitable suspension. A peptizer (sodium triphosphate) was added to obtain a stable suspension. Subsequently the sample was shaken again during one night and analysed using a Micromeritics Sedigraph 5100.

Fraction larger than 250 µm
One-fifth of a sample was used to determine the fraction greater than 250 µm, which is not analysed using the Sedigraph. The sample was wet-sieved and both the fraction smaller than 250 µm and greater than 250 µm was weighed after drying. In this way the fraction larger than 250 µm was obtained.

Grain-size statistics
The EXCEL spreadsheet program GRADISTAT 8 was used to interpolate class boundaries between the raw data size intervals (Blott and Pye, 2001). The program also outputs various grain-size statistics and textural descriptions.

2.2.2. Uncertainties

Grain-size data have been measured using two different methods. This was done because the Sedigraph is dominantly used in Belgium, while laser diffraction is preferred in the Netherlands. To allow comparison of new and older measurements in both countries, the two techniques were applied.

A comparison of the results for eleven samples from borehole B52E0114 shows strongly varying clay-percentages depending on measurement and analysis technique (Table 2-1). When analysed using laser diffraction, the samples have an average clay content (grain size smaller than 2 µm) of 13%. However, Konert and Vandenberghe (1997) have shown that the plate-shape of clay minerals may introduce an over-estimation of their particle size in laser-diffraction measurements. This difference may be up to eight size-classes when compared with traditional pipette measurements. They propose to use the measured fraction smaller than 8 µm as representing the clay fraction, i.e. representing a grain size smaller than 2 µm. When this methodology is used, the average clay content is 41%; more than three times higher than the < 2 µm fraction alone.

The same samples from borehole B52E0114 measured using the Sedigraph method yield an average grain size of 19%, which is 1.5 times the value from the laser-diffraction method. When comparing the Sedigraph results with the laser-diffraction results corrected for the plate-shape of the minerals, the clay percentage based on the Sedigraph is nearly two times lower (41% vs. 19%).

Table 2-1. Comparison of the grain-size measurement results for eleven samples from borehole B52E0114. Shown are the raw data from laser diffraction and sedigraph. These are presented as 0-2 µm and 0-8 µm classes (see text). The lower part of the table shows clay percentages after calculation with Gradistat software. These values compare relatively well with the raw data 0-2 µm class. See text for discussion.

B52E0114											
II1	II2	II3	II4	II5	II6	II7	II8	II9	II10	II11	***MEAN***
Laserdiffraction raw data (%)											
0-2 µm											
8,04	7,67	10,75	20,63	27,51	14,48	16,26	19,81	9,41	11,71	4,05	***13,67***
0-8 µm											
24,22	22,24	43,54	65,59	72,87	41,67	51,89	62,83	51,03	25,41	8,40	***42,70***
Sedigraph raw data (%)											
0-2 µm											
4,62	4,79	20,06	27,49	24,21	9,87	15,74	18,36	18,67	3,79	0,48	***13,46***
0-8 µm											
9,26	9,41	35,24	54,18	48,25	22,48	36,97	37,11	36,54	8,14	2,38	***27,27***
Laserdiffraction clay % according to Gradistat software											
7,52	7,23	9,97	19,11	25,76	13,54	15,16	18,48	8,70	11,15	3,86	***12,77***
Sedigraph clay % according to Gradistat software											
4,92	5,76	25,05	39,07	35,19	11,63	19,41	27,60	36,58	4,38	0,40	***19,09***

Recent studies have shown that the relationships between pipette (like the Sedigraph) and laser-diffraction measurements are different for different types of sediment (Buurman et al., 2001). For marine sediments they found a general under-estimation of the fraction < 50 µm measured using laser diffraction. They further state that it is better to use the two methods separately. The number of measured classes in the fraction < 2 µm in the current study using the Malvern laser-particle sizer, equals 24, which is eight more than in the study of Konert and Vandenberghe (1997). This gives more detail of the present results in the fraction < 2 µm.

Any technique used to measure grain size is known to give a different result. In fact, true grain size does not exist. The combination of measurement technique and the fact that sediment particles rarely have an ideal spherical shape, implies that there is always a degree of uncertainty or noise associated with grain-size measurements. In the present study we will use the laser-diffraction grain-size results *without a correction* for the plate-shape of the clay minerals. Using the laser-diffraction data probably implies a slight under-estimation of the clay content in the samples from the Rupel Clay Member.

2.3.Well-log correlation

To visualize vertical and lateral lithological trends in the Rupel Clay Member, well-log correlation panels were constructed. These panels show gamma ray (GR) values with depth. Higher GR values generally indicate more clay-rich deposits, while low values signify quartz-rich sands. By plotting grain-size data next to the well logs, changes in trends may be visualized.

2.4.Biostratigraphy

For the purpose of completeness an inventory of available biostratigraphic data for the Rupelian stage has been made. For 41 sites in the Netherlands (oil, gas and groundwater wells, outcrop data) biostratigraphic information is available (Appendix 2). Since it is neither the objective nor within the framework of the current project, the biostratigraphic data have not been utilized here.

2.5.Geohydrology

2.5.1. Hydrogeological setting

The hydrogeological framework, i.e. the spatial distribution of the permeability of the subsurface, is characterized by the distribution, thickness and dip of the hydrostratigraphic units and the location of geological structures and tectonic elements of importance for groundwater flow.

The description of the hydrogeological setting of the Rupel Formation (including the Rupel Clay Member) and its overburden requires the integration of different TNO models:

1. Geohydrological model REGIS II (Vernes and Van Doorn, 2005; model available at www.dinoloket.nl);
2. Digital Geological Model DGM (Gunnink et al., 2013; model available at www.dinoloket.nl);
3. Geological model of the deep subsurface (NITG-TNO, 2004; Kombrink et al., 2012) (model available at www.nlog.nl).

The 3D geological framework model DGM consists of 31 stacked lithostratigraphic units (mainly at the geological formation level), that are based on the lithostratigraphy for Neogene and Quaternary deposits in the Netherlands (Westerhoff et al., 2003; Ebbing et al., 2003; Weerts et al., 2004; Gunnink et al., 2013). The model displays units for the upper 500 m. The Paleogene Rupel Formation is only included in the model in the southwestern and easternmost part of the Netherlands where the formation is close to the surface. DGM includes information on the major known onshore faults cutting through the Neogene and Quaternary deposits.

The geohydrological model REGIS II used the lithostratigraphic units of DGM as a basis for the subdivision of the subsurface in hydrogeological units, aquifers and aquitards (Vernes and Van Doorn, 2005). The lithological information is used in combination with groundwater data to characterize the hydrogeological units by hydraulic conductivity, transmissivity and hydraulic resistance. The REGIS model does not cover the entire depth interval of DGM because of limited hydraulic information at greater depth. The REGIS II model includes hydraulic characterization of the Rupel Formation for the southwestern part of the Netherlands, where the formation is present at shallow depth. The Neogene Breda Formation is the basal hydraulic unit in large part of the model. The Breda Formationis not parametrised in the REGIS II model, because of lack of measured hydraulic data.

The current geological model of the deep subsurface covers the whole of the Netherlands (NITG-TNO, 2004; Kombrink et al., 2012). It includes the thickness and depth to base of the Neogene Upper North Sea Group and the Paleogene Super North Sea Group. It provides no information on formation and member level.

At present there is no complete systematic subdivision of the subsurface in aquifers and aquitards and their quantitative hydraulic characterization below the depth of the geohydrological REGIS II model. Ongoing mapping of aquifer units in the Dutch subsurface for geothermal purposes provides information on distribution, depth and thickness of aquifers and regional trends of porosity and permeability (Pluymaekers et al., 2012). These maps are part of a publicly accessible web-based geographical information system ThermoGIS (www.thermogis.nl). Due to a limited amount of measured data for the Paleogene aquifers, porosities were estimated from compaction curves (porosity – depth curves) and permeabilities from fixed porosity-permeability relations for the Roer Valley Graben (Wiers, 2001). These values can only be considered as preliminary estimates of regional porosity and permeability trends of the aquifers directly overlying and underlying the Rupel Clay Formation (Section 3.2).

Two representative cross sections have been compiled from the geohydrological model REGIS II, the Digital Geological Model and the geological model of the deep subsurface to illustrate the hydrogeological setting of the Rupel Formation (Section 3.2).

2.5.2. Hydrodynamic setting

The description of the hydrodynamic setting of the Rupel Formation (Section 3.2) is based on published information, such as Dufour's (2000) overview publication on groundwater in the Netherlands, publications on groundwater flow in the Roer Valley Graben (Bense, 2004; Luijendijk, 2012; Wiers, 2001) and publications on hydrodynamics including compaction-related flow conditions (Kooi, 2000; Kooi et al. 1998; Luijendijk, 2012, Verweij, 1999, 2003).

2.5.3. Porosity and permeability Rupel Clay Member

There is only a limited number of measured porosity and permeability data of the Rupel Clay Member in onshore Netherlands and these are restricted to shallow depths in the order of tens of meters below surface (Appendix 3; Rijkers at al., 1998; Wildenborg et al., 2000). The grain-size data measured by laser diffraction in samples of the Rupel Clay Member taken from boreholes spread across the country (Section 2.2; Figure 1-2) offered an opportunity to generate new porosity and permeability data for the Rupel Clay Member located at greater burial depth. The grain-size measurements revealed the existence of horizontal and vertical lithological variability in the Rupel Clay Member (Section 3.2): texturally it includes muds, sandy muds and to a lesser extent muddy sands.

Porosity decreases with increasing burial depth. At the depths of occurrence of the Rupel Clay Member in the Netherlands porosity reduction is mainly due to mechanical compaction driven by the increase of effective stress. Compressibility, and therefore rate of compaction, is strongly influenced by grain size. Special equations have been developed for calculating porosity and permeability of fine grained sediments (Yang and Aplin, 2004;

Aplin and Macquaker, 2011). These are used to calculate porosity and permeability of the mud part of the Rupel Clay Member.

The porosity and permeability of the sandy muds and muddy sands are calculated using the more generally applicable lithology-dependent porosity-depth and porosity-permeability relations included in the Petromod basin modelling software (Schlumberger) (Hantschel and Kauerauf, 2009). The lithology input for these equations is the percentage mix of standard lithologies (clay, silt and sand). The porosity equation is a porosity-depth/effective stress relation for mechanical compaction based on the conventional Athy's law. The porosity-permeability relation is the multipoint model (Hantschel and Kauerauf, 2009).

Mud porosity and permeability

Muds mostly comprise sediments of fraction < 63 µm, i.e. mostly consisting of a clay fraction (< 2 µm) and a silt fraction (2µm – <63µm). Compressibility of mud, and therefore its rate of compaction, is strongly influenced by grain size: finer-grained muds have higher depositional porosities, but their rate of compaction is higher (Yang and Aplin, 2004; Aplin and Macquaker, 2011). At a given porosity, finer-grained clay-rich muds have smaller pore sizes than silt-rich mudstones. Permeability closely relates to pore size and pore-size distribution. At the same porosity, clay-rich mudstones have lower permeabilities than clay-poor ones.

Yang and Aplin (2004) and Yang and Aplin (2010) developed equations to calculate mud porosity and vertical permeability, respectively. These equations include clay content and burial depth as important parameters. Yang and Aplin (2010) derived their equation based mainly on marine mudstones, using more than 300 samples and most of these samples were from the North Sea and Gulf of Mexico. They assumed the samples to be homogeneous.

Grain-size data have been measured using two different methods (laser diffraction and Sedigraph). The results with respect to clay percentage were found to vary strongly depending on the measurement and analysis technique used (Section 2.2.2). According to Konert and Vandenberghe (1997) the < 8 µm grain-size fraction defined by laser techniques corresponds to a grain size of < 2 µm defined by classical pipette analysis. They propose to use the measured fraction smaller than 8 µm (using laser diffraction) as representing the clay fraction, i.e. representing a grain size smaller than 2 µm.

Given the observed and published variations in the measured clay percentages depending on the technique used, we performed the calculation of porosity and permeability of the mud samples for two 'clay fractions' measured by laser diffraction and analyzed by Gradistat 8 software (Blott and Pye, 2001):

1. Fraction of grain size < 2 µm;
2. Fraction of grain size < 8 µm (corresponding to laser-measured fraction of clay + very fine silt + fine silt).

The approach to calculate mud porosity and permeability includes the following steps:

1. Calculation of porosity

Porosity is calculated using the following equation for void ratio developed by Yang and Aplin (2004):

$e = e100 - \beta \ln[(\sigma_v - P_w)/100]$

where,

$e100 = 0.3024 + 1.6867clay + 1.9505clay^2$

e100 : void ratio at 100 kPa effective stress

clay : clay content (fraction)

$\beta = 0.0407 + 0.2479clay + 0.3684clay^2$

$e = \theta/(1 - \theta)$

e : void ratio

θ : porosity (fraction)

Ϭv-Pw : effective stress (kPa)
Ϭv : vertical stress (kPa)
Pw : formation water pressure (kPa)

The effective stress for the upper part of the North Sea Group is estimated from the following relationship:
Ϭv – Pw = 9.9*z
where,
z : depth (m TVDss)

The vertical stress Ϭv in the Rupel Clay Member is estimated, using a grain-size density of 2700 kg/m^3, pore water density of 1020 kg/m^3 (the Rupel Clay Member is below the fresh-saltwater interface in most parts of the Netherlands; the assumed density corresponds to the density for seawater salinity) and porosity of 40%:
Ϭv = 19.9*z (z in m TVDss; Ϭv = vertical stress in kPa).

The following generalized equation to calculate the pore water pressure (Pw) in the Rupel Clay Member:
Pw = 10.0*z (z in m TVDss; Pw in kPa)

Input required to calculate the porosity using the Yang and Aplin equation (2004):

- Clay content (fraction < 2 µm and fraction 8 µm)
- Depth (z)

2. Calculation of permeability
The vertical permeability is calculated using the relationship published by Yang and Aplin (2010):
$Ln(k) = -69.59-26.79*clay+44.07*clay^{0.5}+(-53.61-80.03*clay+132.78*clay^{0.5})*e + (86.61+81.91*clay-163.61*clay^{0.5})*e^{0.5}$
where,
k : bedding perpendicular permeability (m2)
clay : clay content (fraction)
e : void ratio= θ/(1- θ)

Input required to calculate the permeability using the Yang and Aplin equation (2010):

- Clay content (fraction < 2 µm and fraction 8 µm)
- Porosity (result step 1)

Applicability and uncertainty of the approach
There are a number of uncertainties involved in the application of this method for the Rupel Clay Member. An important uncertainty concerns the clay content to be used. The two methods, laser diffraction and Sedigraph, used to measure grain sizes of the samples produce different results for the clay content (Section 2.2). Several authors have shown that clay content is underestimated by the laser-diffraction method. This is also confirmed by the present study (Section 2.2.1). There is, however, uncertainty about the magnitude of the underestimation. In this study the calculations are performed for two 'clay fractions'. An additional uncertainty results from the assumption of homogeneity of the mud sample that underlies the permeability model of Yang and Aplin (2010). The spatial lithological heterogeneity in muds at cm-m scale is not taken into account in the model. Heterogeneity at this scale occurs in the Rupel Clay Member, especially in the southern and eastern parts of the country. Yang and Aplin (2010) report that for their database (300 samples of marine mudstones, most of these from the North Sea and Gulf of Mexico), an uncertainty of magnitude in permeability at a given porosity is 1 order of magnitude. The mud samples from the Rupel Clay Member belong to one system in contrast to the samples from the Yang and Aplin (2010) study. At this time it is not known if this more

homogeneous sample set reduces the uncertainty in the calculated permeability. At the larger formation scale the Rupel Clay Member is probably anisotropic to a greater or lesser extent: vertical and horizontal hydraulic conductivity measurements performed on the Belgian Boom Clay show that the horizontal conductivity, at the formation scale, can be 5 – 60 times higher than the vertical ones (Wemaere et al., 2008). In order to test the applicability of the Yang and Aplin equations for the Rupel Clay Member, calculations have been performed using grain-size data from Belgian Boom Clay samples at 5 borehole locations (Yu et al., 2011). The results were compared with published porosity and vertical hydraulic conductivity measurements using permeameter or/and migration experiments (Wemaere et al., 2008; Yu et al., 2011, 2012). The permeability was calculated for reported minimum and maximum clay % of the Belgian Boom Formation for each borehole. The published hydraulic conductivity values for the Belgian Boom Clay were estimated using permeameter or/and migration experiments and concern the vertical hydraulic conductivity values representative for the entire Boom Formation. Table 2-2 shows the results of the comparison.

Table 2-2. Calculated vertical permeability for the Boom Formation at 5 well locations in Belgium. The vertical permeability is calculated using the Yang and Aplin (2004, 2010) equations and minimum and maximum clay % (from Yu et al., 2011). Published values for the vertical hydraulic conductivity for the Boom Formation (Yu et al., 2011) are added for comparison.

Well	mTVD below surface	Clay % < 2 µm sedigraph	k_v (m^2) calculated	K_v (m/s) calculated	K_v (m/s) published*
Doel-2b					
Top Boom Formation	54	8,4	6,70E-18	6,70E-11	
Bottom Boom Formation	113	8,4	2,73E-18	2,73E-11	
Top Boom Formation	54	70	6,26E-18	6,26E-11	
Bottom Boom Formation	113	70	1,80E-18	1,80E-11	
Boom Formation					8,00E-11
Zoersel					
Top Boom Formation	89	17	6,33E-18	6,33E-11	
Bottom Boom Formation	187	17	2,43E-18	2,43E-11	
Top Boom Formation	89	70	2,69E-18	2,69E-11	
Bottom Boom Formation	187	70	7,29E-19	7,29E-12	
Boom Formation					5,50E-12
Essen-1					
Top Boom Formation	153,97	11,4	2,32E-18	2,32E-11	
Bottom Boom Formation	280,17	11,4	9,58E-19	9,58E-12	
Top Boom Formation	153,97	47,2	3,53E-18	3,53E-11	
Bottom Boom Formation	280,17	47,2	1,27E-18	1,27E-11	
Boom Formation					8,50E-12
Mol-1					
Top Boom Formation	186	12	1,86E-18	1,86E-11	
Bottom Boom Formation	289	12	9,57E-19	9,57E-12	
Top Boom Formation	186	52	2,22E-18	2,22E-11	
Bottom Boom Formation	289	52	1,01E-18	1,01E-11	
Boom Formation					2,80E-12
Weelde-1					
Top Boom Formation	259	31	1,91E-18	1,91E-11	
Bottom Boom Formation	385	31	9,95E-19	9,95E-12	
Top Boom Formation	259	71	3,63E-19	3,63E-12	
Bottom Boom Formation	385	71	1,69E-19	1,69E-12	
Boom Formation					4,00E-12

Published hydraulic conductivities K_v for the entire Boom Formation (Yu et al., 2011) are the harmonic means of the K_v values of its subunits

3. Results

3.1.Regional-scale geometry and overburden of the Rupel Clay Member

The regional-scale geometry of the Rupel Clay Member (Figure 3-1 to Figure 3-5) clearly demonstrates its presence at shallow depths along the southwestern and eastern borders of the country. Away from these borders, towards the northwest, the member is present at greater depths.

3.1.1. Top and base

In a large area in the southwest of the Netherlands, roughly encompassing the province of Zeeland and the west of the province of Noord-Brabant, the top of the Rupel Clay Member is located at depths shallower than -400 m m.s.l. (Figure 3-1). The same is valid for the east of the country: in the provinces of Groningen, Drenthe, Overijssel and Gelderland east of the River IJssel, and in the northeast of the province of Noord-Brabant and the north of the province of Limburg the top of the clay member lies at depths shallower than -400 m m.s.l.

There are two zones with a burial-depth of the top of the clay member below -800 m m.s.l. These are the Roer Valley Graben (RVG) and the Zuiderzee Low (ZZL), which are known Cenozoic structural elements (Duin et al., 2006). In the RVG the deepest point of the base of the Rupel Clay Member lies around -1600 m m.s.l., in the ZZL this is about -1250 m m.s.l. (Figure 3-2).

3.1.2. Difference with previous CORA study

The depth of the top of the Rupel Clay Member resulting from the present study is compared with the depth of the top of the member resulting from the CORA study, which was based on De Mulder et al. (1984). The difference grid shows where positive and negative deviations occur (Figure 3-3). Large negative differences occur in the south of Limburg, because De Mulder et al. (1984) did not map that region. Large negative and positive deviations occur along the major bounding faults of the Roer Valley Graben, which can be ascribed to the greater detail in the present study resulting from the use of seismic data. The relatively large deviations south of Leiden and west of Amsterdam result from the fact that these areas were mapped as uncertain by De Mulder et al. (1984). Smaller areas with deviations generally result from newly available well data in the present study.

3.1.3. Thickness

The present-day thickness of the Rupel Clay Member does not reflect the original depositional thickness. Due to various geological processes the deposits have experienced vertical movements. Some of these movements have caused parts of the member to become exposed to erosional processes. Due to this, the sequence may have been partly or completely eroded.

The observed thickness variation (Figure 3-4) is likely to be of post-depositional origin. Due to tectonic movements the northern part of the West Netherlands Basin (WNB) was uplifted (inversion) during the Pyrenean Phase around the Bartonian-Priabonian boundary. This caused partial or complete erosion of the Rupel Clay Member, as indicated by the uncertain thickness in the area (Figure 3-4). The effect of the inversion and erosion is clearly visible in an offshore seismic section (Figure 3-6). Near the province of Zeeland, continuous uplift of the London-Brabant Massif has probably caused deposition of a thinner sequence and subsequent partial erosion of the top of the member.

The mean thickness of the Rupel Clay Member is 65 ± 42 m. The member is thickest (> 100 m) in three zones: RVG, ZZL and the southern part of the West Netherlands Basin (WNB). Outside these areas, there are three zones where the thickness is limited to 10 m or less (possibly absent): the north of the WNB, the province of Zeeland, the eastern part of the province of Drenthe and the northeast of the province of Overijssel.

3.1.4. Deeper than 400 m, thicker than 100 m

In some areas the top of the Rupel Clay Member is located deeper than -400 m m.s.l. and the member is thicker than 100 m (Figure 3-5). Two main areas meeting these criteria can be identified: the Roer Valley Graben in Noord-Brabant and Limburg and the eastern part of the Zuiderzee Low, underneath the Veluwe area. In the rest of the country, several small zones meeting the criteria can be identified.

Besides the fact that the above-mentioned criteria are not met in the provinces of Groningen and Drenthe, salt-domes are present there which continue to disturb the subsurface by salt-tectonics.

3.2.Lithological characterization of the Rupel Clay Member

3.2.1. Lithological variability

As a result of the mode of deposition, lithological variability is present in the Rupel Clay Member. Since the Rupel Formation as a whole was deposited in a marine environment, sand deposits are present along the palaeo-coastline of the sea (Figure 1-3). Further away from that coastline, water depths were greater and more fine-grained silt and clay deposits were deposited. Currently these fine-grained deposits are buried at a great depth. Oil and gas wells usually go through this interval without giving much attention to it. Groundwater wells usually do not penetrate the deposits of this formation because they lie too deep. The result is that little is known about the Rupel Formation and its lithological characteristics.

To shed more light on the lithological variability within the Rupel Clay Member in the deeper-buried locations, grain size has been measured on samples from 15 wells. The complete grain-size measurement results and the quality of the old samples from the core shed are discussed in OPERA Task 5.2.1 (Koenen and Griffioen, 2013). The samples were exposed to air, leading to oxidation of pyrite and growth of secondary minerals such as gypsum and carbonate. The results show that the clay-content of most samples is relatively low (<26%, when using laser-diffraction data < 2µm). This implies that in terms of sediment texture most samples do not classify as a clay, but rather as a fine to coarse silt.

In terms of horizontal and vertical grain-size trends and heterogeneity, the number of wells sampled is too low for conclusive results. The first-order results do show that the samples with the coarsest grain size within the Rupel Clay Member are found along the palaeo-coastline, while the samples with the finest grain size are found in the deeper-water basin.

3.2.2. Enhanced conceptual lithofacies model

Generally speaking the distribution of median grain size (D50) in the Netherlands based on the samples from 15 boreholes confirms the palaeogeographic setting (Figure 1-3). According to the palaeogeography the sedimentary basin was deepest in the north and west of the country and finest grained deposits are expected to have accumulated there. The margins of the Rupelian sea were located along the southern and eastern border of the Netherlands. In those regions coarser-grained facies of the Rupel Clay Member are expected due to input from land and reworking by currents and waves. This division is corroborated by the fact that the samples with the finest average median grain size are found in the north and the coarsest are found in the southwest and southeast.

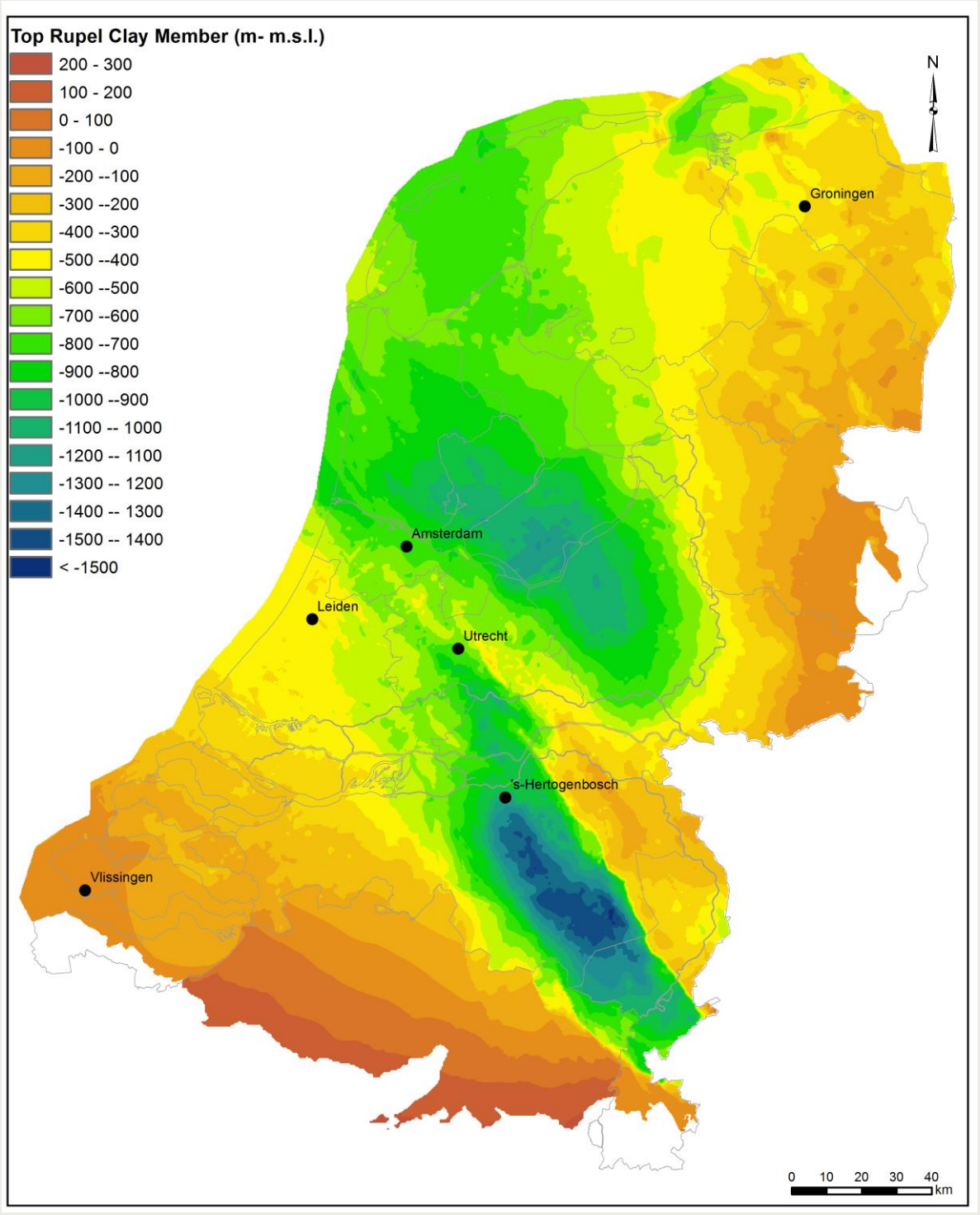

Figure 3-1. The depth (in metres relative to m.s.l. = mean sea level ~NAP) of the top of the Rupel Clay Member. The Belgian data is based on the base of the Formatie van Boom (DOV, 2004). To calculate the top we added 150 m to the base.

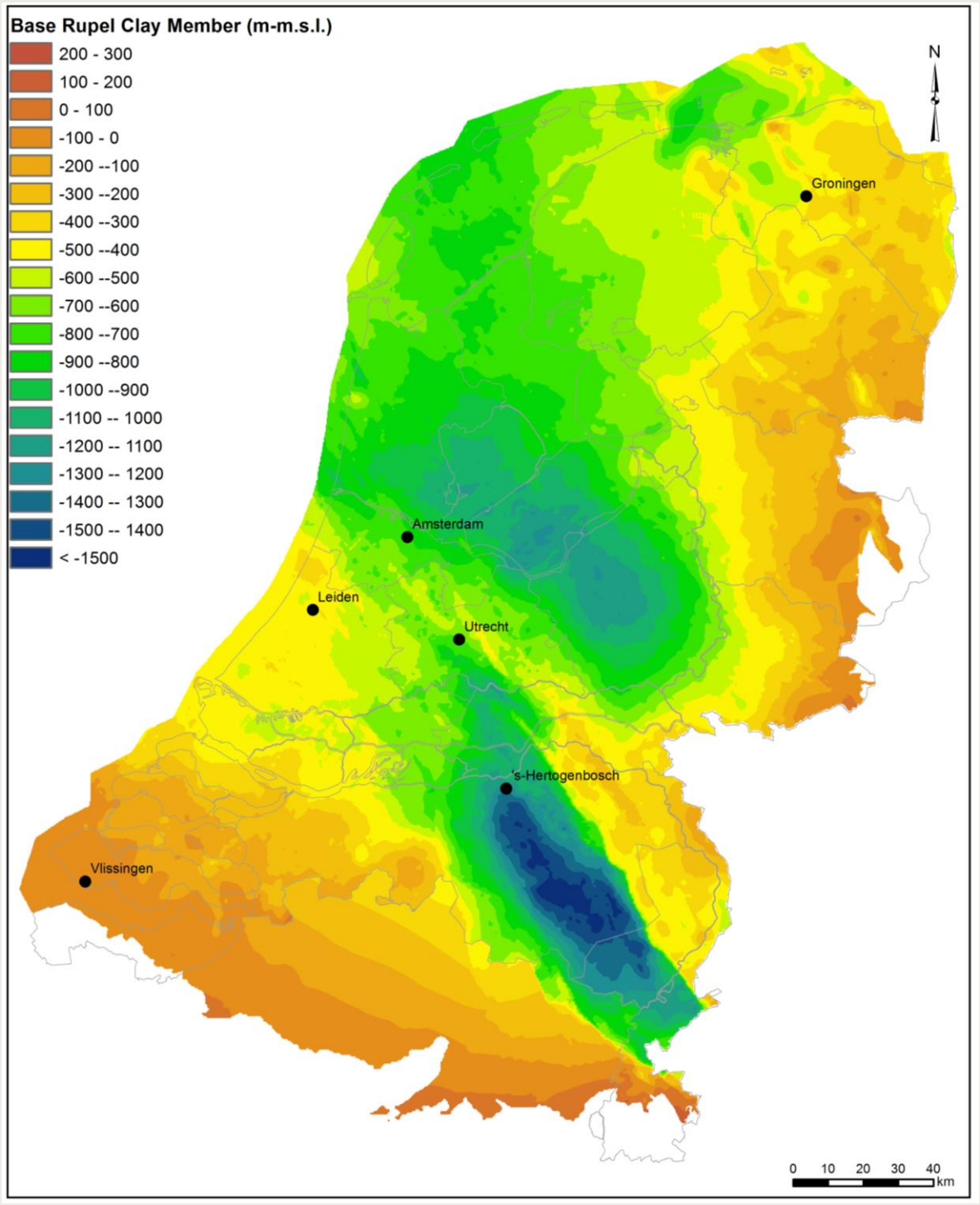

Figure 3-2. The depth (in metres relative to m.s.l. = mean sea level ~NAP) of the base of the Rupel Clay Member. The Belgian data is based on the base of the Formatie van Boom (DOV, 2004).

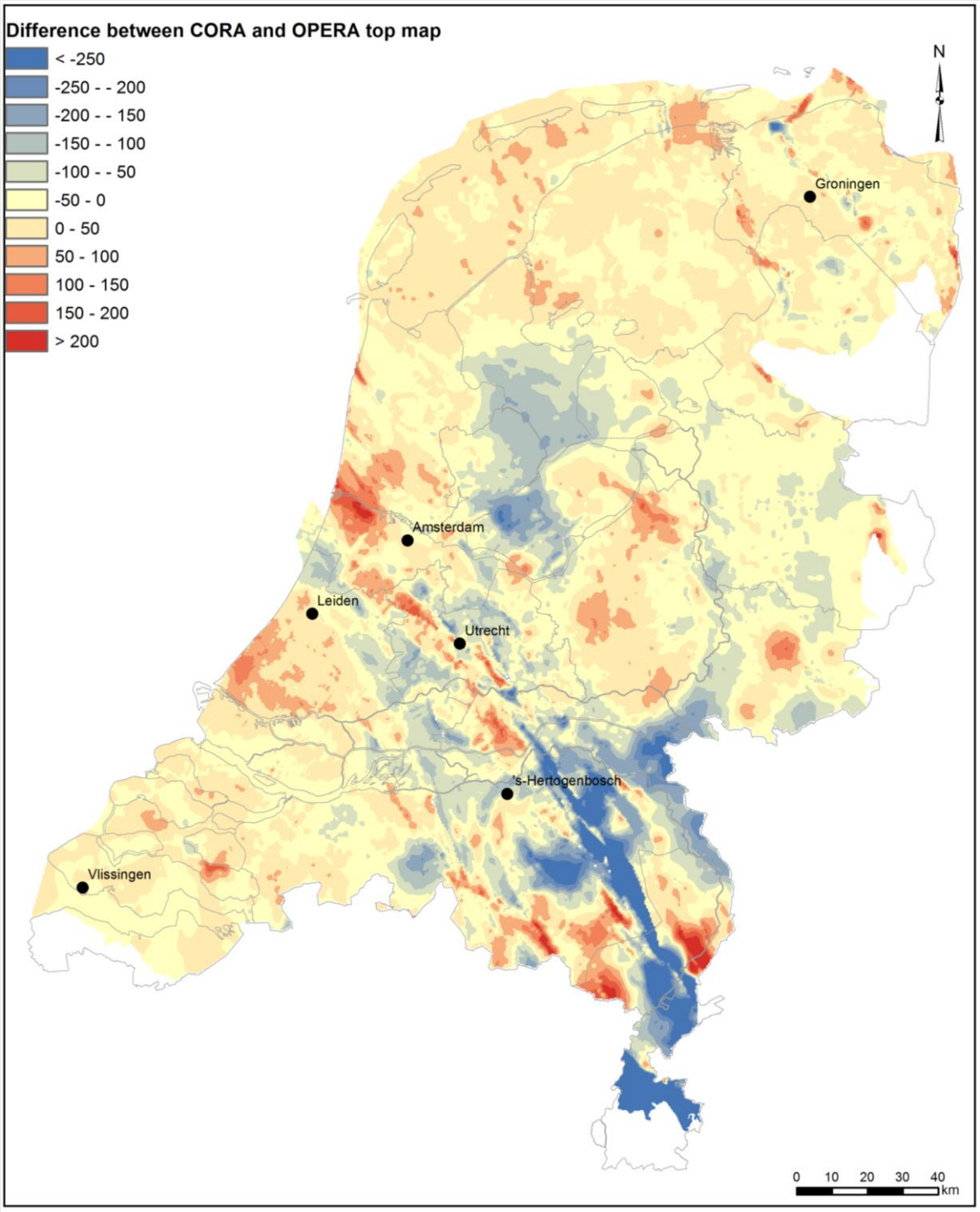

Figure 3-3. The difference between the latest version of the top of the Rupel Clay Member as published in the RGD report by De Mulder et al. (1984) and the top of the member as published in the present OPERA study. Blue = new OPERA grid lies less deep than in De Mulder et al. (1984); red = new OPERA grid lies deeper than in De Mulder et al. (1984).

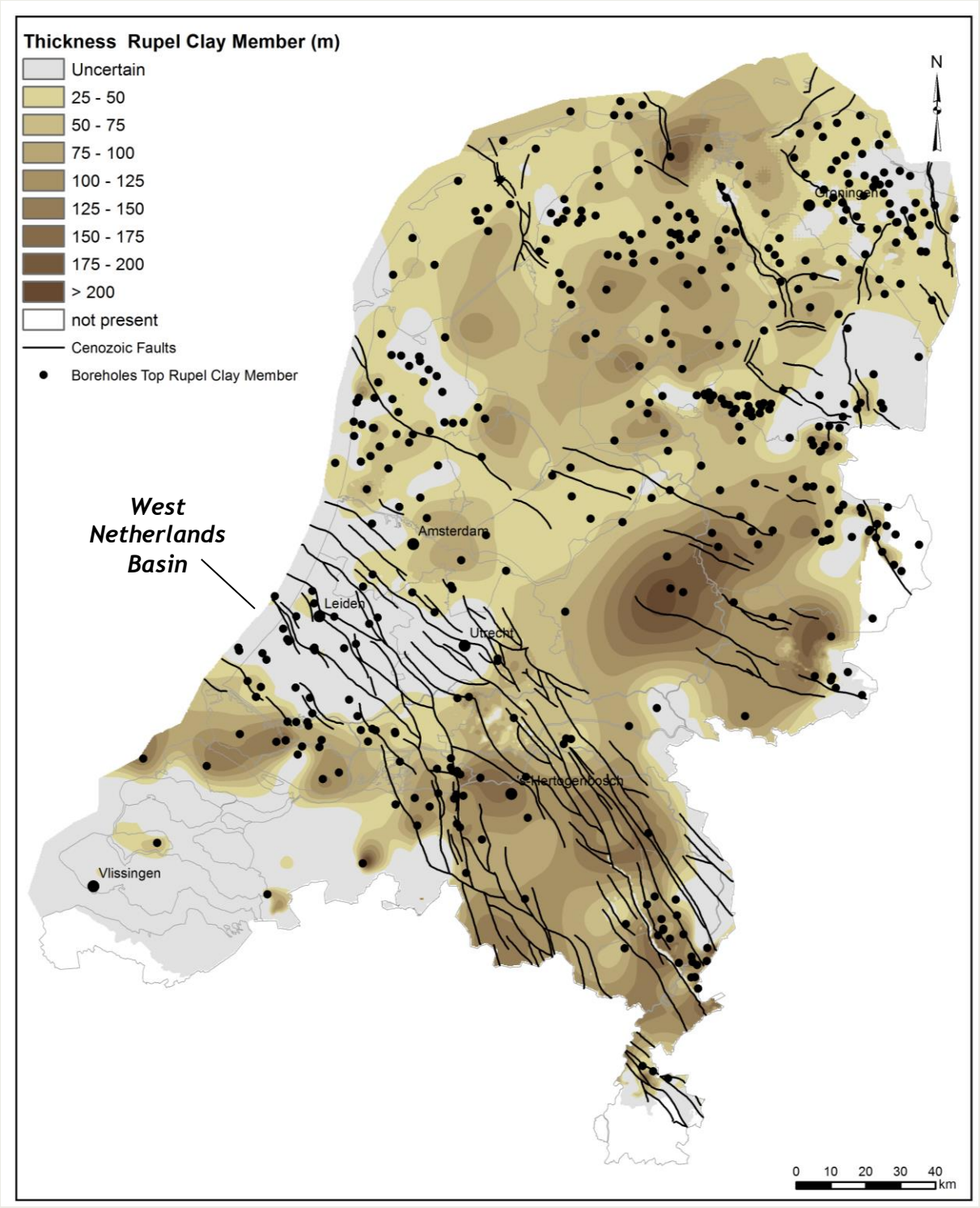

Figure 3-4. The thickness of the Rupel Clay Member between the grids shown in Figures 3-1 and 3-2. Where the thickness is less than 25 m, the Rupel Clay Member may be partially absent, this is therefore indicated as "uncertain".

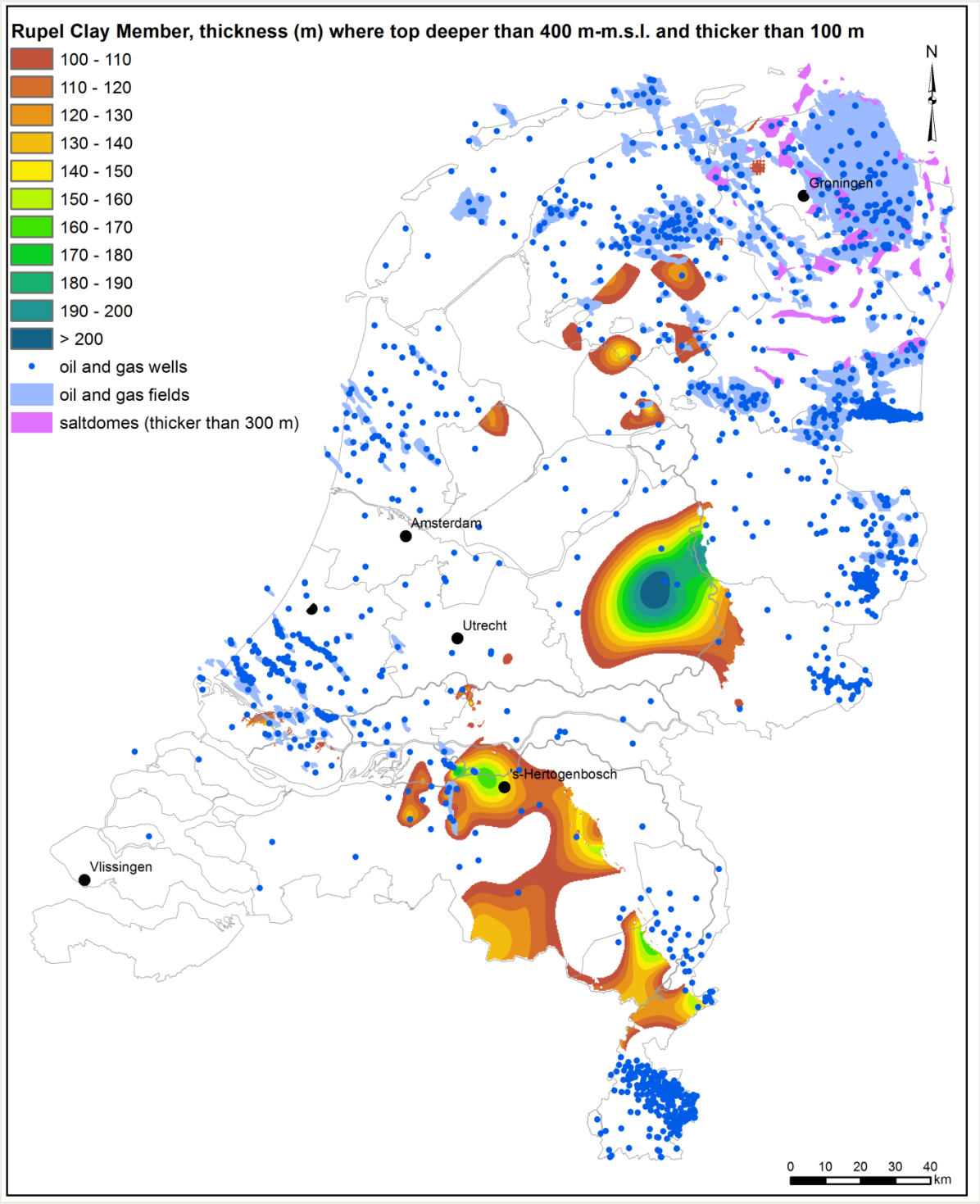

Figure 3-5. The thickness of the Rupel Clay Member, where the top lies deeper than 400 m and the thickness is more than 100 m. Also indicated are oil and gas wells and fields and saltdomes thicker than 300 m.

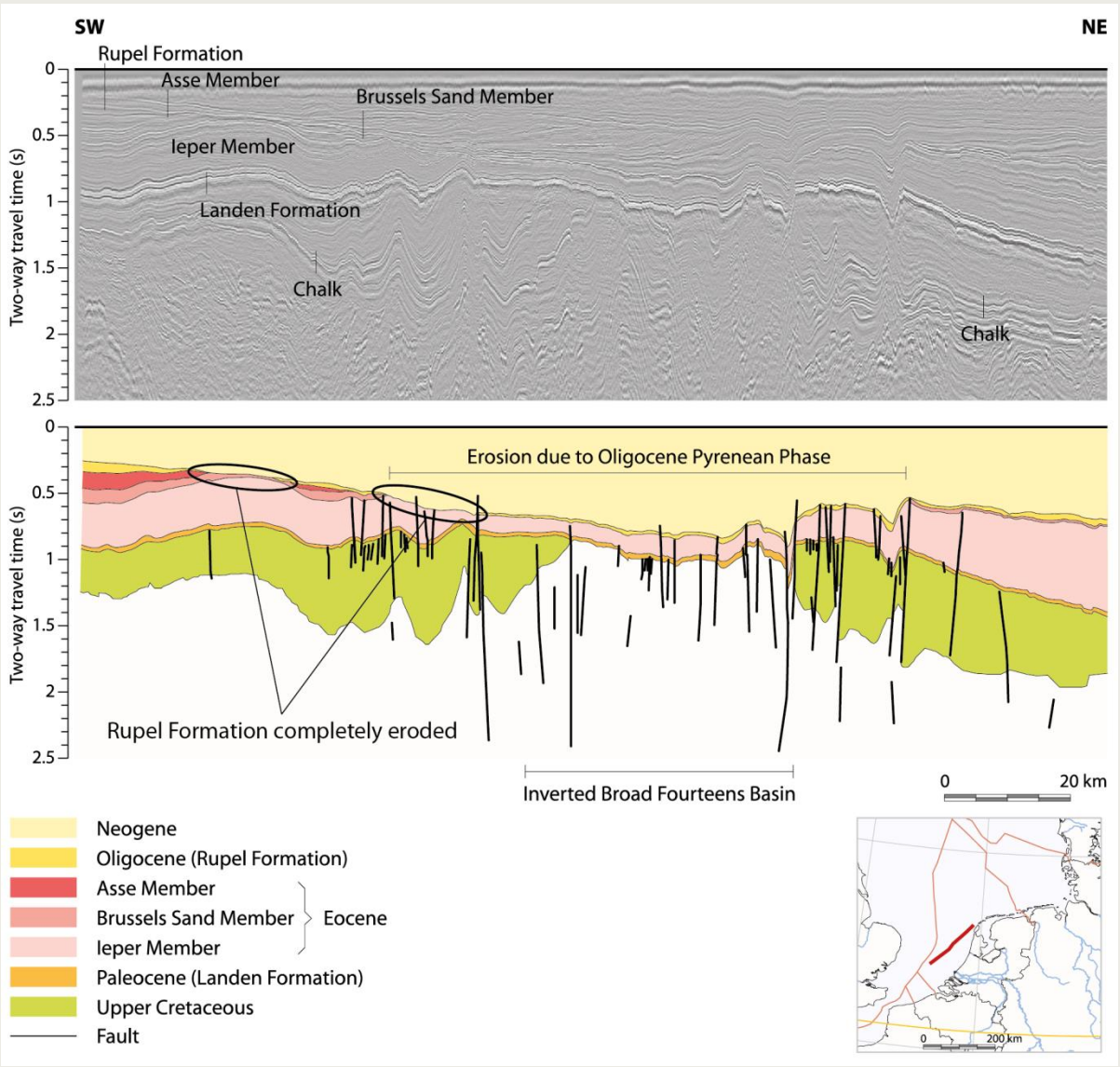

Figure 3-6. Seismic section through Cenozoic sediments below the North Sea (modified after Knox et al., 2010).

Recent studies have found tectonic signals in the Rupelian Boom Clay cycles and indications for regional uplift at the end of the Rupelian stage (Vandenberghe and Mertens, 2013; De Man et al., 2010). Based on a hypothesis proposed by Noël Vandenberghe (2013, pers. com.), older structural elements may have been active during deposition of the Rupel Clay Member in the Netherlands. This implies that structural highs may have caused shallow areas in the sea or even formed islands. To test this hypothesis, structural elements, grain-size data and coastal deposits (Vessem Member) were plotted together on one map (Figure 3-7).

The distribution of boreholes which penetrated the thickest occurrences of the sandy Vessem Member provides some clues on the presence of more shallow parts in the basin. The sediments of the Vessem Member are presently thought to have been deposited as a transgressive sequence resulting from relative sea-level rise (Van Adrichem Boogaert and Kouwe, 1993). When assuming that this sequence is thicker where more land-sourced sand was available, its thickness distribution may suggest the presence of nearby shallow areas or land surfaces during deposition. The map (Figure 3-7) shows clustering of thicker Vessem Member occurrences in the southwest along the Zeeland High, in the southeast on the Peel-Maasbommel Complex, and in the north along the Texel-IJsselmeer High and the Dalfsen High.

The presence of nearby shallow areas or land surfaces during deposition is also expected to be visible in the grain-size data. The median grain size of the analysed boreholes shows coarser Rupel Clay Member grain sizes in the southwest and southeast (Figure 3-7). However, in the north of the country coarser grain sizes are not clearly linked to the suggested highs. Most of the sampled boreholes are not located near the Texel-IJsselmeer High and none are located near the Dalfsen High, so no firm conclusions can be drawn from the median grain-size data in this region.

3.2.3. Focus on areas where deeper than 400 m, thicker than 100 m

In the areas where the Rupel Clay Member is thicker than 100 m and its top is located at depths greater than -400 m m.s.l. (Figure 3-5) limited grain-size data are available. None of the wells analysed for grain size penetrate the focus areas in the Roer Valley Graben in Noord-Brabant and Limburg. The wells are all located on the structurally higher horst blocks on both sides of the graben, where the Rupel Clay Member occurs at depths less than -400 m m.s.l. The well-correlation panel (Figure 3-8) shows that wells B50H0373 and B48G0159 have a slightly larger D50 grain size within the Rupel Clay Member towards top and base. Well B58G0192 contains the coarsest deposits, with D50 grain-size values reaching up to 166 µm. This can be explained by its position near a palaeo-coastline.

Wells in the southwest (B41G0024 and B46C0478) show an average D50 grain size which is similar to that of wells in the north (see below). In the eastern part of the Zuiderzee Low, underneath the Veluwe area no wells have been sampled for grain size. In the north of the country several small zones meeting the depth-thickness criteria have been identified. A well-correlation panel has been constructed for the sampled wells in this area (Figure 3-9). Well GRD-01 penetrates one of these zones. The Rupel Clay Member is about 125 m thick and located at -452-577 m m.s.l. The median grain size (D50) in this well shows low values between 8 and 10 µm, justifying the name of a medium silt. In this well there appears to be no grain-size coarsening towards top and base of the member. Due to absence of a gamma ray (GR) log, well-log correlation with nearby wells is not possible.

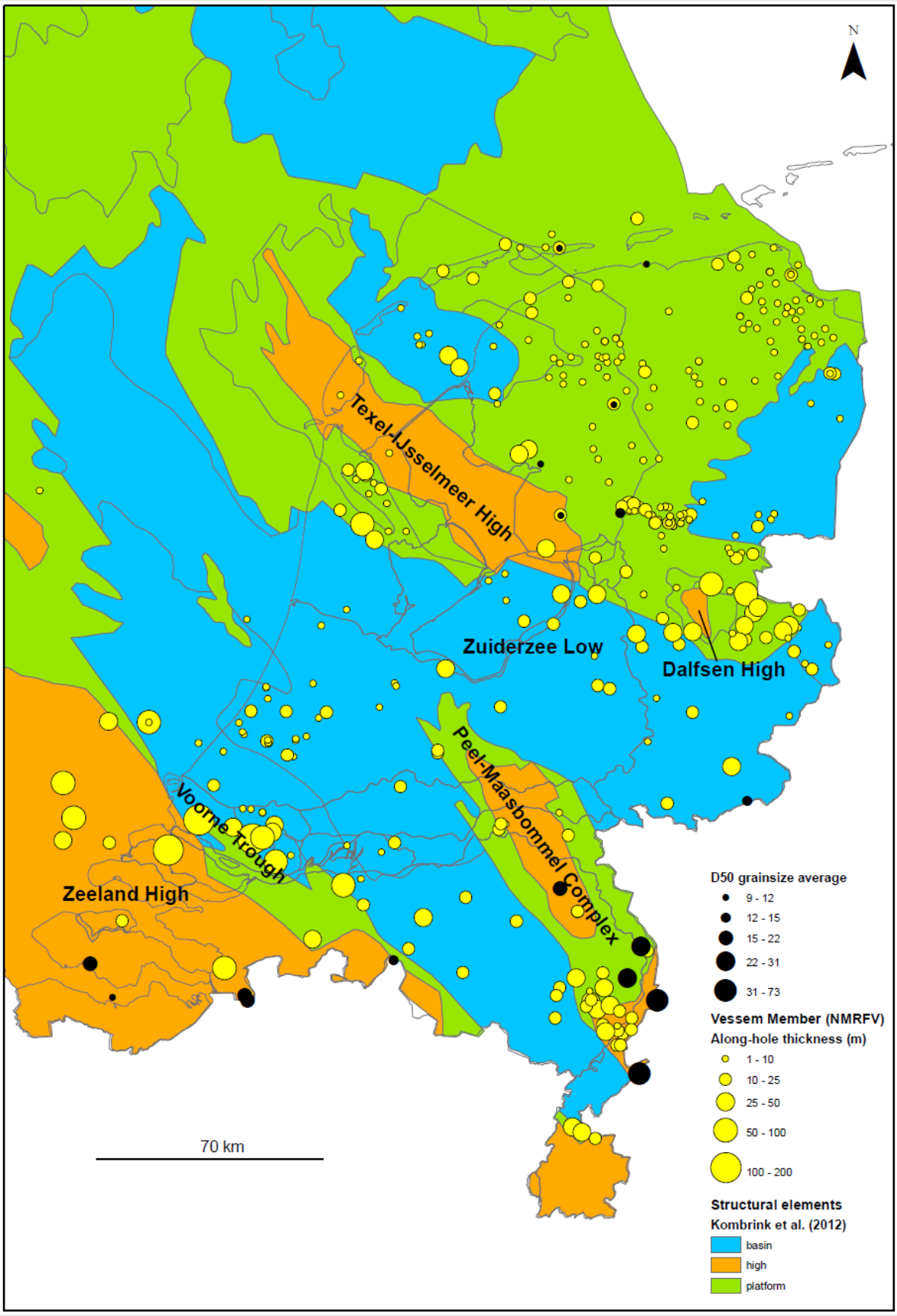

Figure 3-7. On and offshore structural elements, D50 average grain size for each sampled well, and the thickness of Vessem member sands are shown to identify the effect of the structural elements on palaeo-depositional environments and lithofacies (clayey-silty-sandy) in the Rupel Clay Member.

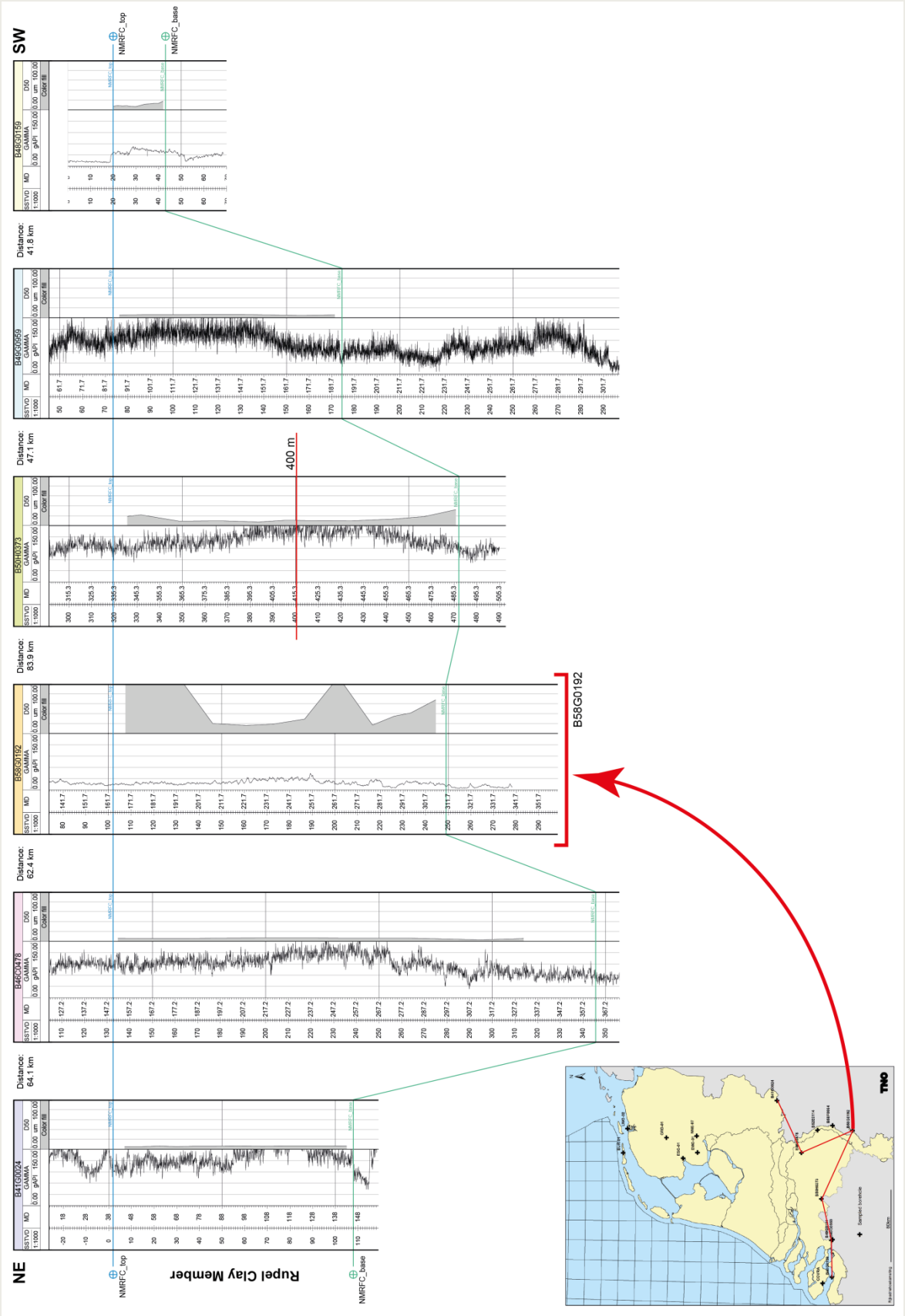

Figure 3-8. Correlation between wells with the Rupel Clay Formation sampled for grain size in the south of the Netherlands. Well B58G0192 shows coarser-grained intervals towards top and base.

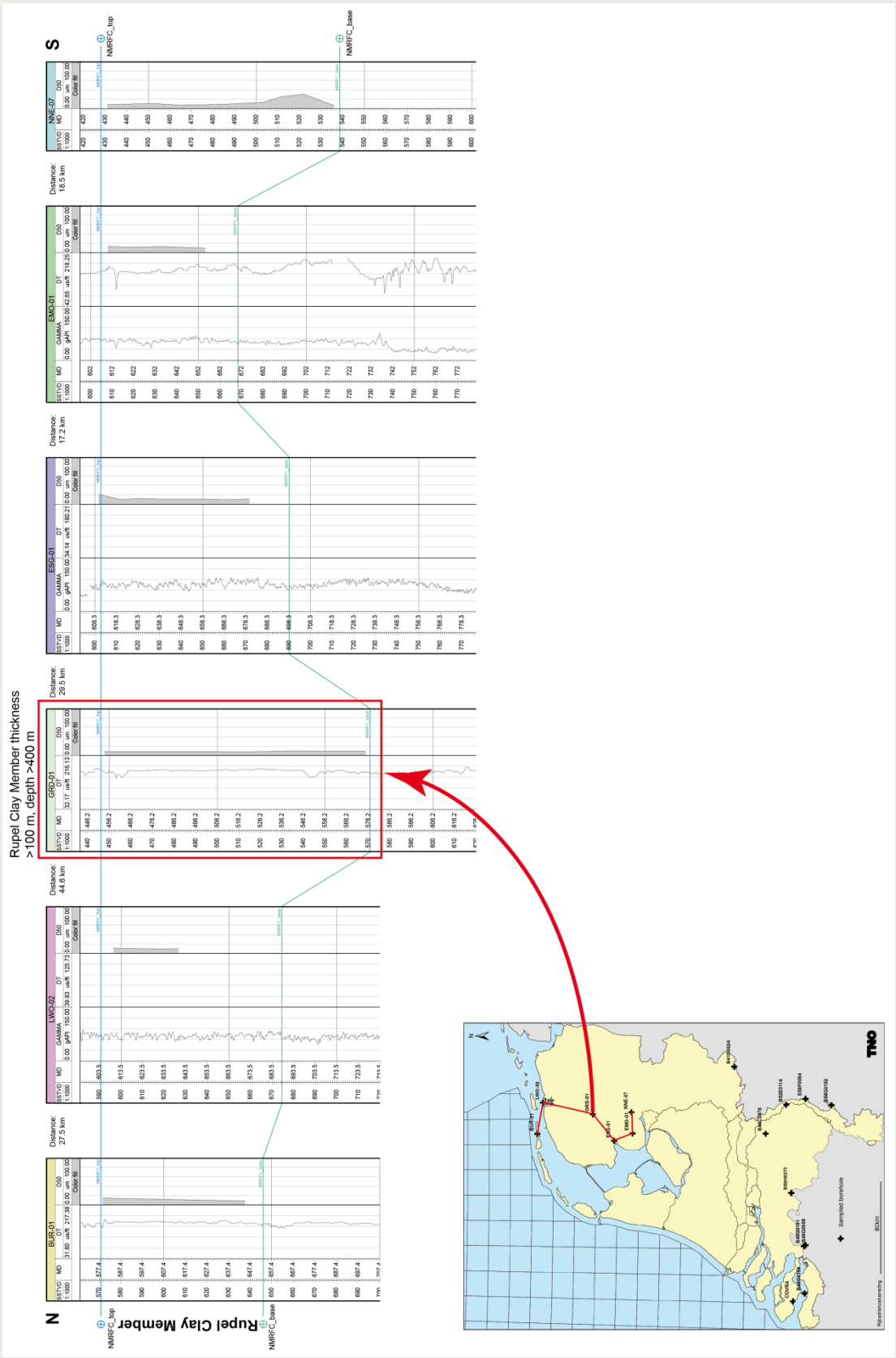

Figure 3-9. Correlation between wells with the Rupel Clay Formation sampled for grain size in the north of the Netherlands. In well GRD-01 the Rupel Clay Member is thicker than 100 m and the top lies deeper than 400 m, it is located in the North Netherlands focus area. A slight grain-size increase towards top and base can be discerned.

3.3.Regional scale geohydrological setting of the Rupel Clay Member

3.3.1. Hydrodynamic setting

The driving forces for water flow through the subsurface are gradients in hydraulic potential, water density differences, and also gradients in salt concentration and electrical potential. All these driving forces are active in the Netherlands to a greater or lesser extent.

The meteoric groundwater flow systems driven by hydraulic gradients are shallow to very shallow systems in most of the Netherlands, especially in the low-lying flat parts of the country (Dufour, 2000). The depth-contour map of the interface between fresh and brackish groundwater (at 150 mg Cl^-/ l) shows that the maximum depth of occurrence of fresh groundwater is in the southeastern onshore part of the country (Figure 3-10).

The response time to changing geohydrological boundary conditions is higher for hydraulic than for hydrochemical systems (Oude Essink, 1996). As a consequence, the maximum depth of occurrence of fresh groundwater provides just a preliminary indication of the depth of penetration of recently active flow of groundwater of meteoric origin. The C14 dating of groundwater in discharge areas of supra-regional groundwater flow systems in the southern Netherlands has revealed Pleistocene ages for the groundwater in this groundwater flow system (> 30,000 years; Stuurman et al., 2000). These ages reveal the long residence times for the groundwater in such a supra-regional meteoric groundwater flow system.

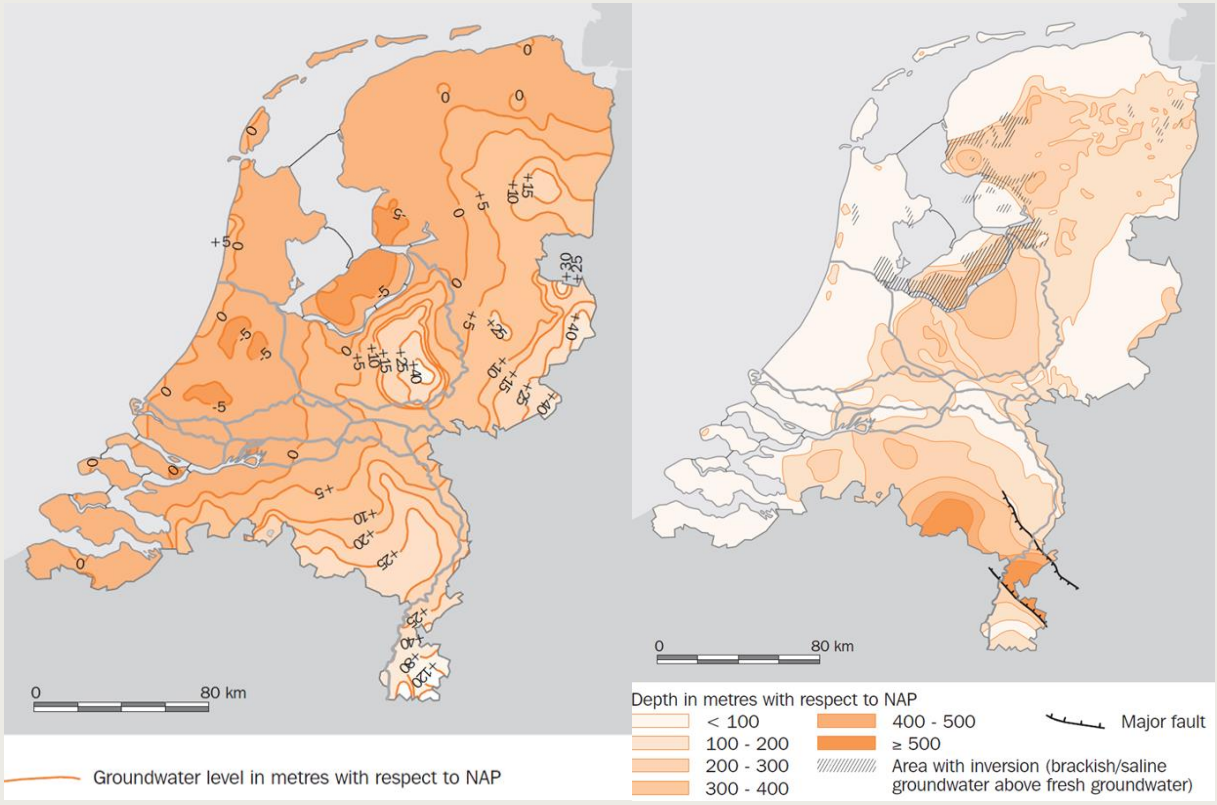

Figure 3-10. Elevation of the water table and depth of the fresh-brackish groundwater interface in the Netherlands (Verweij, 2003; after Dufour, 2000).

The Roer Valley Graben in the southern Netherlands is the only area where the Rupel Clay Member is thicker than 100 m with its top located at depths greater than 400 m below m.s.l., and where the meteoric groundwater flow system extends to a depth of more than 400 m. Wiers (2001) and Luijendijk (2012) modelled groundwater flow along a 2D SW-NE cross section through the central part of the Roer Valley Graben. The modelled hydrogeological framework does not include faults. Luijendijk's model (Figure 3-11 to Figure 3-13) simulated groundwater flow driven by water table gradients, compaction and buoyancy forces generated by salinity and temperature difference. The most active part of groundwater flow is restricted to approximately the upper 500 m and will not affect the Rupel Clay Member in most of the Graben (Figure 3-13). A possible exception is the southern part of the Graben where the Rupel Clay member is present at a shallower depth.

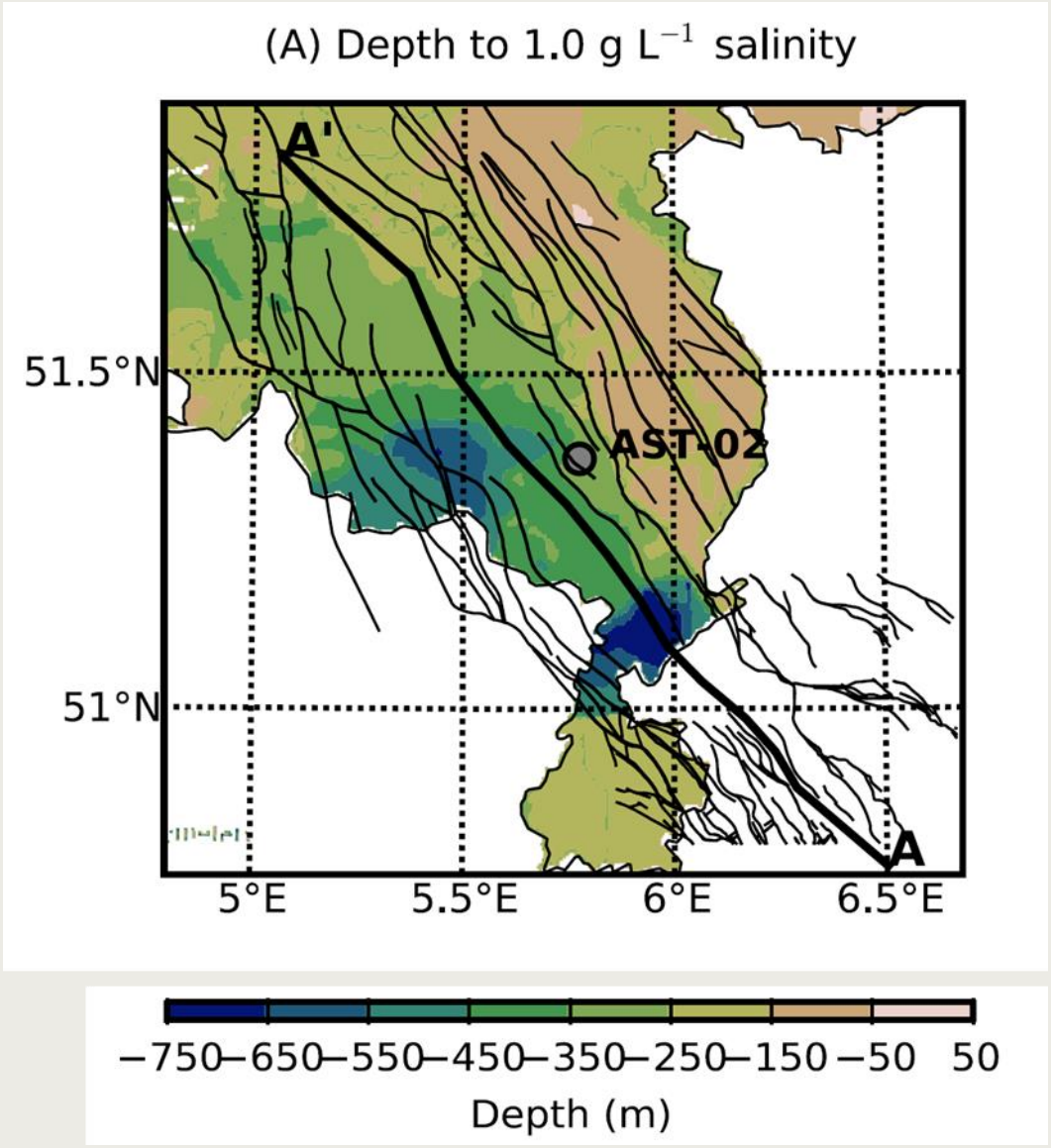

Figure 3-11. Depth of fresh-brackish groundwater interface in the Roer Valley Graben area (from Luijendijk, 2012). A A' is the location of cross section shown in Figure 3-12.

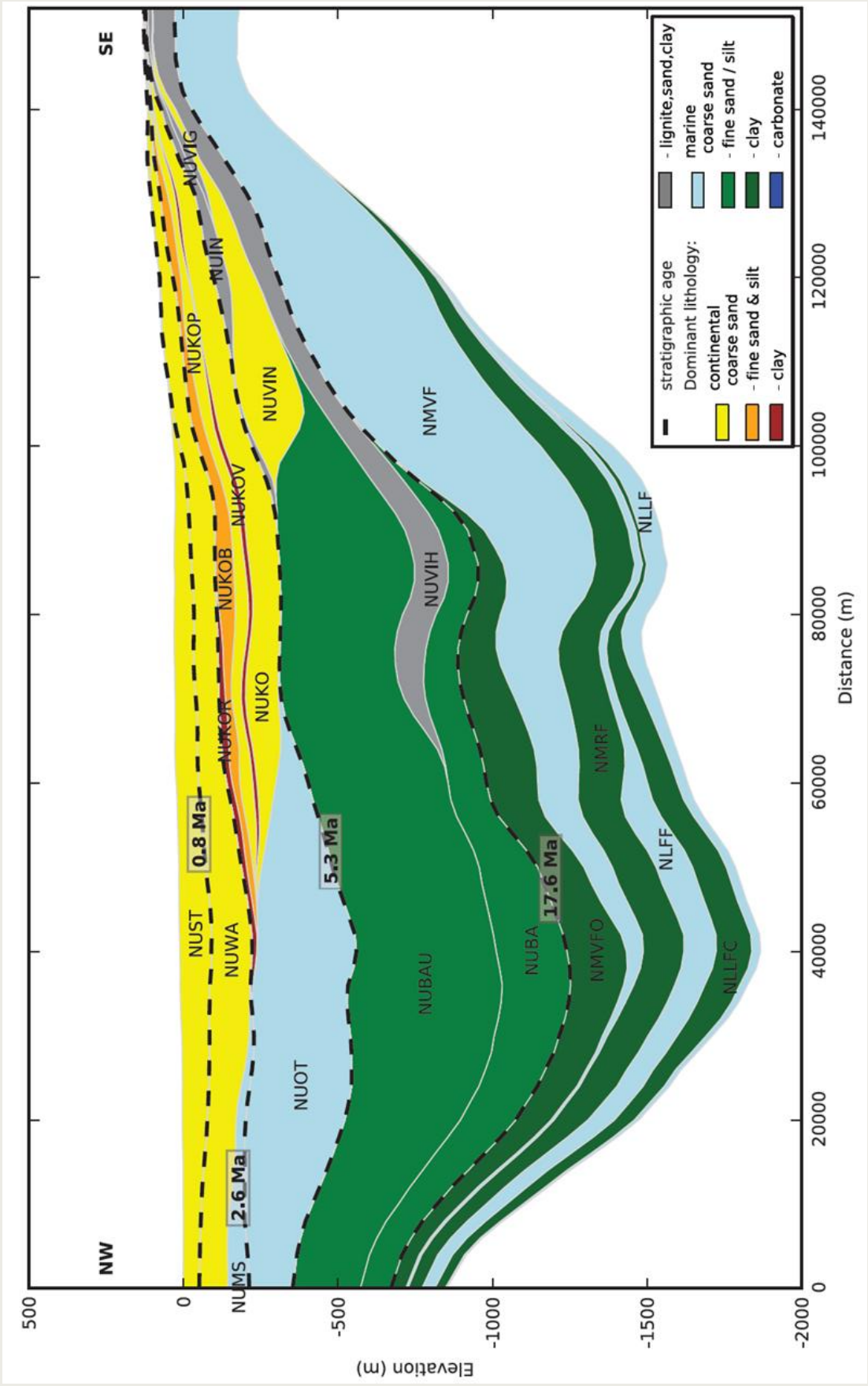

Figure 3-12. 2D lithostratigraphic cross section along the axis of the Roer Valley Graben (from Luijendijk, 2012). NMRF is the Rupel Clay Member. Location of cross section is given in Figure 3-11.

Bense (2004) studied the impact of fault zones on groundwater flow in the Roer Valley Graben and the adjacent areas in Germany. In the Netherlands his research concentrated on assessing hydraulic properties of faults and the influence of faults on groundwater flow at shallow depth. Fault properties were studied in a trenched outcrop over the Geleen Fault. The identified anisotropic nature of the permeability of faults was shown to enhance vertical groundwater flow along the Peel Boundary Fault near Uden. More recent studies (Caro Cuenca, 2012) as well as previous studies of hydraulic heads around shallow faults (such as Ernst and Ridder, 1960; Stuurman and Atari, 1997) confirm the influence of fault zones on groundwater. The southeastern part of the Netherlands is known to be seismically active, and faults may be reactivated (such as the Peel Boundary Fault zone and Feldbiss Fault zones) (Dirkzwager et al., 2000; Houtgast and Van Balen, 2000; Houtgast et al., 2005; Michon and Van Balen, 2005). As a consequence deeper reaching fault zones in the Roer Valley Graben may show dynamic permeability related to fault reactivation. The hydraulic properties of the deeper parts of the fault zones and their influence on groundwater flow are unknown.

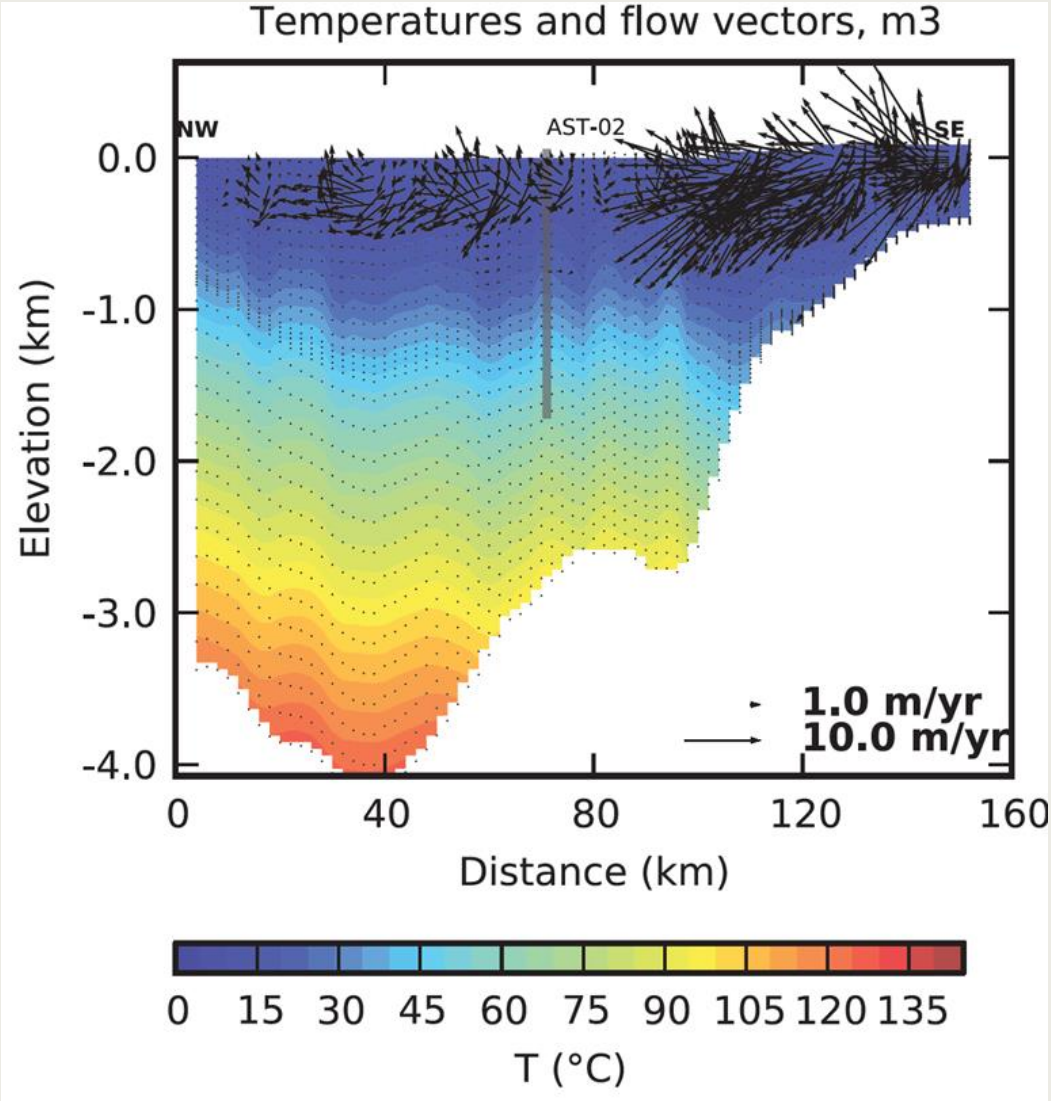

Figure 3-13. Simulation result showing groundwater flow vectors and temperature distribution along the 2D cross section through the Roer Valley Graben for present-day (best fit model scenario from Luijendijk, 2012). Location and lithostratigraphy of cross section is given in Figure 3-11 and Figure 3-12.

Groundwater salinization by upward flow of saline groundwater, including intruded seawater, takes place in the subsurface of the coastal zone of the Netherlands (Oude Essink, 1996, 2001; Post, 2003; Pauw et al., 2012). Modern seawater has intruded laterally about 2 to 6 km from the coastline (Stuyfzand, 1993). Recently, Pauw et al. (2012) performed groundwater flow modelling to quantify the extent of salt water intrusion and salinization due to future sea-level rise. The modelling takes into account density differences between fresh, brackish and saline groundwater. The authors include a no-flow bottom boundary condition at 300 m, indicating that expected active depths of influence of sea water intrusion will be less than 300 m. The seawater intrusion at present-day will probably not influence the Rupel Clay Member in the focus areas located in the northern coastal zone.

A third type of driving force influencing groundwater flow in the Dutch subsurface is sedimentary loading (Kooi, 2000; Kooi and De Vries, 1998; Verweij, 2003; Verweij et al., 2012). Sedimentary loading may induce groundwater flow, porosity reduction by compaction of the rock matrix and/or development of groundwater overpressures (pore pressures higher than hydrostatic pressures). The regional variation in present-day depth of the Rupel Clay Member (Figure 3-1) results from the regional variation in burial history of the Rupel, i.e. the regional variation in sedimentation and erosion since its deposition. TNO performed several basin modelling studies in the onshore Netherlands (for example the basin modelling study of the West Netherlands Basin and the Roer Valley Graben by Nelskamp and Verweij, 2012). These publicly available 3D burial history and compaction models include Cenozoic sedimentary sequences. These models show that compaction of the Dutch subsurface is ongoing from the surface downward to great depths, including the Cenozoic and older sedimentary sequences. These 3D basin models concern large geological time and spatial scales and do not provide specific and detailed information on the burial history, and history of compaction, pressure and groundwater flow at the scale of the Rupel Clay Member and lithostratigraphic members of its overburden. A more detailed 2D basin modelling study of pressure and groundwater flow along a SW-NE cross section offshore the province of North Holland (Verweij, 2003) provides information about the order of magnitude of vertical flow rates induced by sedimentary loading during the Quaternary. Simulated cross formational vertical flow rates are about 0.03 mm/year through the Cenozoic sequence and 0.04 - 0.13 mm/year through the Quaternary sediments.

Another indication of compaction-related flow rates can be deducted from surface subsidence studies. Modelling studies aiming to estimate surface subsidence in the onshore Netherlands due to sedimentary loading and natural compaction were executed using smaller time scales in comparison with the 3D basin modelling studies (Kooi et al., 1998; Kooi, 2000; Kooi and De Vries, 1998). For example, Kooi et al. (1998) simulated the rate of compaction of the Cenozoic sedimentary sequence in the Netherlands during Quaternary times. The simulated rate of compaction of the entire sedimentary sequence increases from southeast to northwest in the direction of increasing thickness of the Quaternary sedimentary sequence, and reaches maximum values of 0.04 mm/year (Figure 3-14). Simulated compaction of the Cenozoic sedimentary sequence in the Roer Valley Graben ranges from < 0.01 mm – 0.015 mm/year.

Chemical osmosis and electro osmosis concern the flow of water driven by a concentration gradient or an electrical potential gradient, respectively. In addition to water potential gradients, the influence of gradients in salt concentration and electrical potential on water flow can be significant in low permeable clayey sediments, such as the Rupel Clay Member. Osmosis has been studied extensively, including modelling approaches as well as in situ experimental studies of the Boom Clay at Mol in Belgium (e.g. Keijzer, 2000; Heister, 2005; Garavito, 2006, Garavito et al., 2007). Specific knowledge on chemical and electro osmosis across the Rupel Clay Member in the Netherlands at the focus depths of > 400 m is lacking.

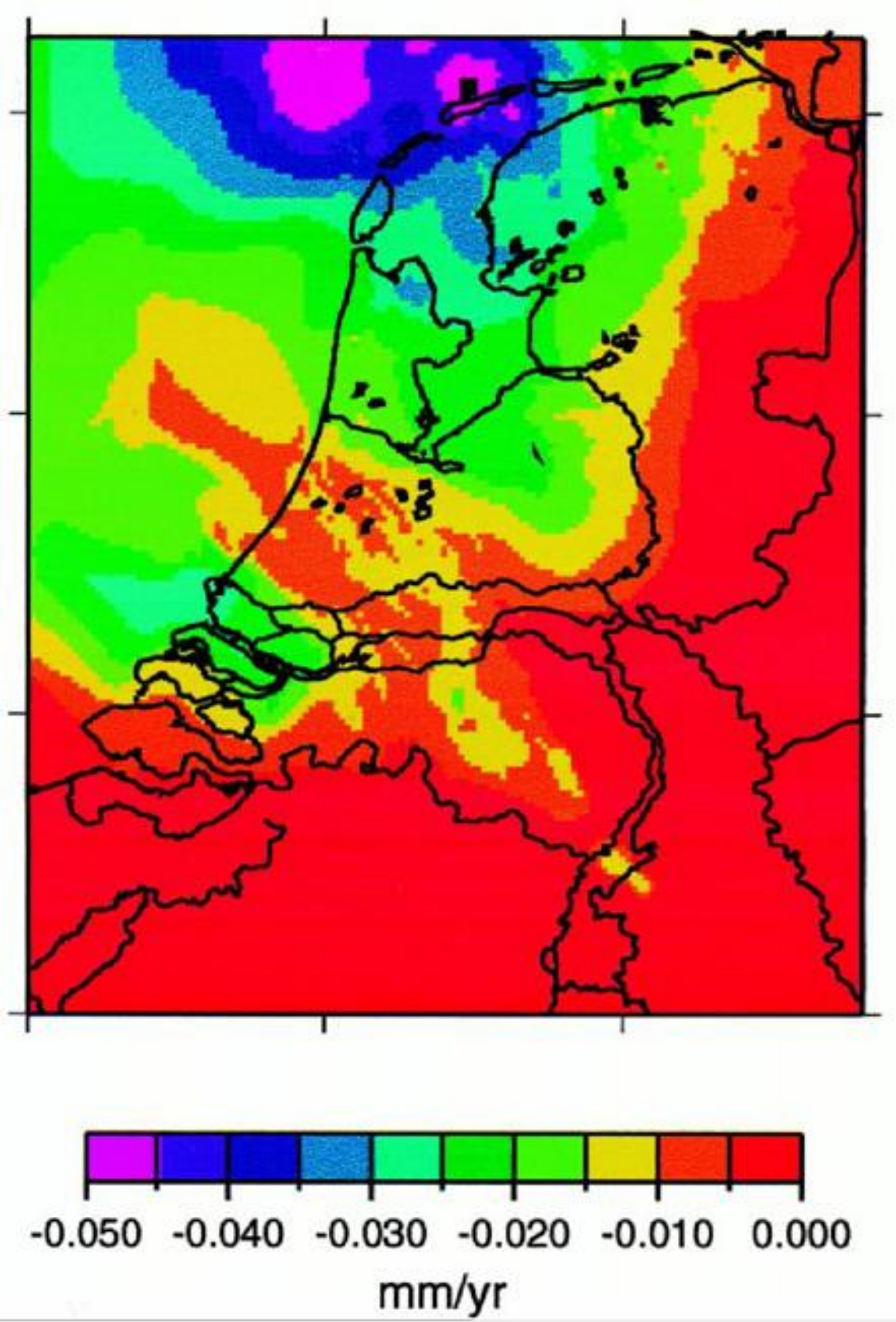

Figure 3-14. Simulated rate of compaction of Tertiary and Quaternary sediments during Quaternary (2.5 – 0 Ma) (from Kooi et al., 1998).

In general pressure tests are only executed in reservoirs/aquitards and not in low-permeable units, such as the Rupel Clay Member. There are no measured pressures of the Rupel Clay Member included in the in-house TNO pressure database. Mudweights measured during drilling of (oil and gas) boreholes can be used as a rough estimation of pore pressure conditions in the drilled geological units, including the low permeable ones. Inventory and interpretation of mudweights as a proxy for pore pressures is time-consuming and not included in this work (Section 1.4).

3.3.2. Hydrogeological setting

The subcrop and supercrop maps of the Rupel Clay Member (Figure 1-5 and Figure 1-6) and two representative cross sections (Figure 3-15 and Figure 3-16) illustrate its hydrogeological setting. The Rupel Clay Member overlies the sandy Vessem Member. This aquifer is characterized by a porosity of 30% and permeability of 321 mD (= 3.2E-13m^2; which corresponds to a hydraulic conductivity of 3.2 E^{-6} m/s) at approximately 500 m depth at MKP-02, located in the province of Zuid Holland. Wiers (2001) reports porosities of 29-35% and permeabilities of 218-941mD for the Vessem unit at depths around 1400 m in the Roer Valley Graben (at AST-GT-02, KB-198, HSW-01).

The supercrop map of the Rupel Clay Member (Figure 1-6) shows that in the southeast of the Netherlands the Rupel is conformably overlain by aquifers consisting of the sandy Steensel and Voort Members. Only limited data are available for the hydraulic properties of these sandy aquifers: core measurements of the Voort Member at three well locations (DON-01, MKP-02, OIW-01) show a variation in permeability between 116 and 429 mD (1.1E^{-13} – 4.2E^{-13} m^2) and in porosity between 27-31%. In the remaining part of the Netherlands the Rupel Clay Member is overlain by an aquitard (Veldhoven Clay Member) and the Breda Formation. The shallow marine sediments of the Breda Formation largely consist of clays, sandy clays and glauconitic sands. There is no detailed information available on the distribution and thickness of sandy intercalations in the Breda Formation. The occurrence of sandy sequences in the Breda Formation are probably largely restricted to the southeastern part of the country (for example the Kakert and Vrijherenberg Members). The Breda Formation constitutes the basal hydraulic unit (geohydrological basis) in large parts of the geohydrological model REGIS II. The Breda Formation is not parametrised in the REGIS II model, because of a lack of measured hydraulic data.

Two representative cross sections were compiled from the geohydrological model REGIS II, the Digital Geological Model and the geological model (Section 2.5.1) (Figure 3-15 and Figure 3-16).

The N-S cross section shows that the Rupel Formation in the northern parts of the Netherlands is overlain by the Breda Formation, which is clay dominated in the north and behaves overall as an aquitard in this region. To the south, in the central parts of the Netherlands (Zuider Zee Low) Neogene deposits of mixed lithology overly the Rupel Clay Member. These are classified as complex hydrogeological units. On top of the Breda aquitard, the hydrostratigraphy is composed of an alternation of complex hydrogeological units, aquifers and aquitards. Detailed information of the subdivision in hydrostratigraphic units and the hydraulic properties overlying the Breda Formation can be obtained from the REGIS II geohydrological model. Information on the hydrostratigraphic build-up of the Breda Formation is missing.

The NW-SE cross section through the Roer Valley Graben (Figure 3-16) shows a detailed subdivision in aquifers and aquitards for the upper ca. 400 m of the cross section. There is no information available from systematic hydrogeological mapping at greater depth. More detailed information concerning hydrostratigraphy of the deeper parts is available from Msc and PhD studies (De Rooij, 2000; Wiers, 2001; Luijendijk, 2012). A schematisation of the Roer Valley Graben is given by De Rooij (2000) (Figure 3-17). The Rupel Clay Member is directly overlain by aquifers (Steensel and Voort members of the Rupel Formation) followed by the low permeable Veldhoven Clay and the moderately low

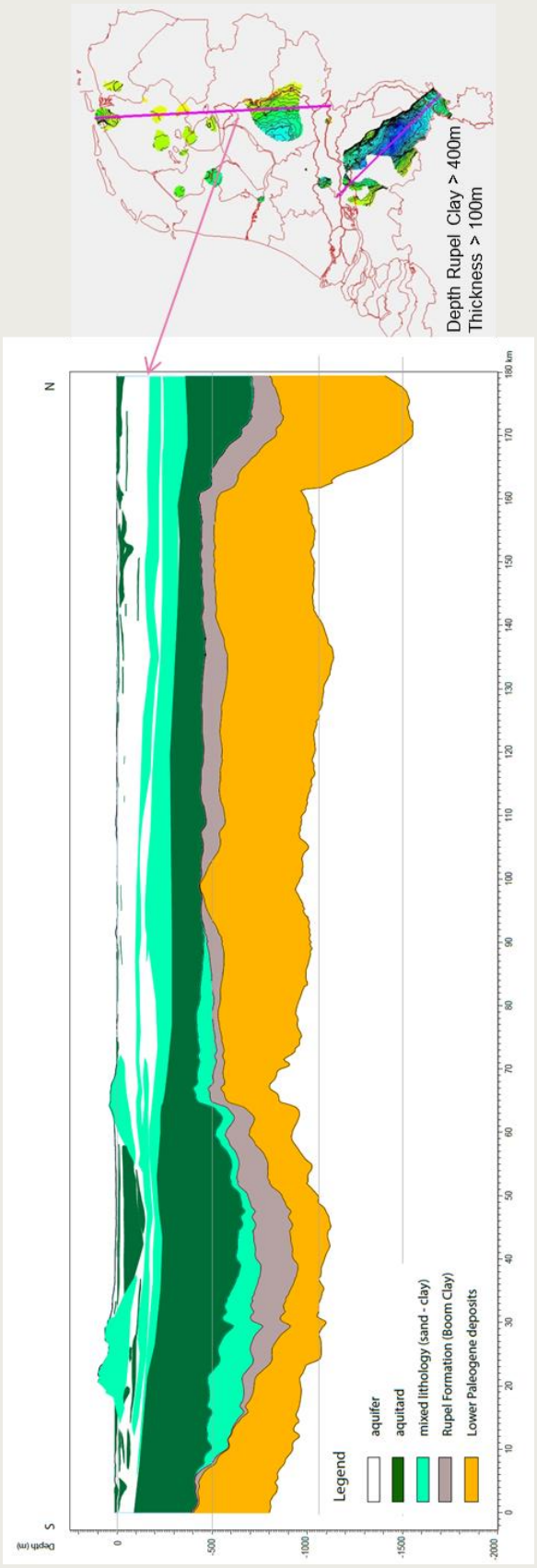

Figure 3-15. N-S cross section showing the regional hydrogeological setting of the Rupel Formation in the central and northern part of the Netherlands.

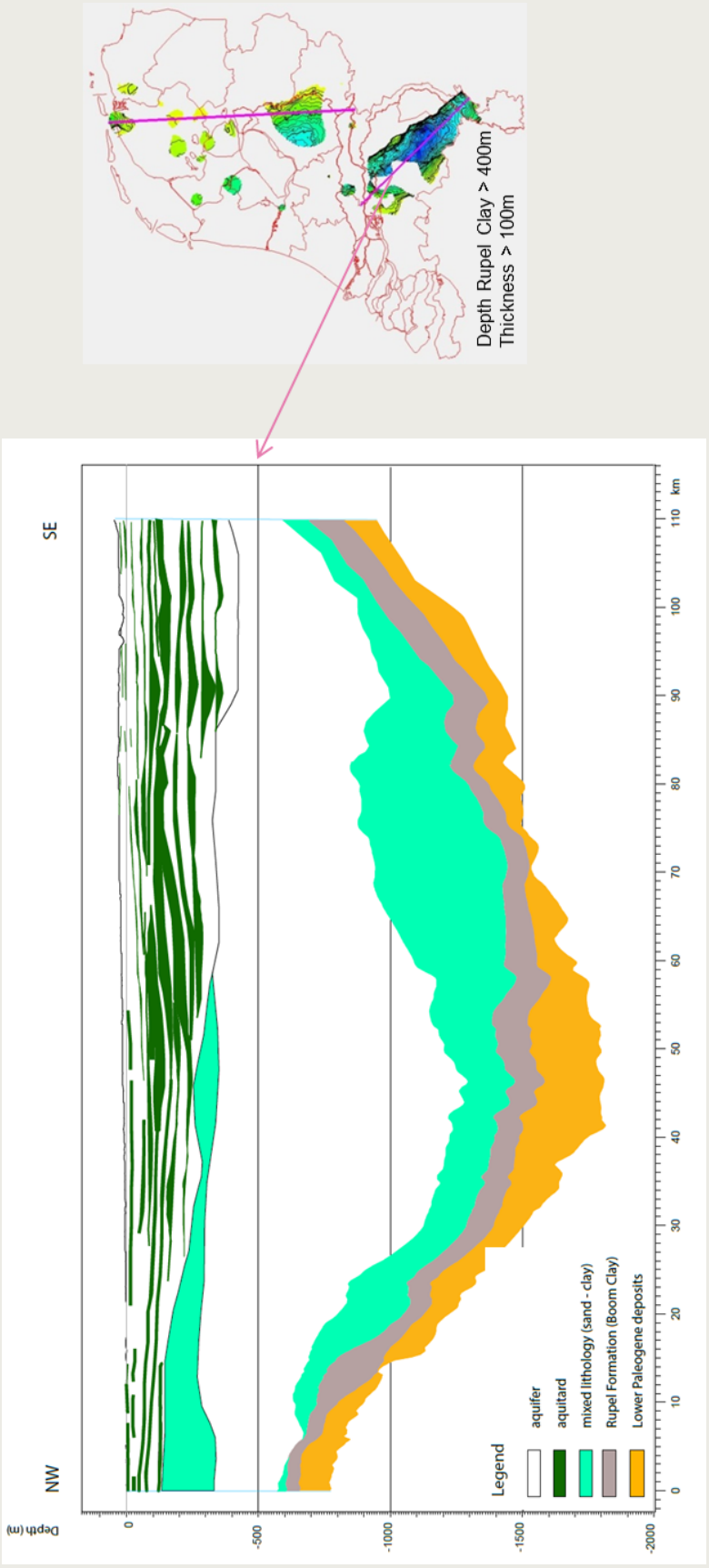

Figure 3-16. NW-SE cross section showing the hydrogeological setting of the Rupel Formation in the Roer Valley Graben.

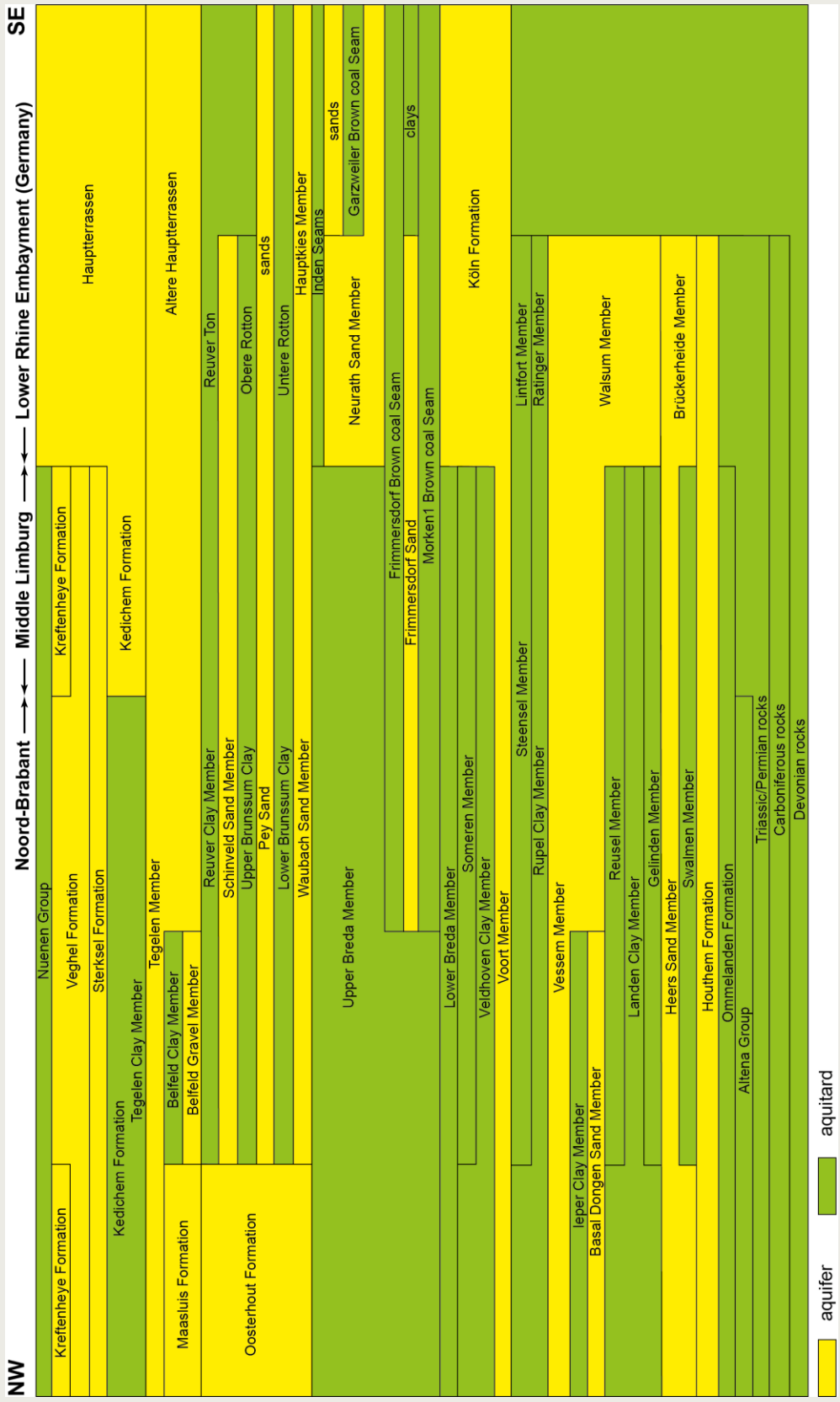

Figure 3-17. Schematic NW-SE cross section through the Roer Valley Graben illustrating the 3D hydrostratigraphic model of the graben used by De Rooij (2000).

permeable Breda Formation, that in part is intercalated with sandy sequences. The NW-SE cross section runs parallel to the direction of the fault systems in the Roer Valley Graben. These fault systems disrupt to a greater or lesser extent the lateral hydraulic continuity of aquifers and aquitards in the graben in the direction perpendicular to the faults.

In general the hydrostratigraphic build-up of the bottom parts of the overburden of the Rupel Clay Member in the southern and southeastern part of the Netherlands is more permeable in comparison with that in the north.

3.4. Geohydrological characterization of the Rupel Clay Member

Measured porosity and permeability (hydraulic conductivity) data of the Rupel Clay Member in the subsurface of the onshore Netherlands are limited and these data are restricted to shallow depths in the order of tens of meters below surface. Some measured data are available for the southwestern part of the Netherlands. For example, the Rupel Clay Member at depths of 21-26 m in three boreholes (B54E0865, B55A0839, B28F1326) has a measured porosity of ca. 43% and a hydraulic conductivity of 1.13-2.11E^{-6} m/d (1.31-2.44E^{-11} m/s). Current porosity and permeability are closely linked to lithological composition and in addition to burial depth and burial history. The difference in burial history of the Rupel Clay Member in the southwest of the Netherlands (influenced by previous uplift and erosion) in comparison to that in the rest of the country, and the widely varying burial depth of the top of the Rupel Clay Member in the onshore Netherlands (Figure 3-1), does not allow the direct use of these measured properties at shallow depth for other regions.

The calculation methods of the porosity and permeability of the Rupel Clay Member on the new samples (Section 2.5.3) take both lithological composition and burial depth into account. The results of the calculations are given in Tables 1 and 2 in Appendix 4.

The lithological composition of the new samples of the Rupel Clay Member shows a spatial variation related to the depositional environment of the sediments (Section 3.2.1). Samples of the boreholes in the north (in the deeper-water part of the palaeo-basin) show the least vertical variation and have the finest grain size. These samples belong to the textural group of muds. Samples of the boreholes in the southern and southeastern part of the Netherlands (along the palaeo-coastline) are vertically more heterogeneous and contain the coarsest grain size within the Rupel Clay Member (Section 3.2.1). The Rupel Clay Member found in these boreholes includes muds, sandy muds, muddy sands, and even sands.

Tables 1 and 2 (Appendix 4) show that the vertical permeability of the 'mud' part of the Rupel Clay Member at depths of > 400 m is in the 10-19 m^2 range (vertical hydraulic conductivity of 10-12 m/s) (Figure 3-18).

The spatial variation in lithological composition induces spatial variation in hydraulic properties (Appendix 4, Table 1). The samples of the boreholes in the northern Netherlands (LWO-02, GRD-01, EMO-01; seven out of eight samples of ESG-01) are all muds and show the least vertical variation in permeability. For example, the vertical permeability of the Rupel Clay Member in RGD-01 varies between 1.3 E^{-19} – 4.5 E^{-19} m^2 over a depth interval of 448-569 m TVDss. In both the east-southeastern and the southwest-southern areas the 'mud' part of the Rupel Clay Member is overlain and/or underlain by coarser grained sediments: the vertical variation in permeability over the Rupel Clay Member reflects this heterogeneity. For example, the vertical permeability of the Rupel Clay Member in B52E0114 (E-SE area) varies between 4.6E^{-14} and 3.3E^{-19} m^2 over a depth interval of 381-524 m TVDss, and that in B50H0373 (S area) varies between 6.0E^{-17} and 4.1E^{-19} m^2 over a depth interval of 325-470 m TVDss.

Spatial variation in the calculated permeability of the Rupel Clay Member also results from differences in its burial depth (Figure 3-1). The calculated permeabilities for the samples in the southwest and southern area also clearly show this influence. The calculated vertical permeability decreases for mud samples from 2.3E^{-17} m^2 at a very shallow depth of 21 m (B48G0159), 5.0E-18 m^2 (B49G0191; 82 m), 3.5E^{-18} m^2 (B49G0959;129 m), to 4.2E^{-19} m^2 at 442 m (B50H0373). None of the boreholes analysed for grain size and

permeability calculations penetrate the focus area in the Roer Valley Graben where the Rupel Clay Member is thicker than 100 m and its top is located at depths greater than 400 m. Deep burial of the Rupel Clay Member in the graben is expected to result in both low porosity and permeability of the mud part of the member.

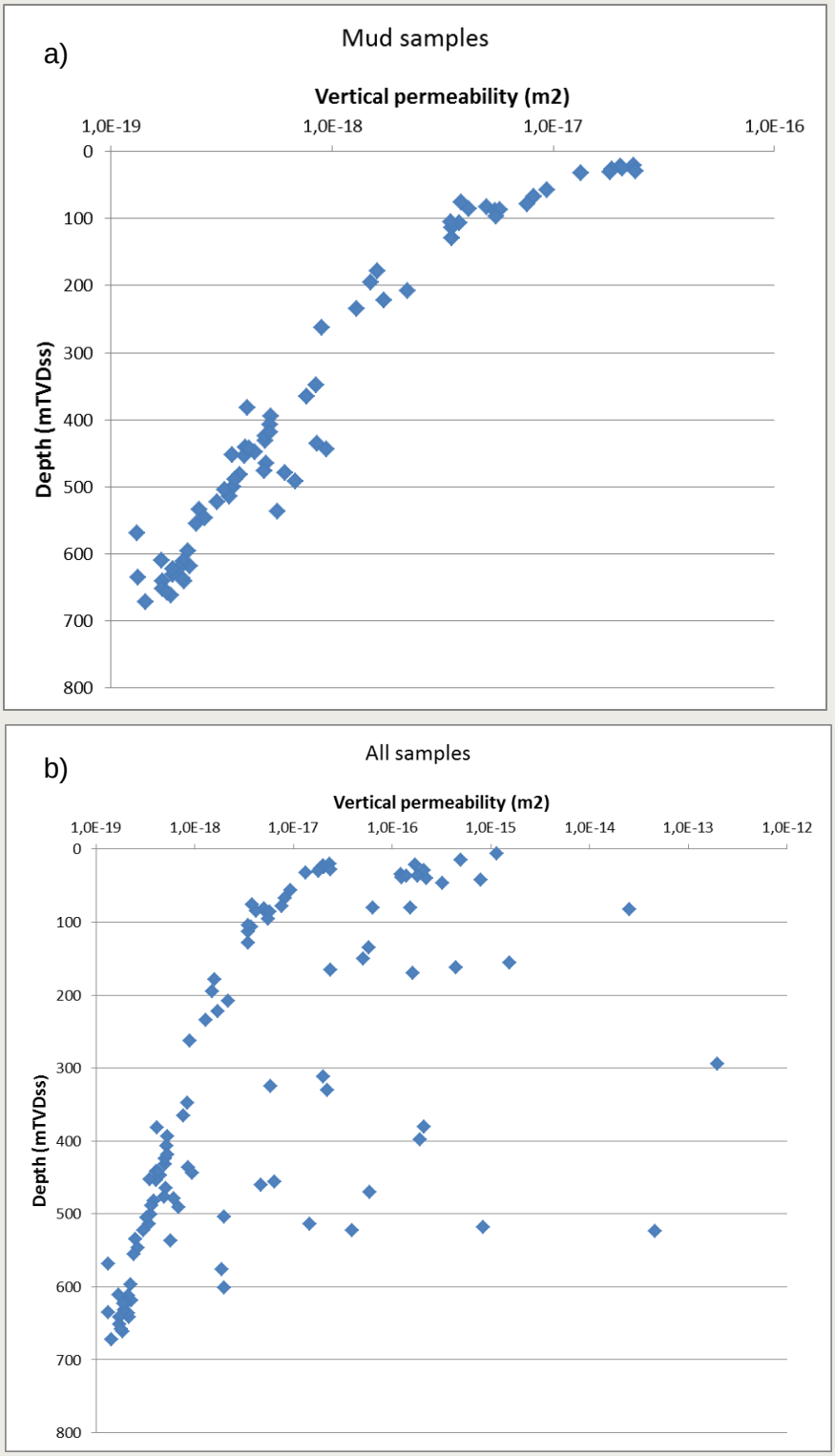

Figure 3-18. Cross plot of a) calculated vertical permeability versus depth for mud samples and b) for all samples of the Rupel Clay Member (calculations based on clay% < 2µm given Table 1 in Appendix 2).

4. Discussion

As part of the Safety Case a collection of arguments supporting or rejecting long-term safety of a repository for low-, medium- and high-level radioactive waste needs to be collected. The geological and geohydrological characterization of the Boom Clay and its overburden primarily contribute to the safety functions 'isolation' and 'delay and attenuation of the releases' (Smith et al., 2009).

Long-term safety of a radioactive repository in a geologic formation is basically determined by the depth, thickness and permeability/hydraulic conductivity of the host-rock. With respect to the latter, the host-rock preferably is a homogeneous fine-grained sediment with a high clay content. Further, the host-rock should be thick enough to perform the required task of isolation, and it should be buried deep enough to be out of reach of future geologic developments such as glaciations, groundwater flow etc.. The integrity of the host-rock should be high, which means that no or limited disturbances or discontinuities are present to prevent groundwater flow through the host-rock.

For this study we have chosen the host-rock to have a minimum burial depth of the top of the Rupel Clay Member of -400 m m.s.l. and a minimum thickness of 100 m. These values are partly somewhat arbitrary and partly based on geological knowledge. The minimum burial depth is based on the fact that glacier advances during future ice ages may scour up to several hundreds of metres in depth. For the disposal concept to be investigated a repository depth of 500 meter and a thickness of the Rupel Clay Member of 100 meter was assumed (Verhoef et al., 2011).

4.1. Stratigraphic interpretation

Stratigraphic interpretation is the basis of geologic mapping. Of the stratigraphic interpretations of the Rupel Formation in the ~5000 onshore Mining Law-related wells, about 20% have been properly quality controlled during the 1980's. Since then about 20% has been quality controlled for mapping purposes. The remainder of the onshore wells has stratigraphic interpretations which were taken from the composite well logs as supplied by the owners of the wells.

Since the 1980's new litho- and chronostratigraphic insights have been developed. Further, it is clear that the Dutch stratigraphic nomenclature does not always match well with the nomenclature in Belgium and Germany for the investigated time-interval. The lack of recent stratigraphic (re-)interpretation of the Rupel Formation and the mismatch with neighbouring countries limits the reliability of the presented results in this study. Future studies should pay special attention to these topics in order to improve the quality of produced maps.

4.2. Geometry, distribution and lithology of focus areas

Two main areas meeting the depth-thickness criteria can be identified: the Roer Valley Graben in Noord-Brabant and Limburg (Figure 4-1) and the eastern part of the Zuiderzee Low (Figure 4-2), underneath the Veluwe area. Some smaller zones meeting the criteria can also be identified in the north of the country (Figure 4-3). The smaller zones in the north measure 5-25 km in width, and are therefore still interesting for a disposal facility. Currently no minimum area requirement for zones thicker than 100 m exist. Despite the fact that these small spots may partly be artifacts resulting from the interpolation, we will consider them here. We do that since at least the spot penetrated by well GRD-01 is proven to be about 125 m thick assuming a correct stratigraphic interpretation.

4.2.1. Roer Valley Graben

This focus area consists of several sub areas (Figure 4-1). The top of the Rupel Clay Member is located between -400 and -1500 m m.s.l. in this focus area. In the graben the Rupel Clay Member is penetrated by 18 wells. Of these wells, 15 wells have

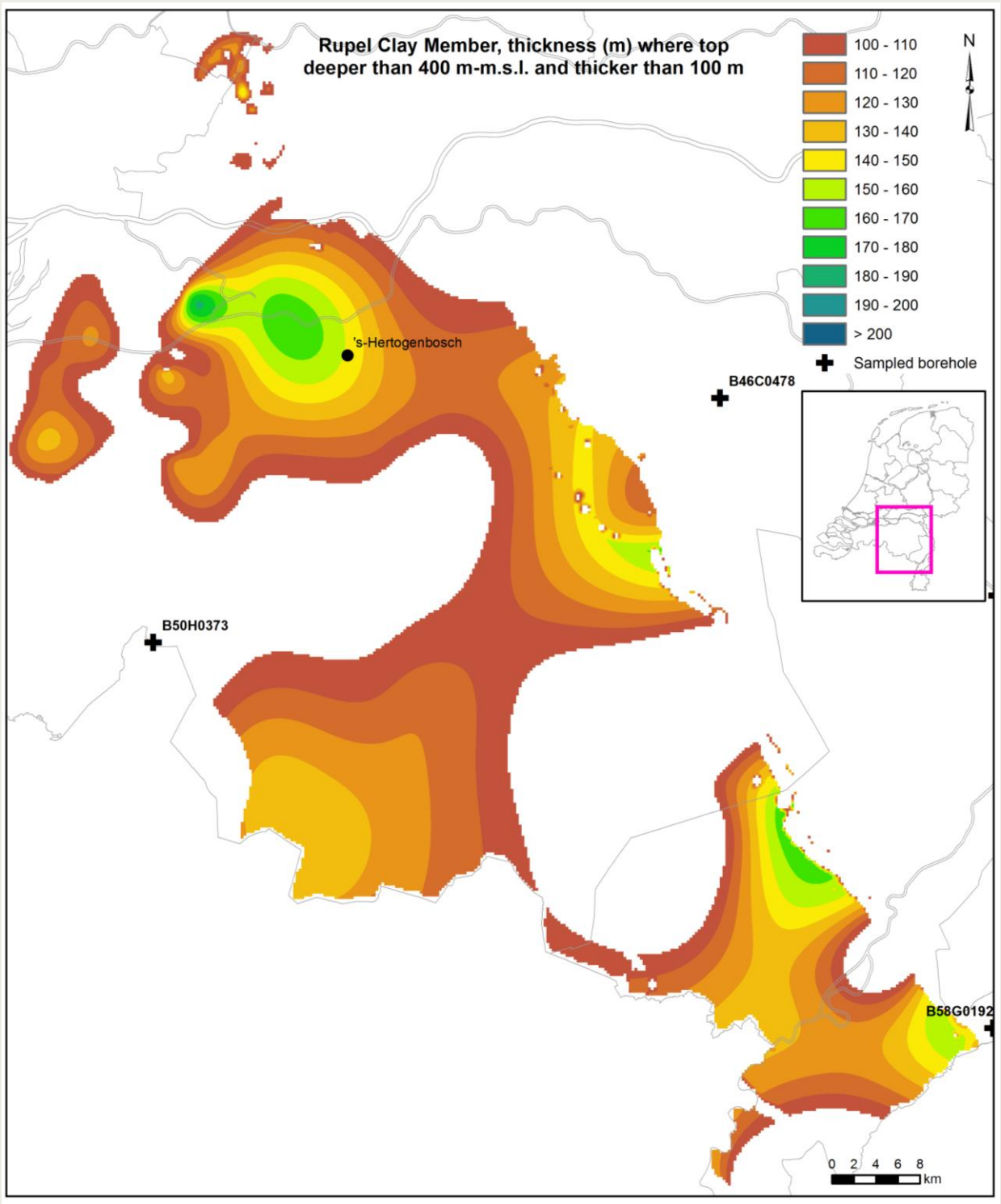

Figure 4-1. Thickness of the Rupel Clay Member in the Roer Valley Graben focus area, where the top of the Rupel Clay Member lies deeper than 400 m and the thickness is more than 100 m.

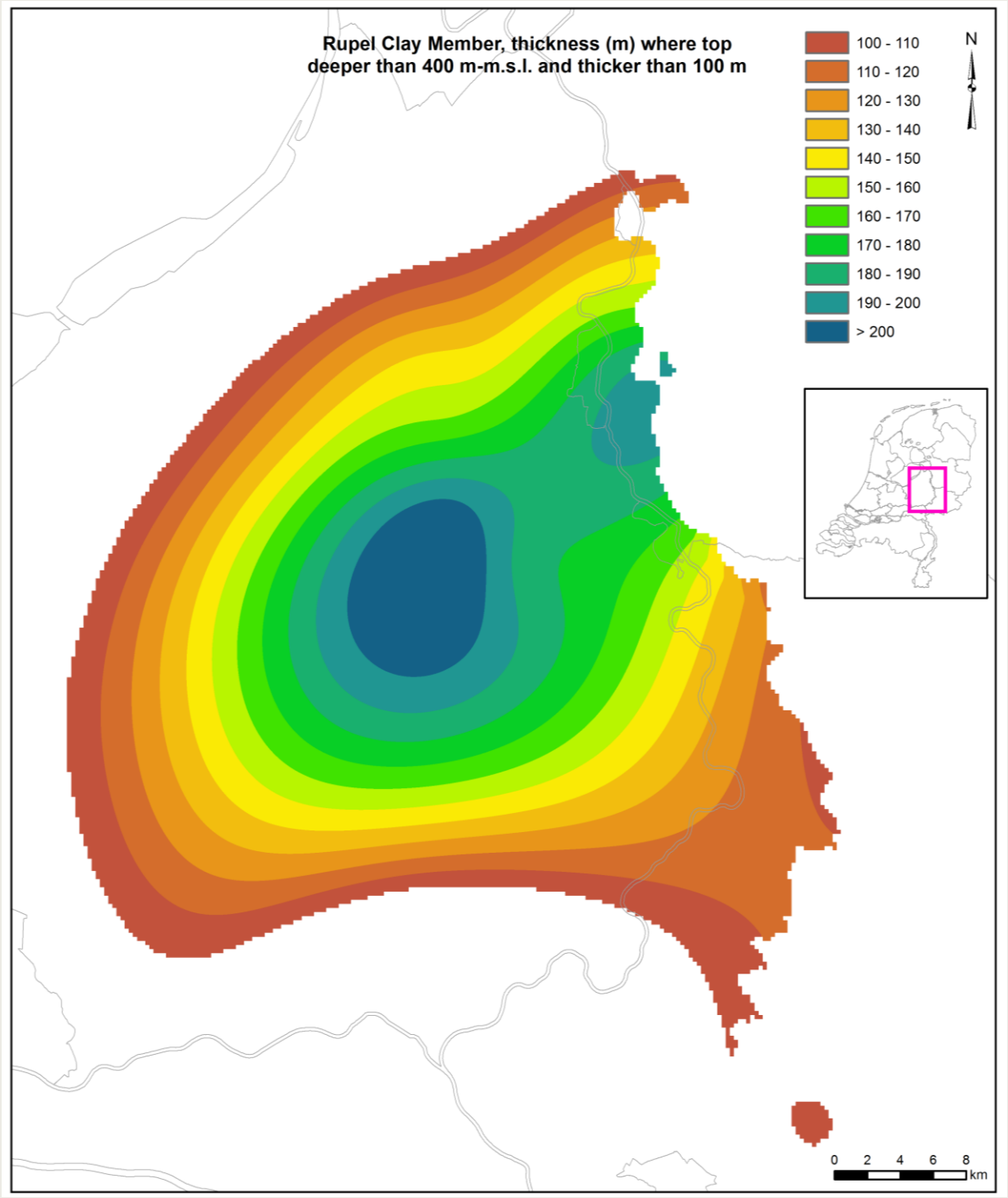

Figure 4-2. Thickness of the Rupel Clay Member in the Zuiderzee Low focus area, where the top of the Rupel Clay Member lies deeper than 400 m and the thickness is more than 100 m.

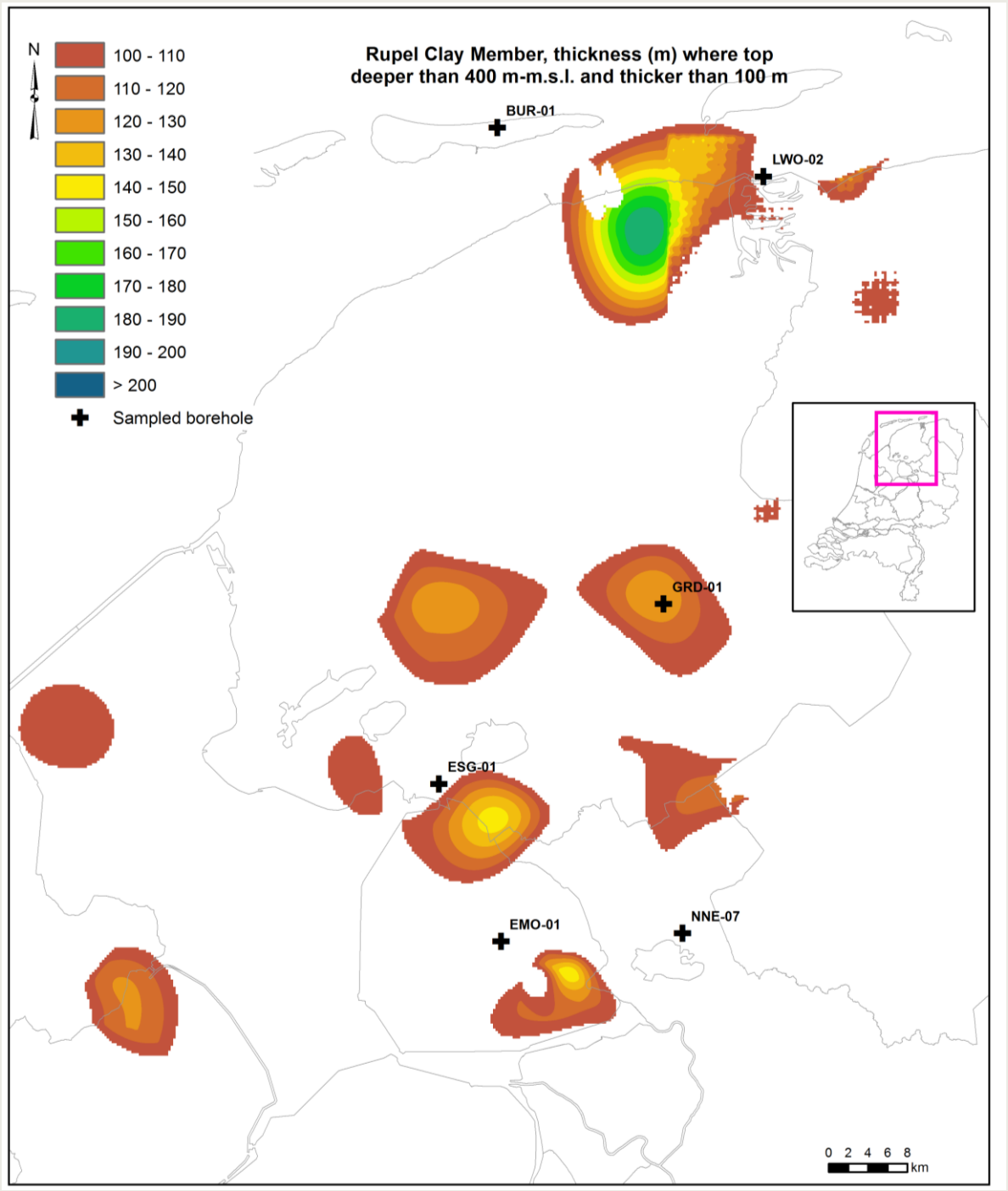

Figure 4-3. Thickness of the Rupel Clay Member in the North Netherlands focus area, where the top of the Rupel Clay Member lies deeper than 400 m and the thickness is more than 100 m.

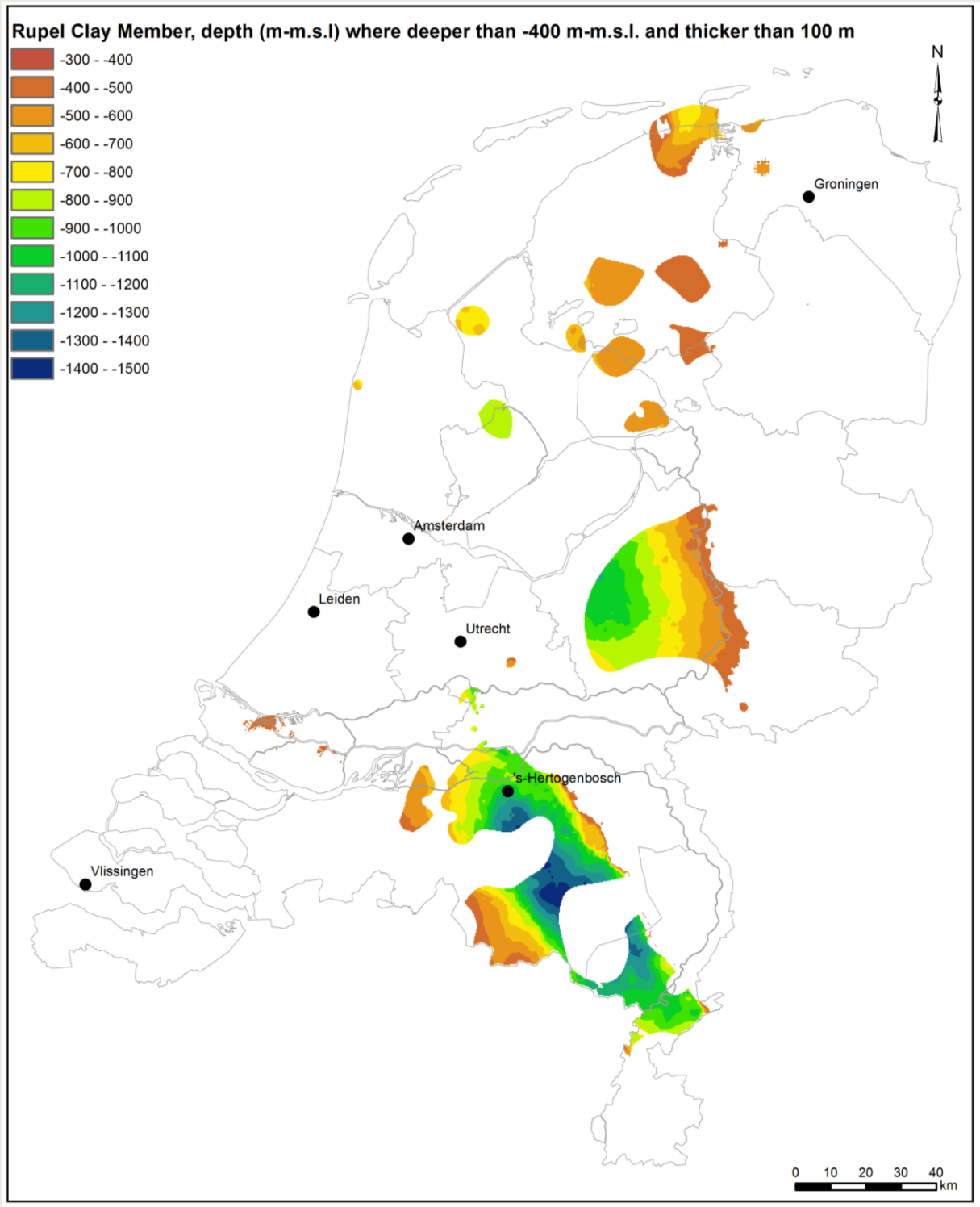

Figure 4-4. Depth of the Rupel Clay Member, where the top lies deeper than 400 m and the member is thicker than 100 m.

encountered a thickness of at least 100 m. The limited number of wells is a positive aspect for the clay layer in the Roer Valley Graben, since that implies a relatively limited number of possible vertical conduits for fluid flow along (future) degrading boreholes. Nearby well AST-GT-02 has been drilled by TNO in 1986 for research purposes and may be used for future studies of the characteristics of the clay layer, depending on sample quality.

None of the boreholes sampled for grain size is located in this focus area. Based on nearby wells and the palaeogeography (Figure 1-3a) we expect the most fine-grained low energy facies to be found towards the northwest, while coarser-grained coastal sand facies are expected near the borders with Germany and Belgium, as corroborated by well B58G0192 (Figure 3-8).

The Rupel Clay Member in this focus area is cut by several larger faults (Figure 4-5). The faults have created offsets of the clay layer in the order of tens to hundreds of metres, creating compartmentalization and fragmentation. It must be noted that the focus area thickness map does not show this compartmentalization (Figure 4-1). Besides the mapped faults, more faults may be present which either have not been identified due to the limited 2D seismic data availability or which are below the seismic resolution.

The permeability of—especially the deeper parts—of the faults in the Roer Valley Graben is unclear. However, some indication may be obtained from a recent study based on radar inferometry. Based on that study vertical surface movements have been observed resulting from groundwater flow and not fault movement (Caro Cuenca, 2012). The surface movements of several millimetres per year occur in fault-bounded compartments which move independently. This implies limited or absent lateral fault permeability. If vertical fault-block movement occurs, it is Vertical flow may still be present in these cases. These results are based on shallow aquifers (up to 200 m depth). Whether the results are valid for deeper layers with different conditions is unknown.

4.2.2. Zuiderzee Low

In this focus area the top of the Rupel Clay Member is located between -400 and -1200 m m.s.l. (Figure 4-2). Four wells have penetrated the clay member in this area, which is a similarly positive aspect as in the Roer Valley Graben.

Boreholes sampled for grain size are not located in this focus area. Based on our conceptual lithofacies model, there is a possibility of the presence of coarser silty or fine-sandy intervals in the north of the area. This would be sourced from the topographic high that may have been present north of this area. Due to lack of data it is unclear whether the structural high that is present south of the focus area, could have generated a similar coarser-grained sediment input. The middle part of the focus area is expected to be most fine-grained.

Several faults have been mapped in the Zuiderzee Low, however they have not been mapped in Cenozoic sediments (Figure 4-5). The mapping campaign only used 2D seismic data because 3D seimic data was not available. Presently still no 3D seismic data cover this area, making a more detailed analyses using 3D seismic data impossible. The Rupel Clay Member is nonetheless expected to be crossed by several faults. Because the Zuiderzee Low is more a depression than a graben, the fault offsets are probably less than in the Roer Valley Graben. At this stage we cannot make any predictions on the density, scale and permeability of the faults in this area.

4.2.3. North Netherlands

The top of the Rupel Clay Member in this region lies between -400 and -850 m m.s.l. Near the island of Ameland a salt dome has lifted the Rupel Clay Member up to depths around -250 m m.s.l. (Figure 4-3). The clay member in this region has been penetrated by only six wells. Although this is positive for the integrity of the clay layer, it obviously also limits reliability and hampers analyses of its properties.

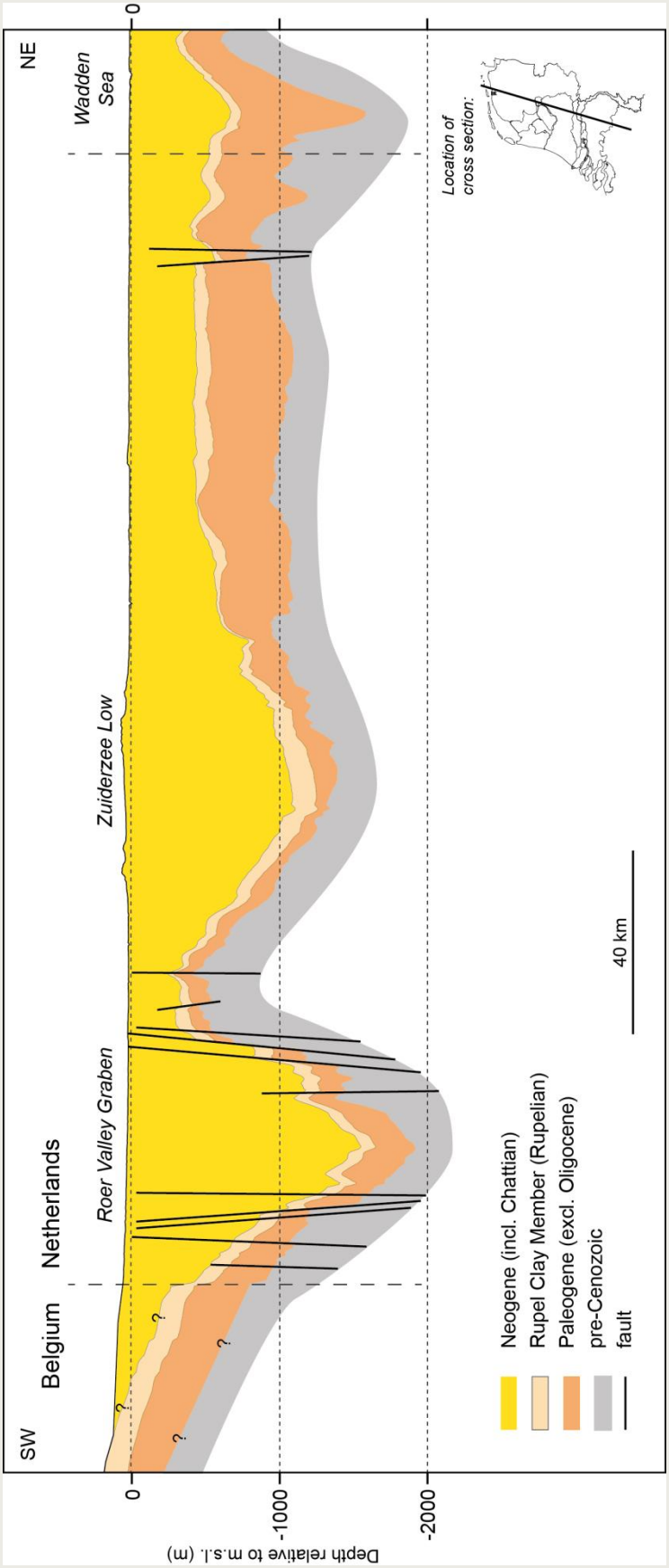

Figure 4-5. Cross-section through the 3D layer model which forms the basis of the presented grids. The cross-section clearly shows the variable depth of the Rupel Clay Member through the Netherlands. The absence of faults in the Zuiderzee Low area reflects the lack of data there.

Wells GRD-01 penetrates one of the blobs and has been sampled for grain-size analyses. The median (D50) grain size lies around 8-10 µm. The relatively fine grain size corresponds with the proposed deeper water facies north of the Texel-IJsselmeer High (Figure 3-7) and with the palaeogeographic setting of a deeper marine basin (Figure 1-3).

Faults have been mapped in the north of the country, but they have not been mapped to cross the Rupel Clay Member (Figure 4-5). The mapping campaign only used 2D seismic data because 3D seimic data was not available. The Rupel Clay Member is nonetheless expected to be crossed by several faults. Presently the area is covered by 3D seismic data and a new mapping campaign is underway at TNO and due to be finished late 2014. These new data will allow a more accurate and detailed analyses of the depth of the Rupel Clay Member and the presence of faults.

4.2.4. Remaining onshore Netherlands

In the remainder of the country the thickness of the Rupel Clay Member is more than 100 m in an area east of the Zuiderzee Low focus area and in the south of the West Netherlands Basin (in the south of Zuid Holland; Figure 4-6). However, the Rupel Clay Member is located deeper than 400 m only in limited locations (Figure 4-4).

Due to uplift after deposition (inversion) in the West Netherlands Basin, the Rupel Clay Member was partially eroded. This is clearly illustrated by an offshore cross section (Figure 3-6). In the North Sea the thickness of the Rupel Formation decreases towards the centre of the cross section. In the south it has locally been completely eroded.

If potential repository locations are to be considered outside the focus areas, special attention should be given to the post-depositional erosion in the West Netherlands Basin area. It should also be kept in mind that the thickest occurrences of the Rupel Clay Member not always coincide with a burial depth below 400 m. On the other hand, the base of the member is buried deeper than -1000 m m.s.l. in the Roer Valley Graben and Zuiderzee Low, possibly creating practical and technical limitations for the construction of a repository.

4.3.Integrity

The main geological and sedimentological features affecting the integrity of the Rupel Clay Member will be discussed here. Integrity is defined here as the amount of natural or man-made disturbances of the deposit, which may increase or reduce fluid flow and thereby affect the efficiency of the geological barrier.

4.3.1. Faults and seismicity

As indicated above, faults cross-cut the Rupel Clay Member. Offsets caused by faults may reach up several hundreds of meters in the most faulted regions (Roer Valley Graben). These offsets may juxtapose both permeable and impermeable layers against the Rupel Clay Member. The fault planes themselves can be conduits for fluid flow along the planes. They can also be barriers for flow through them. Fault characteristics such as location, offset, activity and permeability are crucial parameters for the OPERA Safety Case. A limited amount of data limits possibilities to list all these characteristics for the onshore faults.

Natural seismicity is common in the southeast of the the Netherlands in the Roer Valley Graben, where natural (tectonic) earthquakes occur regularly along the existing natural faults. The largest earthquake ever recorded in the Netherlands (magnitude 5.8 on the Richter Scale) occurred in 1992 along the Peel Boundary Fault close to Roermond, which is the main northern bounding fault of the graben. Smaller-scale (induced) earthquakes are known from the northeast of the Netherlands, where large-scale gas extractions cause induced seismicity. The largest induced earthquake occurred in 2012 near Huizinge (Groningen) and measured 3.6 on the Richter Scale.

Up to 2012, a maximum magnitude for induced seismicity was defined at a level of 3.9. Since the Huizinge event, however, this maximum magnitude is under discussion. In general, the magnitude of an induced event depends on the scale of the changes in the subsurface. For natural (tectonic) seismic events, the magnitude depends on the stresses existing on the faults. Induced events and tectonic events could both be damaging to structures in the afflicted area. Summarizing, it is advisable to take the chance of both natural and induced seismic events into consideration when planning a disposal site.

4.3.2. Salt domes

Salt domes are present mainly in the provinces of Groningen and Drenthe, where the thickness of the Rupel Clay Member is generally thinner than 100 m (Figure 3-5). One salt dome is present in the North Netherlands focus area, in the blob near Ameland. Due to the upward movement of salt in salt domes, the overlying rocks and sediments are lifted up which is accompanied by small-scale faulting or salt tectonics. These faults may alter the integrity of the Rupel Clay Member, as described above. It is therefore advisable not to locate a repository in a host-rock in an area near active salt-dome formation, i.e. not in the provinces of Groningen, Drenthe and the northeast of Friesland. The Zuiderzee Low and the Roer Valley Graben are known to have thin Zechstein salt layers (<300 m), which are not susceptible to salt-dome formation. Future geologic developments will be studied in OPERA Task 4.1.2, and will shed more light on the (im-)possibilities of disposal in host-rock near locations with thick salt layers and salt domes in the subsurface.

4.3.3. Calcareous septaria

Calcareous septaria are hard concretions with fractures in them, occurring in the Rupel Clay Member. They are more brittle than the surrounding clay and occur concentrated in layers. From outcrops in Belgium, groundwater has been observed to flow preferentially along these layers. They may therefore form groundwater conduits and require special attention with respect to integrity.

From Belgian outcrops they are known to have elongate flattened spheroidal shapes with long axes parallel to bedding planes (Figure 4-7). They generally measure 0.3-1 m in width and 0.1-0.2 m in thickness (De Craen et al., 1999). The following section on the characteristics of the calcium carbonate septaria is taken from De Craen et al. (1999):

> “Boom Clay carbonate concretions consist of authigenic micritic to microsparitic calcite and minor amounts of framboidal pyrite. The diagenetic carbonate cements fill porosity between detrital clay minerals and silt-size quartz. There are also minor amounts of muscovite, glauconite, feldspar, collophane, and iron oxide (most likely oxidized pyrite). Ostracods, gastropods, foraminifera, coccoliths, and bivalves, usually in life position, contribute to the concretion matrix. Burrow pipes and fossil traces (< 2 mm in diameter) are common, as are fecal pellets. Large and hard shell parts are commonly disrupted and broken by later septarian fracturing, with sparry calcite infilling the fracture porosity. Breakage of burrows and hard pyrite concentrations by septarian fractures is also observed.”

The actual formation of the concretions (lithification) started very early in diagenesis close to the sediment-water interface and before significant compaction occurred (De Craen et al., 1999). The mineral composition of the calcite and pyrite in the concretions indicates that formation of the concretions was dominated by bacterial sulphate reduction (De Craen et al., 1999).

In Belgium the presence of calcareous-rich layers seems unrelated to Milankovitch cycles, grain size and organic matter (De Craen et al. 1999). According to Laenen (1997 in De Craen 1999) glacio-eustatic sea-level movements may explain their distribution. The calcareous-rich layers are usually present at the bases of major water-deepening events after sea-level lowstands. In Belgium, the cyclic occurrence of calcareous septaria is linked to intervals with a higher content of sedimentary carbonate (De Craen et al. 1999). They

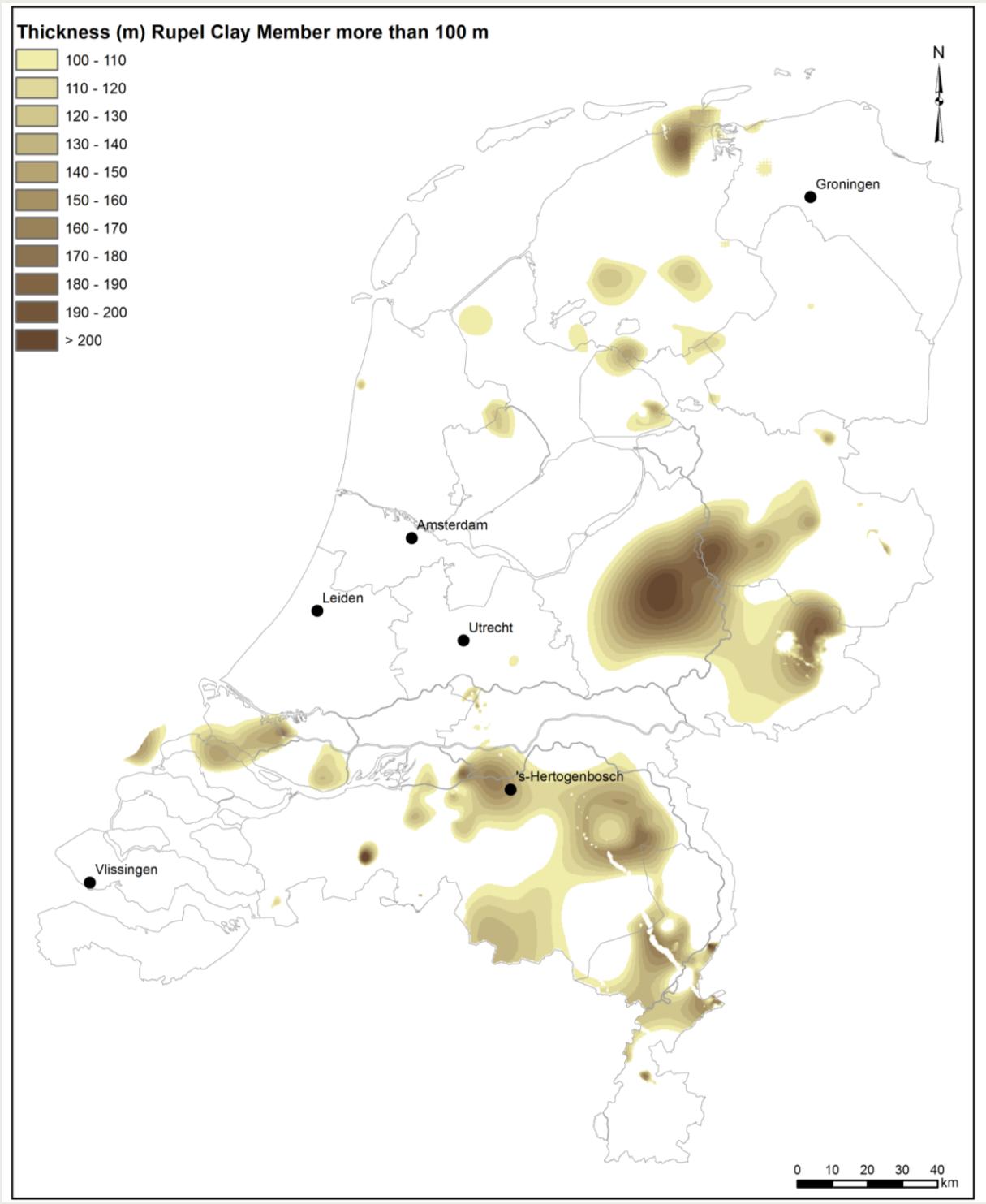

Figure 4-6. Thickness of the Rupel Clay Member, where thicker than 100 m.

Figure 4-7. A calcareous concretion in a Belgian quarry, width is about 60 cm.

can be correlated over long distances across different facies using resistivity and density logs (Leroi 1995 in De Craen 1999). The glacio-eustatic sea-level control on the deposition of calcareous-rich layers is considered to control the occurrence of calcareous septaria as well (De Craen et al 1999). Nearly all calcareous septaria layers appear to result from deposition of carbonate planktonic blooms that occurred during flooding events at the ends of glacial periods (Vandenberghe and Laga 1986).

More than 18 horizons characterized by the presence of septarian carbonate concretions have been identified in Belgium (Gaemers 1993). In the Winterswijk area a study of the Brinkheurne Formation, which is equivalent to the Rupel Clay Member, shows the presence of calcareous septaria in the Netherlands. Ten distinct layers were identified there, which are independent of reported carbonate-free and carbonate-rich levels. If in a borehole no septaria were found, usually a carbonate band or carbonate-rich clay layer was identified. As in Belgium, the septaria have formed soon after sediment deposition and occur over greater distances, making them well-suited for correlations (Van den Bosch and Hager, 1984). Where erosion has taken place, the remaining gravel lag contains many reworked septaria in the Winterswijk area (Van den Bosch et al., 1975).

For a large part of the Dutch subsurface, we are unaware of the presence of carbonate septaria. Sea-level movements have occurred basin wide, and the presence of the calcareous septaria layers as reported in Belgium is expected in the subsurface of the Netherlands as well. The Rupel Clay Member in the Dutch subsurface may reach thicknesses up to twice as much as in Belgium, and the total number of global glacio-eustatic sea-level movements is the same as in Belgium. However, it is unclear which of these movements is registered in both countries. The marine basin was deeper in the Netherlands and therefore the deposits there may contain additional eustatic sea-level cycles. On the other hand the top of the Rupel Clay Member has been eroded in places, which implies that some cycles in the top of the sequence are missing. It is therefore not possible to simply use the number of global eustatic cycles to predict the number of septaria layers in the vertical succession in the Netherlands.

4.3.4. Sedimentation and bioturbation

Some degree of lamination is expected to be present in the Rupel Clay Member sediments. In marine environments laminae are often destroyed by bioturbation. Mixing of more permeable silt and sand-rich layers with less permeable clay-rich layers may result in an overall permeability reduction of the deposit. No quantitative data on bioturbation frequency, or on variations in sedimentation rate, have been published for the Rupel Clay Member so far (De Craen et al 1999).

4.3.5. Boreholes

Boreholes penetrating the Rupel Clay Member may cause vertical connectivity within the member and with overlying and underlying deposits (Figure 3-5). Around depths of 500 m most oil and gas wells have an outer width of 0.3-0.5 m. The quality of casing and cement depend on the age of the borehole. For geological disposal of radioactive waste the density and future degradation of boreholes needs to be considered.

In the near future the number of boreholes penetrating the Rupel Clay Member may increase considerably due to the recent interest in geothermal energy. The Cenozoic aquifers above and below the Rupel Clay Member are targets for that.

4.4. Organic matter and hydrocarbons

4.4.1. Organic layers

Organic layers do not affect integrity directly, but their presence does have the capacity of affecting a disposal site in various ways and is therefore discussed here. In Belgium the Rupel Clay Member is known to contain substantial amounts of organic matter, with an average value of 1.7 wt.% for total organic carbon (Decleer et al., 1983). The organic matter is of type II (of planktonic origin) and type III (of terrestrial origin) and in Belgium it shows a low level of maturity with vitrinite reflectance levels around 0.25-0.4% (Vandenberghe 1978; Laenen, B., 1998; Van Geet et al., 2003; Blanchart, 2011; Bruggeman and De Craen, 2012). The relevance of knowledge on the organic matter content is its behaviour when heated. According to Deniau et al. (2004) the heat generated by radioactive waste may release various compounds from the kerogen. These compounds may affect the effectiveness of the sediment as a barrier to waste migration, for example through complexation of radio-nuclides with some of the released compounds. This is a topic of other work packages in the OPERA program.

In the Netherlands the Rupel Clay Member is buried at greater depths and is subject to higher temperatures than in Belgium. Around 1000 m depth, the natural average temperature is 40°C. The bitumen in the organic matter can be converted to crude oil when the host sediment is lowered into the oil window (temperatures between 60-160°C). In the Netherlands this would be below roughly 1750 m depth, so in the Roer Valley Graben (Bonté et al., 2012). Gas is generated when the host sediment is lowered into the gas window (temperatures between 150-200°C), which is not applicable for the Rupel Clay Member.

Organic matter and bitumen have been identified in the Rupel Clay Member in the Netherlands. For example in hydrocarbon exploration well Grashoek-01 on the Peel-Maasbommel Complex, where at around 400 m depth organic matter, bitumen and tarry oil were reported by NAM in the composite well log. Other oil shows in rocks of a similar age in that region have been reported by Van Waterschoot van der Gracht (1909, 1918) and Van Riessen and Vandenberghe (1996). The latter are most likely related to oil seepage originating from from deeper Mesozoic or Carboniferous source rocks, remobilized by Pyrenean-phase tilting.

The presence of organic matter and bitumen may pose both a threat and an opportunity for disposal of radioactive waste. As explained above the high temperatures released from the waste may generate compounds which may act as a barrier for radio-nuclides. On the other hand the presence of bitumen and generated oil in deeper buried

Rupel Clay Member deposits may provide a risk during the construction of a repository. The deepest occurrence of the base of the Rupel Clay Member occurs in the Roer Valley Graben, around -1600 m m.s.l., which is above the oil window. In the graben the Rupel Clay Member has not been buried deeper than its current depth. This implies that the clay in the Roer Valley Graben has never been in the oil window, and is thus expected to contain no thermogenic hydrocarbons. On the other hand, gas produced by microbial organisms from the organic matter in the Rupel Clay Member may be present. The optimal temperature-range for microbial gas generation lies between 30 and 50°C (Clayton, 2010).

4.4.2. Hydrocarbons

In the Netherlands many oil and gas fields are known (Figure 3-5). Next to that, oil and gas companies define their own prospects, where oil or gas may be present. These prospects are confidential and not proven. We do know that the major source rocks in the Netherlands are the gas-generating Carboniferous (Westphalian) coal layers and the oil-generating Early-Jurassic (Toarcian) black shales. The Westphalian coal layers are present in almost the complete onshore part of the Netherlands. The Toarcian black shales are present in the Roer Valley Graben and in the Zuiderzee Low. Reservoir rocks for oil and gas fields in the onshore part of the Netherlands are located stratigraphically below the Rupel Clay Formation. However, small (shallow) hydrocarbon occurrences may be present in permeable layers which lie stratigraphically below and above the Rupel Clay Member (e.g. De Wijk gas field in the Basal Dongen Tuffite). In the Roer Valley Graben focus area only the Waalwijk gas field is present at the westernmost extremity. In the Zuiderzee Low focus area, no oil or gas fields have been found. In the North Netherlands focus area, several smaller gas fields are present. The localization of a future disposal site should take the presence of hydrocarbon fields and dispersed hydrocarbons into consideration.

4.5. Geohydrology of focus areas

There is only limited measured data and information available on the geohydrological properties of the Rupel Clay Member for the burial depth and thicknesses considered in this study (i.e. minimum burial depth of the top of the Rupel Clay Member of -400 m m.s.l. and minimum thickness of 100 m) .

However, geohydrological properties are known to vary as a function of heterogeneity, lithological composition and compaction of a lithostratigraphic unit. In general, the Netherlands were located in the coastal zone of the Cenozoic Southern North Sea Basin. The depocentre of this basin is located to the north northwest of the Netherlands in the Central North Sea. Sediments deposited in the Southern North Sea Basin decrease in grain size in a north-northwestward direction towards the depocentre. This can be observed in the changes in grain size in the Rupel Clay Member and the lithostratigraphic units on top and below this member.

According to the conceptual lithofacies model of the Rupel Clay Member (Section 3.2.2) the coarser grain sizes are found along the margins of the Rupelian sea, along the southern and eastern border of the Netherlands and finest grained deposits in the deeper water part of the paleo sea in the north and west of the country. The grain sizes of the samples show that the Rupel Clay Member in the north is not only more fine-grained but also more homogeneous. The spatial variation in lithology, heterogeneity and also burial depth is apparent in the variation of the calculated permeability using the grain-size analyses of the samples of the Rupel Clay Member. The samples from the north of the country consist almost entirely of muds with calculated vertical permeabilities of less than $8.3E^{-19}$ m^2 ($8.3E^{-12}$ m/s) (calculated using for clay+very fine silt+fine silt % from laser diffraction). The vertical variation in permeability in the more heterogeneous Rupel Clay Member in the southern and east southeastern part of the country can reach several orders of magnitude due to increased permeability of the coarser grained layers. The calculated porosities and permeabilities for the focus area in North Netherlands provides a first estimation of the geohydrological properties of the Rupel Clay member: overall relatively

low permeable and homogeneous. Quantitative information on the geohydological properties of the Rupel Clay Member in the Zuiderzee Low are missing, because of a lack of samples. No boreholes were sampled for grain size in the Roer Valley Graben as well. Previous basin modelling studies suggest that deep burial of the Rupel Clay Member in the graben is expected to result in low porosity and permeability of the mud part of the member.

The two representative cross-sections (Figure 3-15 and Figure 3-16) illustrate the influence of the regional changes in grain size on the hydrostratigraphy of the overburden of the Rupel Clay Member: the bottom parts of the overburden of the Rupel Clay Member in the southern and southeastern part of the Netherlands (Roer Valley Graben) is more permeable in comparison with that in the north.

The geohydrological framework of the Rupel Clay Member and its over- and underburden is not only determined by the distribution, thickness and dip of the hydrostratigrahic units, but also by geologic structures and tectonic elements of importance for groundwater flow. Fault systems cutting through the Rupel Clay Member are more numerous in the southern focus area (Roer Valley Graben) in comparison with the Zuider Zee Low and North Netherlands.

4.6.Data quality and limitations of the work

As stated in the introduction, this work is a desk-study giving an overview of the Rupel Clay Member. This study updates previous studies performed in the framework of radioactive waste disposal.

The results presented here reflect a greatly increased dataset and improved knowledge and technical possibilities which have been gathered over the last 30 years. As such the new results were timely. Nonetheless the new results should be handled with care, since no new stratigraphic interpretation of boreholes was performed. Further, the correlation of Dutch stratigraphic nomenclature is known not to match well with the Belgian-German nomenclature. No effort was made to improve that within this study. We also did not interpret the Rupel Clay Member on seismic data. Faults that were used are known to be of limited reliability, especially in the Zuiderzee Low region in the middle of the country.

The conceptual lithofacies model is based on a limited number of wells with grain size data and therefore should be merely taken as a broad geologic setting. Future work on for example the focus areas should concentrate on the gathering of dedicated core data from new boreholes, 3D seismic data and extensive analyses and interpretations. The present study can serve as a guideline for such a more detailed study.

5. Conclusions and knowledge gaps

5.1. Conclusions

This study presents an update of the geometrical, geological and geohydrological properties of the Rupel Clay Member in the onshore part of the Netherlands. Existing borehole and seismic interpretations were evaluated and integrated with results from recent literature. Additionally, grain-size samples from 15 boreholes have been analysed and interpreted for lithofacies and geohydrological properties. We present the most detailed depth and thickness maps of the Rupel Clay Member since the last Rupel Clay Member maps were made, some 30 years ago. The maps provide insight in the 3D geometry and distribution of the member in the Dutch onshore subsurface.

Following the OPERA research plan we divide our conclusions into the following four subjects:

1. **Regional-scale geometry and overburden:**
    - The Rupel Clay Member is present in nearly the entire onshore part of the Netherlands;
    - The mean thickness is 65 ± 42 m;
    - Along the southwestern and eastern borders of the country the Rupel Clay Member is present within ~50 m from the land surface;
    - The deepest occurrences of the top of the Rupel Clay Member lie in the Roer Valley Graben in Noord-Brabant and Limburg (-1500 m m.s.l.) and in the Zuiderzee Low (-1150 m m.s.l.);
    - Three focus areas (deeper than 400 m, thicker than 100 m) have been identified: 1. Roer Valley Graben (Noord Brabant); 2. Eastern part of the Zuiderzee Low (Gelderland); and 3. Several smaller zones in the north of the country (Friesland).

2. **Lithological characterization:**
    - In the north of the country the member is more fine-grained and homogeneous than in the southeast and southwest, where palaeo-coastlines are responsible for a more sandy component;
    - Within the Rupel Clay Member the sediments generally are more silty towards the top and base of the member. This pattern is most pronounced in the south of the Netherlands;
    - Within the Rupel Clay Member regular lamination at decimetre to metre scale has been identified in Belgium and is expected to be present in the Netherlands as well. Towards the centre of the palaeo-basin, the lamination may be less pronounced due to a higher overall clay content;
    - Our conceptual lithofacies model suggests more sandy lithofacies around the Texel-IJsselmeer and Dalfsen Highs.

3. **Regional scale geohydrological setting:**
    - The geohydrological setting of the Rupel Clay Member in the south of the country is significantly different from that in the north with respect to both geohydrological framework and groundwater flow conditions;
    - The geohydrological framework of the Rupel Clay Member and its over- and underburden are determined by the distribution, thickness and dip of the hydrostratigraphic units and by geologic structures and tectonic elements of importance for groundwater flow. Fault systems cutting through the member are known to be more numerous in the Roer Valley Graben. This is unknown for the Zuiderzee Low;

- Two representative hydrostratigraphic cross-sections show that the overburden directly overlying the Rupel Clay Member in the southern and southeastern parts of the Netherlands is more permeable than in the north;
- The meteoric groundwater-flow systems are shallow to very shallow systems in most of the Netherlands. The Roer Valley Graben is the only focus area where the active meteoric groundwater flow extends to a depth of more than 400 m and may reach the Rupel Clay Member;
- Compaction of the Cenozoic sedimentary sequence, including the Rupel Clay Member, is on-going. Modelling studies indicate that compaction-related vertical groundwater flow rates through the Cenozoic sediments range between < 0.01 and 0.04 mm/year.

4. **Geohydrological characterization:**
   - In line with the lithofacies distribution, the calculated permeability of the Rupel Clay Member is lowest in the north of the Netherlands and higher and more variable in the south and southeast;
   - Generally the permeability decreases with increasing depth for the same lithology.

Additional factors possibly affecting the integrity of the Rupel Clay Member are:
- Faults;
- Salt domes;
- Layers of calcareous septaria;
- Organic matter and bituminous layers;
- Present and future boreholes;
- Natural and induced seismicity.

5.2. Knowledge gaps and recommendations for future work

- There is a mismatch with respect to the Cenozoic lithostratigraphic nomenclature of the Netherlands, Belgium and Germany, which urgently needs to be resolved, before further geologic studies can take place;
- The lithofacies distribution in the Rupel Clay Member is still poorly understood due to a lack of data. New wells with geophysical logging campaigns are needed to resolve this. An option may be to run detailed logs in hydrocarbon and geothermal wells penetrating the Rupel Clay Member;
- Lithostratigraphy and geohydrological properties (porosity, permeability, storage coefficient/compressibility) of the Rupel Clay Member and the deposits directly overlying and underlying it, are still poorly understood;
- Detailed mapping of distribution and thickness of the lithostratigraphic units of the Breda Formation, especially in the southeastern parts of the Netherlands, are required as first step to assess the spatial variation in geohydrological properties in the Breda Formation;
- In the two largest focus areas (Roer Valey Graben and Zuiderzee Low), where the Rupel Clay Member is thicker than 100 m and its top is located at depths greater than -400 m m.s.l. no grain-size data are available. None of the boreholes sampled for grain size is located in this focus area. Future studies should obtain high-quality cores and sediment samples from all focus areas to enable thorough comparisons;
- Faults in the onshore part of the Netherlands form a potential risk but are poorly mapped;
- Fault properties (horizontal and vertical offset, geohydrological properties, connectivity) are unknown but may be vital with respect to the Safety Functions;
- Geohydrological properties of the Rupel Clay Member and the deposits directly overlying and underlying it can be obtained by combining the grain size-based method to calculate porosity and permeability using grain-size analyses of - new - samples with basin modelling approaches;

- There are no measured data on pressure and groundwater flow conditions in and around the Rupel Clay Formation (where the Rupel Clay Formation is located at depths greater than 400m);
- In the north of the Netherlands sub-glacial tunnel valleys (Peelo Channels) are present which have recently been shown to reach further south and deeper (up to 600 ms or ~500 m depth) than previously known. Further work needs to be done to map these valleys, to aid magnitude estimates of future sub-glacial erosion.

References

Abels, H.A., Van Simaeys, S., Hilgen, F.J., De Man, E., Vandenberghe, N., 2006. Obliquity-dominated glacio-eustatic sea level change in the early Oligocene; evidence from the shallow marine siliciclastic Rupelian stratotype (Boom Formation, Belgium). Terra Nova 19, 65-73.

Aplin, A.C., Macquaker, H., 2011. Mudstone diversity: origin and implications for source, seal, and reservoir properties in petroleum systems. AAPG Bulletin 95-12, 2031-2059.

Bense, V.F., 2004. The hydraulic properties of faults in unconsolidated sediments and their impact on groundwater flow. PhD thesis, VU University Amsterdam, 143 p.

Blanchart, P., 2011. Influences de l'oxydation et de la biodégradation anaerobie sur la matière organique de l'argile oligocène de Boom (Mol, Belgique): Conséquences sur la formation d'espèces organiques hydrosolubles, Institut National Polytechnique de Lorraine, Université de Nancy.

Blott, S.J., Pye, K., 2001. GRADISTAT: a grain size distribution and statistics package for the analysis of unconsolidated sediments. Earth Surface Processes and Landforms 26, 1237-1248.

Boisson, J.-Y. (ed.), 2005. Clay Club Catalogue of Characteristics of Argillaceous Rocks. NEA rapport 4436/ISBN: 92-64-01067-X, Paris, p. 27-72.

Bonté, D., Van Wees, J.D., Verweij, J.M., 2012. Subsurface temperature of the onshore Netherlands: new temperature dataset and modeling. Netherlands Journal of Geosciences 91-4, 491-515.

Bremmer, C.N., Simmelink, H.J., Heidema, A.H., Hoogendoorn, A., Pagnier, H.J.M., 1997. Kartering slecht-doorlatende laagpakketten van Tertiaire formaties - CAR Fase I. RGD report: GB 2514, 27 p. including appendices.

Bruggeman, C., De Craen, M., 2012. Boom Clay natural organic matter – status report 2011. External Report of the Belgian Nuclear Research Centre, Mol, Belgium: SCK•CEN-ER-206, 149 p.

Buurman, P., Pape, Th., Reijneveld, J.A., De Jong, F., Van Gelder, E., 2001. Laser-diffraction and pipette-method grain sizing of Dutch sediments: Correlations for fine fractions of marine, fluvial, and loess samples. Netherlands Journal of Geosciences 80-2, 49-57.

Caro Cuenca, M., 2012. Improving radar interferometry for monitoring fault-related surface deformation. Applications for the Roer Valley Graben and coal mine induced displacements in the southern Netherlands. PhD Thesis Delft University of Technology, the Netherlands. 142 p.

Clayton,C. 2010. Incorporation of biogenic gas generation into petroleum system models. Oral presentation at the Geological Society of London meeting 'Modelling sedimentary basins and their petroleum systems', London, 22-23 April 2010.

De Craen, M., Swennen, R., Keppens, E.M., Macaulay, C.I., Kiriakoulakis, K., 1999. Bacterially mediated formation of carbonate concretions in the Oligocene Boom Clay of northern Belgium. Journal of Sedimentary Research 69-5, 1098-1106.

De Lang, F.D., Ebbing, J.H.J., 2003. Rupel Formatie. In: Lithostratigrafische Nomenclator van de Ondiepe Ondergrond. Retrieved 12-08-2013 from http://www.dinoloket.nl/rupel-formatie.

De Man, E., Van Simaeys, S., Vandenberghe, N., Harris, W.B., Wampler, J.M., 2010. On the nature and chronostratigraphic position of the Rupelian and Chattian stratotypes in the southern North Sea basin. Episodes 33-1, 3-14.

De Mulder, E.F.J., Schokking, F., Van Rooijen, P., 1984. Inventarisatie van slecht-doorlatende laagpaketten in de ondergrond van het Nederlandse vasteland. RGD rapport: OP 6009, 137 p. met bijlagen.

De Rooij, R., 2000. A hydrogeological schematization of the Roer Valley Graben. MSc Thesis Centre of Hydrology Utrecht (ICHU), Utrecht University. TNO report NITG 00-200-A.

Decleer, J., Viane, W., Vandenberghe, N., 1983. Relationships between chemical, physical and mineralogical characteristics of the Rupelian Boom clay, Belgium. Clay Minerals 18, 1-10.

Dehandschutter, B., Vandycke, S., Sintubin, M., Vandenberghe, N., Gaviglio, P., Sizun, J.P., Wouters, L., 2004. Microfabric of fractured Boom Clay at depth: a case study of brittle–ductile transitional clay behaviour. Applied Clay Science 26, 389-401.

Dehandschutter, B., Vandycke, S., Sintubin, M., Vandenberghe, N., Wouters, L., 2005. Brittle fractures and ductile shear bands in argillaceous sediments: inferences from Oligocene Boom Clay (Belgium). Journal of Structural Geology 27, 1095-1112.

Deniau, I., Derennea, S., Beaucaireb, C., Pitschb, H., Largeaua, C., 2004. Occurrence and nature of thermolabile compounds in the Boom Clay kerogen (Oligocene, underground Mol Laboratory, Belgium). Organic Geochemistry 35, 91-107.

Dirkzwager, J.B., Van Wees, J-D., Cloetingh, S.A.P.L., Geluk, M.C., Dost, B., Beekman, F., 2000. Geomechanical and rheological modeling of upper crustal faults and their near-surface expression in the Netherlands. Global and Planetary Change 27, 67-88.

DOV, 2004. Isohypsen van de basis van de Tertiaire Formatie van Boom, T07Bm_FormatievanBoom_IH_Basis_20040116.
https://dov.vlaanderen.be/dovweb/html/services.html#Isohypsen Tertiair

Dufour, F.C., 2000. Groundwater in the Netherlands: Facts and Figures. Netherlands Institute of Applied Geoscience TNO (Delft), 96 p.

Duin, E. (1995). Stability of benchmarks Groningen. Subproject 16 II, Seismic interpretation of Tertiary. RGD report 95KAR08

Duin, E., Doornenbal, J.C., Rijkers, R.H.B., Verbeek, J.W., and Wong, T.E., 2006, Subsurface structure of the Netherlands; results of recent onshore and offshore mapping: Netherlands Journal of Geosciences 85-4, 245-276.

Ebbing, J.H.J., Weerts, H.J.T., Westerhoff, W.E., 2003. Towards an integrated land-sea stratigraphy of the Netherlands. Quaternary Science reviews 22, 1597-1587.

Ernst, L.F., De Ridder, N.A., 1960. High resistance to horizontal groundwater flow in coarse sediments due to faulting. Geologie en Mijnbouw 39, 66-85.

Gaemers, P.A.M., 1993. Refined correlations by means of lithostratigraphy and gadid otolith zonation of the Rupelian of the North Sea Basin: a progress report: Belgische Vereniging voor Geologie, Bulletin 102, 147-158.

Garavito, A.M.F., 2006. Chemical osmosis in clayey sediments; field experiments and numerical modeling. PhD thesis, Vrije Universiteit Amsterdam.

Garavito, A.M.F., De Cannière, P., Kooi, H., 2007. In situ chemical osmosis experiment in the Boom Clay at the Mol underground research laboratory. Physics and Chemistry of the Earth 32, 421-433.

Gunnink, J.L., Maljers, D., Gesssel, S.F., Menkovic, A., Hummelman, H.J., 2013. Digital Geological Model (DGM): a 3D raster model of the subsurface of the Netherlands. Netherlands Journal of Geosciences 92-1, 33-46.

Gradstein, F.M., Ogg, J.G., Schmitz, M.D., Ogg, G.M., 2012. The Geologic Time Scale 2012. Elsevier, 1176 p.

Hantschel, T., Kauerauf, A.I., 2009. Fundamentals of basin and petroleum systems modeling. Springer Verlag Berlin Heidelberg, 476 p.

Heister, K., 2005. Coupled transport in clayey materials with emphasis on induced electrokinetic phenomena. PhD. Thesis, Utrecht University, Utrecht, the Netherlands,118 p.

Houtgast, R.F., Van Balen, R.T., 2000. Neotectonics of the Roer Valley Rift System, the Netherlands. Global and Planetary Change 27, 131-146.

Houtgast, R.F., Van Balen, R.T., Kasse, C., 2005. Late Quaternary evolution of the Feldbiss Fault (Roer Valley Rift System, the Netherlands) based on trenching, and its potential relation to glacial unloading. Quaternary Science Reviews 24, 491-510.

Keijzer, T.J.S., 2000. Chemical Osmosis in Natural Clayey Materials. PhD Thesis, Utrecht University, Utrecht, The Netherlands, 166 p.

Knox, R.W.O.B., Bosch, J.H.A., Rasmussen, E.S., Heilmann-Clausen, C., Hiss, M., De Lugt, I.R., Kasińksi, J., King, C., Köthe, A., Słodkowska, B., Standke, G. & Vandenberghe, N., 2010. Cenozoic. In: Doornenbal, J.C. and Stevenson, A.G. (editors): Petroleum Geological Atlas of the Southern Permian Basin Area. EAGE Publications b.v. (Houten): 211-223.

Koenen, M., Griffioen, J., 2013. Mineralogical and geochemical characterization of the Boom Clay in the Netherlands. COVRA report: OPERA-PU-5-2-1-TNO-1, 77 p.

Kombrink, H., Doornenbal, J.C., Duin, E., Den Dulk, M., Van Gessel, S.F., Ten Veen, J.H., and Witmans, N., 2012, New insights into the geological structure of the Netherlands; results of a detailed mapping project: Netherlands Journal of Geosciences 91-4, 419-446.

Konert, M., Vandenberghe, J., 1997. Comparison of laser grain size analysis with pipette and sieve analysis: a solution for the underestimation of the clay fraction. Sedimentology 44, 523-535.

Kooi, H., De Vries, J. 1998. Land subsidence and hydrodynamic compaction of sedimentary basins. Hydrology and Earth System Sciences 2, 159-171.

Kooi, H., Johnston, P., Lambeck, K., Smither, C., Molendijk, R., 1998. Geological causes of recent (~100 yr) vertical land movement in the Netherlands. Tectonophsics 299, 297-316.

Kooi, H., 2000. Land subsidence due to compaction in the coastal area of The Netherlands: the role of lateral fluid flow and constraints from well-log data. Global and Planetary Change 27, 207-222.

Laenen, B., 1997. The geochemical signature of relative sea-level cycles recognised in the Boom Clay. Unpublished PhD Thesis Katholieke Universiteit Leuven, Belgium, 396 p.

Laenen, B., 1998. The geochemical signature of relative sea-level cycles recognised in the Boom Clay. Aardkundige Mededelingen, University Press Leuven 9, 61-82.

Lear, C.H., Elderfield, H., Wilson, P.A., 2000. Cenozoic deep-sea temperatures and global ice volumes from Mg/Ca in benthic foraminiferal calcite. Science 287, 269-272.

Leroi, S., 1995. Stratigrafische correlaties in de Rupel Groep tussen Belgie en het Nederrijngebied in Duitsland. Unpublished Licentiaatsthesis Katholiek Universiteit Leuven, Belgium, 41 p.

Luijendijk, E., 2012. The role of fluid flow in the thermal history of sedimentary basins. Inferences from thermochronology and numerical modeling in the Roer Valley Graben, southern Netherlands. PhD Thesis, VU University Amsterdam, 198 p.

Maréchal, R., Laga, P. (eds.), 1988. Voorstel lithostratigrafische indeling van het Paleogeen. Nationale Commissies voor stratigrafie, commissie: Tertiair.

Michon, L., Van Balen, R.T., 2005. Characterization and quantification of active faulting in the Roer valley rift system based on high precision digital elevation models. Quaternary Science Reviews 24, 457-474.

Nelskamp, S., Verweij, J.M., 2012. Using basin modeling for geothermal energy exploration in the Netherlands – an example from the West Netherlands Basin and Roer Valley Graben. TNO report TNO-060-UT-2012-00245, 113 p.

NITG-TNO, 2004, Geological Atlas of the Subsurface of the Netherlands - onshore: Utrecht, Netherlands Institute of Applied Geoscience TNO, 104 p.

Oude Essink, G.H.P., 1996. Impact of sea-level rise on groundwater flow regimes, a sensitivity analysis for the Netherlands. PhD Thesis, Delft University of Technology, Delft, the Netherlands, 411 p.

Oude Essink, G.H.P., 2001. Salt water intrusion in a three-dimensional groundwater system in the Netherlands: A numerical study. Transport in Porous Media 43, 137-158.

Pauw, P., De Louw, P.G.B., Oude Essink, G.H.P., 2012. Groundwater salinisation in the Wadden Sea area of the Netherlands: quantifying the effects of climate change, sea-level rise and anthropogenic interferences. Netherlands Journal of Geosciences 91-3, 373-383.

Pluymaekers, M.P.D., Kramers, L., Van Wees, J-D., Kronimus, A., Nelskamp, S., Boxem, T., Bonte, D. 2012. Reservoir characterisation of aquifers for direct heat production: methodology and screening of the potential reservoirs for the Netherlands. Netherlands Journal of Geosciences 91-4, 621-636.

Post, V.E.A., 2003. Groundwater salinization processes in the coastal area of the Netherlands due to transgressions during the Holocene. PhD Thesis, VU University, Amsterdam, the Netherlands, 138 p.

Rijkers, R.H.B., Huisman, D.J., De Lange, G., Weijers, J.P., Witmans-Parker, N., 1998. Inventarisatie geomechanische, geochemische en geohydrologische eigenschappen van Tertiaire kleipakketten - CAR Fase II. TNO report NITG 98-90-B, 167 p.

Smith, P., Cornélis, B., Capouet, M., Van Geet, M., 2009. The Long-Term Safety Strategy for the Geological Disposal of Radioactive Waste, SFC1 level 4 report: second full draft. ONDRAF/NIRAS, NIROND-TR REPORT 2009-12 E, Geological Disposal Programme, www.nirond.be. Brussels, Belgium, 52 p.

Stuurman, R.J., Atari, R.H. 1997. De grondwatersituatie rond de Wijstgronden bij Uden. TNO report NITG 97-212-a, 83 p.

Stuurman, R., Van Beusekom, G., Reckman, J., 2000. Watersystemen in beeld. Een beschrijving en kaarten van de grondwater- en oppervlaktewatersystemen van Noord Brabant. Nederlands Instituut voor Toegepaste Geowetenschappen TNO, Report 00-10-A.

Stuyfzand, P.J., 1993. Hydrochemistry and hydrology of coastal dunes of the western Netherlands. PhD thesis, VU University, Amsterdam, the Netherlands, 366 p.

Tweede Kamer (1993). Opbergen van afval in de diepe ondergrond, Kamerstukken II 1992-1993, 23 163, nr. 1, 1-10.

Van Adrichem Boogaert, H.A., Kouwe, W.F.P., 1993, Stratigraphic nomenclature of the Netherlands, revision and update by RGD and NOGEPA, Section A, General: Mededelingen Rijks Geologische Dienst 50, 1-24.

Van Dalfsen, W., Doornenbal, J.C., Dortland, S., Gunnink, J.L., 2006. A comprehensive seismic velocity model for the Netherlands based on lithostratigraphic layers: Netherlands Journal of Geosciences 85-4, 277-292.

Van de Vate, L., 2012. Research on the disposal of radioactive waste in the Netherlands. In: Floor, P. (coord. Ed.), 2012. Dutch Earth Sciences – development and impact. The Hague, KNGMG, 202-204.

Van den Bosch, M., Cadée, M.C., Janssen, A.W., 1975. Lithostratigraphical and biostratigraphical subdivision of Tertiary Deposits (Oligocene-Pliocene) in the Winterswijk and Almelo region (eastern part of the Netherlands): Scripta Geologica 29, 1-167.

Van den Bosch, M., Hager, H., 1984, Lithostratigraphic correlation of Rupelian deposits (Oligocene) in the Boom area (Belgium), the Winterswijk area (The Netherlands) and the Lower Rhine district (F.R.G.): Mededelingen van de Werkgroep voor Tertiaire en Kwartaire Geologie 21-3, 123-138.

Van Echelpoel, E., Weedon, G.P., 1990. Milankovitch cyclicity and the Boom Clay Formation: an Oligocene siliciclastic shelf sequence in Belgium. Geological Magazine 127, 599-604.

Van Geet, M., Maes, N., Dierckx, A., 2003. Characteristics of the Boom Clay organic matter, a review. Geological Survey of Belgium, Professional paper 2003/1, N. 298, 1-23.

Van Riessen, E.D., Vandenberghe, N., 1996. An Early Oligocene oil seepage at the southern rim of the North Sea Basin, near Leuven (Belgium): Geologie en Mijnbouw 74-4, 301-312.

Van Waterschoot van der Gracht, W.A.J.M., 1909. The deeper geology of the Netherlands and adjacent regions, with special reference to the latest borings in the Netherlands, Belgium and Westphalia. Memoires of the Governmental Institute for Geological Exploration in the Netherlands 2 (R.O.V.D.), The Hague.

Van Waterschoot van der Gracht, W.A.J.M., 1918. Eindverslag over de onderzoekingen en uitkomsten van de Dienst der Rijksopsporing van Delfstoffen in Nederland, Amsterdam.

Vandenberghe, N., 1978. Sedimentology of the Boom Clay (Rupelian) in Belgium. Verhandeling Koninklijke Academie voor Wetenschappen, Letteren en Schone Kunsten van Belgie, Klasse Wetenschappen XL, nr. 147, 137 p.

Vandenberghe, N., Laga, P., 1986. The septaria of the Boom clay (Rupelian) in the type area in Belgium: Aardkundige Mededelingen 3, 229–238.

Vandenberghe, N., Laenen, B., Van Echelpoel, E., Lagrou, D., 1997. Cyclostratigraphy and climatic eustacy. Example of the Rupelian stratotype. C R Acad. Sci. II A, 325, 305-315.

Vandenberghe, N., Hager H., Van den Bosch M., Verstraelen A., Leroi S., Steurbaut E., Prüfert J., Laga P., 2001. Stratigraphic correlation by calibrated well logs in the Rupel Group between North Belgium, the Lower Rhine area in Germany and Southern Limburg, and the Achterhoek in the Netherlands. In: Contributions to the Paleogene and Neogene Stratigraphy of the North Sea Basin (N. Vandenberghe, ed.), Aardkundige Mededelingen 11, 69–84. Leuven University Press, Leuven, Belgium.

Vandenberghe, N., Mertens, J., 2013. Differentiating between tectonic and eustatic signals in the Rupelian Boom Clay cycles (Lower Oligocene, Southern North Sea Basin). Newsletters on Stratigraphy, DOI: http://dx.doi.org/10.1127/0078-0421/2013/0034.

Verhoef, E., Neeft, E., Grupa, J., Poley, A., 2011. Outline of a disposal concept in clay. COVRA report: OPERA-PG-COV008, 17 p.

Vernes, R.W., Van Doorn, Th.H.M., 2005. Van gidslaag naar hydrogeologische eenheid-Toelichting op de totstandkoming van REGIS II. TNO report NITG 05-038-B, 105 p.

Verweij, J.M. 1999. Application of fluid flow systems analysis to reconstruct the post-Carboniferous hydrogeohistory of the onshore and offshore Netherlands. Marine and Petroleum Geology 16, 561-579.

Verweij, J.M., 2003. Fluid flow systems analysis on geological timescales in onshore and offshore Netherlands. With special reference to the Broad Fourteens Basin. PhD Thesis, VU University Amsterdam, 278 p.

Verweij, J.M., Simmelink, H.J., Underschultz, Witmans, N. 2012. Pressure and fluid dynamic characterisation of the Dutch subsurface. Netherlands Journal of Geosciences 91-4, 465-490.

Weerts, H.J.T., Westerhoff, W.E., Cleveringa, P., Bierkens, M.F.P., Veldkamp, J.G., Rijsdijk, K.F., 2004. Quaternary geological mapping of the lowlands of the Netherlands, a 21st century perspective. Quaternary International 133-134, 159-178.

Welkenhuysen, K., De Ceukelaire, M., 2009. Tertiair lithostratigrafische interpretatie op basis van geofysische boorgatmetingen van de boringen van meetnet 1 VMM - Afdeling Water uitgevoerd in 2005-2006: 306 p.

Wemaere , I., Marivoet, S. Labat, S., 2008. Hydraulic conductivity variability of the Boom Clay in north-east Belgium based on four core drilled boreholes. Physics and Chemistry of the Earth 33, S24–S36.

Westerhoff, W.E., Wong, T.E., Geluk, M.C., 2003. De opbouw van de ondergrond. In: De Mulder, E.F.J., Geluk, M.C., Ritsema, I., Westerhoff, W.E., Wong, Th.E. (eds). De ondergrond van Nederland. Nederlands Instituut voor Toegepaste geowetenschappen TNO (Utrecht), 247-352.

Wiers, J., 2001. A hydrogeological characterization and groundwater model of the Roer Valley Graben. Msc Thesis. Centre of Hydrology Utrecht (ICHU), Utrecht University and Netherlands Institute of Applied Geoscience TNO – National Geological Survey.

Wildenborg, A.F.B., Orlic, B., De Lange, G., De Leeuw, C.S., Zijl, W., Van Weert, F., Veling , E.J.M., De Cock, S., Thimus, J.F., Lehnen-de Rooij, C., Den Haan, E.J., 2000. Transport of Radionuclides disposed of in Clay of Tertiary Origin (TRACTOR). TNO report NITG 00-223-B, 223 p.

Yang, Y., Aplin, A.C., 2004. Definition and practical application of mudstone porosity-effective stress relationships. Petroleum Geoscience 10, 153-162.

Yang, Y., Aplin, A.C., 2010. A permeability-porosity relationship for mudstones. Marine and Petroleum Geology 27, 1692-1697.

Yu, L., Gedeon, M., Wemaere, I., Marivoet, J., De Craen, M., 2011. Boom Clay Hydraulic Conductivity-a synthesis of 30 years of research. External report of Belgian Nuclear Research Centre, SCK•CEN-ER-122, 101 p.

Yu, L., Rogiers, B., Gedeon, M., Marivoet, J., De Craen, M., Mallants, D., 2012. Hydraulic conductivity of Boom Clay in north-east Belgium. Transfert 2012, 11 p.

Appendix 1

Boreholes used to compute the thickness of the Rupel Clay Member.

1	ACA-11	51	BGM-09	101	DRO-01	151	HBG-03
2	AHM-01	52	BHG-01	102	DSP-01	152	HEI-01
3	AHO-E-55	53	BHM-01	103	DSP-02	153	HEK-01
4	AKM-01	54	BHM-02	104	DVD-01	154	HEL-05-A
5	AKM-02	55	BHM-03	105	DVD-02	155	HEL-07
6	AKM-03	56	BIR-01	106	DVN-01	156	HES-01
7	AKM-04	57	BIR-02	107	DZL-01	157	HEW-01
8	AKM-05	58	BIR-03	108	EHV-01	158	HGM-01
9	ALD-01	59	BKL-01	109	EIB-01	159	HIL-01
10	ALE-01	60	BKN-01	110	EKL-01	160	HLD-01
11	ALK-01	61	BKP-01	111	EKR-104	161	HLE-01
12	ALM-01	62	BLA-01	112	EKR-208	162	HLM-01
13	ALP-01	63	BLF-101	113	ELV-101	163	HLO-01
14	ALT-01	64	BLG-01	114	EMM-07	164	HND-01
15	AME-205	65	BLG-02	115	EMO-01	165	HOA-03
16	AML-01	66	BLH-01	116	ENA-02	166	HOK-01
17	AMO-01	67	BNT-01	117	ENS-02	167	HOK-02
18	AMO-02	68	BOL-01	118	EPE-01	168	HOO-01
19	AMO-03	69	BOZ-01	119	ETV-01	169	HPT-01
20	AMR-01	70	BRAK-01	120	EVD-01	170	HRL-01
21	AND-01	71	BRG-01	121	FIN-01	171	HRL-02
22	AND-02	72	BRH-01	122	FLN-01	172	HRL-03
23	AND-04	73	BRK-04	123	FRB-01	173	HRL-08
24	AND-05	74	BRL-01	124	GAG-03	174	HRL-09
25	ANJ-01	75	BRN-15	125	GAG-04	175	HRS-01
26	ANS-01	76	BRT-01	126	GEL-01	176	HRV-01
27	APN-01	77	BRW-01	127	GEL-05	177	HTM-01
28	APN-02	78	BRW-02	128	GGT-01	178	HVB-01
29	APS-01	79	BSKP-01	129	GIT-01	179	HVS-01
30	ARV-01	80	BSL-01	130	GLH-01	180	IJD-01
31	ASN-01	81	BTA-01	131	GOU-01	181	IJM-01
32	AST-01	82	BUM-01	132	GRD-01	182	ILP-01
33	AST-GT-02	83	BUR-01	133	GRH-01	183	JLD-01
34	BAC-01	84	BWD-01	134	GRK-01	184	JPE-01
35	BAR-NE-01	85	CLD-01	135	GRL-01	185	KAM-01
36	BAS-01	86	CLDV-01	136	GRT-01	186	KDZ-01
37	BDK-01	87	COC-01	137	GRT-02	187	KDZ-02
38	BDM-01	88	COR-01	138	GRT-03	188	KES-10
39	BEE-12	89	COV-01	139	GRT-04	189	KGB-01
40	BEE-72	90	COV-03	140	GRT-05	190	KHM-01
41	BER-01-A	91	COV-05	141	GRT-06	191	KOL-02
42	BER-03	92	DAL-01	142	GRT-07	192	KPK-01
43	BER-04	93	DAL-02	143	GRW-01	193	KRD-01
44	BFD-14	94	DEW-03	144	GSB-01	194	KRL-01
45	BGM-01	95	DIV-01	145	GST-01	195	KTG-01
46	BGM-02	96	DJM-01	146	GSV-01	196	KWK-01
47	BGM-03	97	DKK-01	147	GTV-01	197	LAD-01
48	BGM-04	98	DKK-02	148	GWD-01	198	LBR-01
49	BGM-07	99	DKK-03	149	HBG-01	199	LEK-01
50	BGM-08	100	DON-01	150	HBG-02	200	LEL-01

201	LEW-01	251	NSN-01	301	ROW-05	351	STN-02
202	LIE-22	252	NSS-GT-34	302	RPL-01	352	STR-01
203	LIR-14	253	NVG-01	303	RSB-01	353	STW-01
204	LIR-23	254	NWD-01	304	RSK-01	354	SUW-01
205	LKM-01	255	NWK-01	305	RST-01	355	SWD-01
206	LMB-01	256	OAS-01	306	RSW-01	356	SWM-21
207	LNH-01	257	OBL-01	307	RSW-02	357	SWM-73
208	LOD-01	258	OBLZ-01	308	RTD-05	358	SWO-01
209	LOM-01	259	ODK-01	309	RTD-10	359	TBR-01
210	LOZ-01	260	ODP-01	310	RTD-11	360	TBR-04
211	LRM-01	261	ODS-01	311	RTD-12	361	TBR-OBS
212	LSM-01	262	OEG-01	312	RUI-02	362	TER-01
213	LTV-02	263	OFL-01	313	RVR-76	363	TES-01
214	LUT-02	264	OIS-01	314	SAN-01	364	TID-101
215	LVD-01	265	OIW-01	315	SAP-11	365	TID-103
216	MAB-13	266	OLD-01	316	SCB-01	366	TID-201
217	MAL-01	267	OLE-01	317	SDB-01	367	TID-202
218	MAN-74	268	OLR-02	318	SDM-01	368	TID-203
219	MAR-101	269	OLZ-01	319	SDM-OBS	369	TID-301
220	MDM-01	270	OMM-01	320	SEV-19	370	TID-OBS
221	MDZ-01	271	OMM-02	321	SIB-01	371	TJM-01
222	MED-01	272	OMM-03	322	SLB-02	372	TUB-02
223	MEE-01	273	OOT-01	323	SLD-01	373	TUB-08
224	MEL-08	274	OPE-01	324	SLD-02	374	TUM-01
225	MID-101	275	OPE-02	325	SLD-03	375	TUM-02
226	MKN-01	276	OPH-01	326	SLD-04	376	TUS-OBS
227	MKO-01	277	OPL-16	327	SLK-01	377	UHM-01
228	MKZ-01	278	OPL-GT-59	328	SMA-01	378	UHZ-01
229	MNT-01	279	OPO-01	329	SMG-01	379	URE-01
230	MOL-01	280	OVE-01	330	SML-01	380	URS-01
231	MOL-02	281	OVS-01	331	SMR-01	381	USQ-01
232	MRS-18	282	OWG-01	332	SMR-OBS	382	VAL-01
233	MSB-01	283	PAU-01	333	SND-01	383	VEH-01
234	MSB-02	284	PEI-01	334	SNK-01	384	VHZ-01
235	MSL-01	285	PLG-01	335	SNM-GT-01	385	VLO-01
236	MWD-02	286	POS-01	336	SOL-03	386	VLR-01
237	NAG-01	287	PRW-01	337	SOW-01	387	VLV-01
238	NBG-01	288	PSP-01	338	SPC-01	388	VLW-02
239	NDP-01	289	PTH-01	339	SPD-01	389	VRE-01
240	NDW-01	290	RAA-01	340	SPH-01	390	VRS-05
241	NER-71	291	RAL-01	341	SPK-01	391	VRS-101
242	NGA-01	292	RAL-02	342	SPKO-01	392	VRS-201
243	NGA-04	293	REU-01	343	SPKO-03	393	VRV-01
244	NGA-07	294	RID-01	344	SPL-01	394	WAA-01
245	NKK-01	295	RID-02	345	SPW-01	395	WAK-01
246	NLM-01	296	RID-03	346	STA-03	396	WAP-01
247	NOR-01	297	ROD-101	347	STH-01	397	WAS-01
248	NOR-02	298	ROD-102	348	STK-01	398	WAS-05
249	NOR-03	299	ROT-01	349	STM-01	399	WAV-01
250	NRZ-01	300	ROT-OBS	350	STN-01	400	WAV-02

401	WAV-03	451	WYK-06
402	WAV-04	452	WYK-07
403	WAV-06	453	WYK-09
404	WAV-09	454	WYK-10
405	WAV-10	455	WYK-11
406	WAV-11	456	WYK-12
407	WAV-12	457	WYK-13
408	WAV-13	458	WYK-14
409	WAV-15	459	WYK-15
410	WAV-16	460	WYK-16
411	WAV-18	461	WYK-19
412	WAW-01	462	WYK-20
413	WAZ-01	463	WYK-21
414	WBL-01	464	WYK-22
415	WDL-01	465	WYK-23
416	WDR-01	466	WYK-24
417	WDV-01	467	WYK-25
418	WDV-04	468	WYK-27
419	WDV-05	469	WYK-29
420	WED-01	470	WYK-30
421	WED-02	471	WYK-31
422	WED-03	472	WYK-32
423	WEP-01	473	ZAD-01
424	WGF-01	474	ZDW-01
425	WHM-01	475	ZDW-02
426	WIM-01	476	ZDW-03
427	WIR-01	477	ZDW-A-01
428	WLO-01	478	ZED-01
429	WMR-01	479	ZEW-01
430	WOB-01	480	ZLN-01
431	WRF-01	481	ZND-01
432	WRG-01	482	ZND-04
433	WRM-01	483	ZND-09
434	WRM-02	484	ZND-10
435	WRV-01	485	ZND-11
436	WRW-01	486	ZOM-01
437	WSM-01	487	ZOM-04
438	WSN-01	488	ZOM-05
439	WSN-02	489	ZOM-06
440	WSN-03	490	ZOM-12
441	WSP-01	491	ZPD-01
442	WWK-01	492	ZRP-01
443	WWN-01	493	ZST-01
444	WWN-02	494	ZUW-01
445	WWN-03	495	ZUW-01
446	WWS-01	496	ZWA-01
447	WYH-01	497	ZWD-01
448	WYK-02	498	ZWO-01
449	WYK-04		
450	WYK-05		

Appendix 2

Inventory of palynological reports from the Rupelian in the Netherlands (by Dirk Munsterman, TNO 2013).

Well	Lab. nr.	Rep. nr. (year)	Conf.	Chronostratigraphy
Outcrop samples Winterswijk, groeve IV	2051-1	2430 NITG 05-026-B	N	2.20 and 1.00-1.50 m below bolder clay Zone NP 22 = Zone O 2
30F470 (Noordwijk)	3154	2348 NITG 99-108-B	N	453.1-454.1 m: Rupelian
41G0024 (De Haart)	3252	2554 60-UT-2011-02173	N	40-40.5 m: O 5-6 42-62.5 m: O 5a 82-82.5 m: O 4b 94-94.5 m: O 4a 108-146.5 m: O3 151-152 m: O2
46A260 (Heumensoord)	3192	2384 NITG 01-232-B	N	No Rupelian, t.d. at 418-419 m: Chattian
OPL-16 Diepboring 16 (Oploo)	3167	2335A NITG 98-14-B	N	314.9-319.4 m: Rupelian
46C0478 (Mill)	2434	2508 2008-U-R1065	?	294-301 m: O4a 308-314 m: O3 332-338 m O2-3
48E0224 ('s Heer-Arendskerke	2249	2396 NITG 03-061-B	N	70-128 m: Rupelian
48H0328 (Kapelle)	2414	2488 2007-U-R1015/B	N	69-70 m: Rupelian undiff. 80-81 m: O4a 90-131 m: O3 142-143 m: O1/O2
49G0959 (Putten)	3246	2525 034-UT-2009-02485/B	N	85-86 m: early Chattian, or older 100-101 m: O5 150-181 m: O3 190-191 m: O2 195-221 m: E8-O1
50H0373 (Goirle)	3241	2508 2008-U-R1065	?	461-462 m: O2-3 503-504 m: O1 507-508 m: E8 (Priabonian)
52E114 (Broekhuizervorst)	3159	2384 NITG 01-232-B	N	420-447.5 m: Rupelian
54A0088 (Waterlandkerkje)	3208	2415 NITG 04-080-B	N	15.90 m: O2-4a
54B0085 (Biervliet)	3206	2407 NITG 04-016-B	N	21.70-33.50 m: Rupelien
54E0335 (Schapenbout)	3215	2440 NITG 05-050-B	N	17.6-21.5 m: O3 25.5-35.5 m: O2 37.5-40.5 m: O1 45.5-65.5 m: Priabonian
54F0093 (Axel)	3198	2396 NITG 03-061-B	N	10-55 m: Rupelian
54F0097 (Axel)	3205	2407 NITG 04-016-B	N	21.70-33.50 m: early Rupelian
54H0021 (Koewacht)	3212	2431 NITG 05-016-B	N	18.50-20.50 m: O2 (Ruisbroek) 25.50-27.50 m: O1 (Bassevelde)
55A0364 (Hulst)	3197	2396 NITG 03-061-B	N	50-115 m: Rupelian 116-127 m: Priabonian
58F0064 (Groote Heide)	3175	2384 NITG 01-232-B	N	629-689 m: earliest Chattian-Rupelian
				continued on next page

Well	Lab. Nr.	Rep. nr. (year)	Conf.	Chronostratigraphy
6A127 (Blija)	3174	2351A NITG 00-118-B	N	448.5-502.5 m: Rupelian
A17-1	2227-1	2506 2008-U-R1045/B	N	1140-1150 m: O5 1170 m: O3-4a 1180 m: O1
BUM-01 (Buurmalsen-1)	3127	2285A NITG 00-262-B	N	840-850 m: Chattian 860-890 m: Rupelian
DON-01 (Dongen-1)	3176	2354 NITG 99-194-B	N	532-537.4 m: earliest Chattian 613-616 m Rupelian
EVD-01 (Everdingen-1)	3126	2286A NITG 00-263-B	N	810-870 m: Chattian 870-910 m: Rupelian
F17-10		confidential	Y	xxxxxxxx
G10-1	2167-1	*2275 (1993) *2408 (2004) *2460 (2005) 2543 (2010)	N	1000 m: early Chattian, O6
G16-6	2156-6	2518 034-UT-2009-1794	N	940 m: Chattian, O6 980-990 m: Priabonian
HVS-01 (Hellevoetsluis-1)	3195	2394 NITG 02-187-B	N	420-480 m: Rupelian
L06-2	2168-2	*2413 (2004) *2424 (2004) 2452 NITG 05-124-B	N	880 m: O4a or older 900-920 m: O3
L06-3	2168-3	2452 NITG 05-124-B	N	1000 m: Rupelian 1030 m: O3
L07-6	2122-6	2485 2007-U-R0873	N	700-730 m: O5a 750 m: O4 770-790 m: O3 810 m: Priabonian
LBR-01 (Limbricht-1)	3158	2330 NITG 97-109-B 2330A NITG 97-193-B	N	305-326 m: late Chattian 344.5-361.5 m: early Chattian 381.5-489.5 m: Rupelian
N04-1	2225	2483 2007-U-R0704-B	N	500 m: Serravallian 515-545 m: O3 or older 560 m: Bartonian
NDW-01 (Nederweert-1)	2036	2284A NITG 98-260-B	N	1105-1255 m: early Chattian 1270-1295 m: earliest Chattian 1320-1370 m: Rupelian 1390 m: Early Eocene, Ypresian
OBLZ-01 (Oud Beijerland Zuid-1)	3196	2394 NITG 02-187-B	N	460-530 m: Rupelian 540-570 m: Priabonian
Q11-03	2231-03	2529 034-UT-2010-00610	N	520 m Early Miocene 530-550 m: O3 560 m Early Eocene, Ypresian
Q13-5	2231-5	2530 (2010)	N	490-500 m: Middle Miocene, Serravallian 510 m: Rupelian 530 m: Middle Paleocene
RAA-01 (Raath-1)	3157	2328 NITG 97-108-B	N	599-648 m: latest Rupelian-earliest Chattian 663-672.5 m: Rupelian
SMG-01 (St Michelsgestel)	3169	2342 NITG 98-161-B	N	1400-1430 m: early Chattian 1445-1530 m: Rupelian 1550 m latest Eocene/earliest Rupelian
				continued on next page

Well	Lab. Nr.	Rep. nr. (year)	Conf.	Chronostratigraphy
SPKW-10 (Spijkenisse West-1)	3194	2394 NITG 02-187-B	N	370 m late Serravallian 380-500 m Rupelian 530-560 m Priabonian
VEH-01 (Veldhoven-01)	3030	2376 NITG 01-146-B	N	912-1007 m: Aquitanian-early Burdigalian 1009-1095 m: Chattian 1105-1120 m: latest Rupelian-earliest Chattian 1125-1130 m: Rupelian
				end of table

Appendix 3

Reference list of geohydrological properties of the Rupel Formation/Rupel Clay Member in onshore Netherlands

I Geohydrological properties of the Rupel Formation, SW part of the Netherlands (Zeeland)

I.1 Source: TNO database

Borehole	Depth interval m	Porosity	Hydraulic Conductivity (m/d at 10oC)	Hydraulic Conductivity (m/s)	Method
B28F1326	18,62-18,67	0,385	0,067865934	7,85485E-07	GU-FH_Falling head
B28F1326	18,9-18,95	0,413	0,061507151	7,11888E-07	GU-FH_Falling head
B28F1326	20,55-20,60	0,408	0,069795188	8,07815E-07	GU-FH_Falling head
B28F1326	20,80-20,85	0,429	0,085692525	9,91812E-07	GU-FH_Falling head
B28F1326	24,70-24,72	0,426	1,38087E-06	1,59823E-11	fall
B28F1326	25,65-25,70	0,432	0,00521716	6,03838E-08	GU-FH_Falling head
B28F1326	25,77-25,82	0,452	0,001578149	1,82656E-08	GU-FH_Falling head
B54E0865	21,31-21,33	0,437	2,11243E-06	2,44495E-11	fall
B55A0839	25,82-25,84	0,437	1,13434E-06	1,31289E-11	fall

Borehole	Depth interval m	Unit	Lithological composition		
			Lutum	Silt	Sand
B28F1326	18,60-19,00	RURAOO	0,01	0,05	0,94
B28F1326	18,60-19,00	RURAOO	0,01	0,05	0,94
B28F1326	20,30-21,00	RURAOO	0,01	0,05	0,94
B28F1326	20,30-21,00	RURAOO	0,01	0,05	0,94
B28F1326	24,04-25,00	RURA	0,4	0,58	0,02
B28F1326	25,40-26,00	RURAOO	0,03	0,15	0,82
B28F1326	25,40-26,00	RURAOO	0,03	0,15	0,82
B54E0865	20,99-21,46	RUBO	0,4	0,58	0,02
B55A0839	25,23-26,00	RUBO	0,55	0,45	0

I.2 Source: Rijkers, R.H.B., Huisman, D.J., De Lange, G., Weijers, J.P., Witmans-Parker, N., 1998. Inventarisatie geomechanische, geochemische en geohydrologische eigenschappen van Tertiaire kleipakketten - CAR Fase II. NITG-TNO. TNO report NITG 98-90-B, 167 p.

The following table (next page) includes clay content and porosity values for the Rupel Clay Member at shallow depths in Zeeland. The report also provides information on clay content for the same borehole locations and geomechanical parameters.

Borehole	Depth m-msl	Clay <2µm	Porosity	Borehole	Depth m-msl	Clay <2µm	Porosity
54E0290	30,3		0,43	48G0208	46,7	0,57	0,45
	31,45	0,64	0,47	48G0209	30,4	0,69	0,43
	36,3		0,42		37,15	0,5	0,43
	39,35	0,34	0,45		42,1	0,29	0,44
	42	0,1	0,33	48G0210	29,95	0,57	0,39
	45,3	0,13	0,36		37,4	0,49	0,41
54E0293	39,45	0,4	0,41		37,7	0,64	0,42
	45,5	0,36	0,43		43,45	0,5	0,43
	47,5	0,25	0,4	48G0211	22,8	0,28	0,49
54E0294	48,1		0,36		23,85	0,39	0,42
	58,1		0,4		28,8	0,71	0,43
54E0296	40	0,41	0,44		29,35	0,51	0,42
	42,25	0,66	0,4		33,6	0,68	0,42
	46	0,34	0,39		39,8	0,51	0,41
48G0205	35,7	0,326	0,43		44,65	0,42	0,42
	39,85	0,498	0,47		48,7	0,34	0,45
	44,3	0,471	0,46		50	0,59	0,44
	46,05	0,259	0,44	48G0212	35,2	0,58	0,4
48G0206	25,27		0,4		40,7	0,59	0,42
	31,75		0,4		45,33	0,3	0,43
	34,15	0,36	0,47	48G0213	35,7	0,64	0,4
	34,75	0,52	0,4		50	0,66	0,45
	37,5		0,41		46,35	0,26	0,44
	39,9	0,42	0,42	48G0214	31,85	0,58	0,43
	42,35		0,42		35,8	0,64	0,42
	43,55	0,67	0,42		38,45	0,62	0,46
	44,45		0,46		41,75	0,57	0,42
	45,2	0,25	0,42		45,95		0,41
48G0207	25,2		0,32		46,9	0,54	0,41
	31,45		0,39		49,8	0,37	0,43
	31,9	0,43	0,38		50,6		0,43
	33,5		0,42		53,45	0,4	0,42
	37,1	0,58	0,41		57,95	0,57	0,44
	41,25		0,41	48G0215	41,2	0,63	0,43
	43,3	0,52	0,41		44,3	0,57	0,43
48G0208	22,35	0,55	0,44		46,85	0,41	0,4
	25,25	0,65	0,39		51,2	0,38	0,43
	28,35	0,75	0,45	48G0216	40,54	0,63	0,4
	32,35	0,63	0,41		46,12	0,57	0,42
	33,4		0,42		49,02	0,35	0,45
	35,55	0,48	0,41		55,03	0,5	0,45
	36,6	0,26	0,42	48G0218	43,85	0,65	0,41
	40,4	0,37	0,45		46,5	0,61	0,41
	41,45	0,36	0,43		50,6	0,56	0,4
	41,6		0,41	48G0219	43,1	0,58	0,41
	45,2	0,22	0,44		48	0,7	0,44

II Geohydrological properties Rupel Clay Member, Roer Valley Graben

Source: Wiers, J., 2001. A hydrogeological characterization and groundwater model of the Roer Valley Graben. Msc Thesis. Centre of Hydrology Utrecht (ICHU), Utrecht University and Netherlands Institute of Applied Geoscience TNO - National Geological Survey.

Borehole	Depth interval m	Unit	Porosity	Permeability mD	Hydraulic conductivity m/s	Calculation Method
AST-GT-02	1415-1495	NMRFC	0,27	3	2,78E-08	average porosity from density log; permeability from porperm relation
HSW-01		NMRFC	0,32	7,5	6,94E-08	average porosity from sonic log; permeability from porperm relation
WWK-01	783-888	NMRFC	0,32	3,8	3,47E-08	average porosity from sonic log; permeability from porperm relation
(The Rupel Formation in HSW-01 occurs between 1182 and 1288 m depth)						

III Geohydrological properties Rupel Clay Member, Blija, Friesland

Source: Wildenborg, A.F.B., Orlic, B., De Lange, G., De Leeuw, C.S., Zijl, W., Van Weert, F., Veling , E.J.M., De Cock, S., Thimus, J.F., Lehnen-de Rooij, C., Den Haan, E.J., 2000. Transport of Radionuclides disposed of in Clay of Tertiary Origin (TRACTOR). Netherlands Institute of Applied geoscience TNO – National Geological Survey. TNO report NITG 00-223-B, 223 p.

One of the topics in this report concerns lab experiments on the Rupel Clay Member using samples from depths of 453 and 561 m at borehole Blija (Friesland) and samples from Belgian boreholes. The lab experiments are conducted to assess geomechanical properties of the clay. No present-day permeability values for the Blija samples are reported. It was found that the Blija samples have an overconsolidation ratio of 1.3-1.8. The authors state that the overconsolidation is to a large degree caused by aging effects, which includes the processes of creep and diagenesis. They indicate that there is no conclusive evidence for ice-loading consolidation in the samples of the formerly glaciated northern part of the Netherlands.

IV Geohydrological properties of overburden and underburden of the Rupel Clay Member

Source: Speelman, H. and Breunese, J.N., 1985. Permeabiliteit, porositeit en kleigehalte van Tertiaire en onder-Kwartaire afzettingen in Nederland. Rijks Geologische Dienst Rapportnummer 84KAR13EX, 75 p. plus bijlagen.

This report presents tables with porosity and permeability values for the sandy units of Cenozoic and Early Quaternary age at borehole locations in different parts of onshore Netherlands (depth range 50-1000 m). It includes tables with clay contents (Vsh) and porosity derived from logs; porosity and permeability measured on core samples; permeability from well tests; and permeability calculated from porosity and grain size data using three different methods (Van Baaren, Kozeny-Carman, Breddin).

Source: Heederik, J.P., et al., 1989, Geothermische reserves Centrale Slenk, Nederland. Exploratie en Evaluatie., TNO-rapport OS 89-18.

This report includes measurement values of geohydrological properties (porosity, permeability) of Tertiary sandy units from the geothermal borehole AST-GT-02.

V.Hydrogeological schematization of Cenozoic and Quaternary units and their geohydrological parameters

The following reports and publications provide hydrogeological schematizations of the subsurface and associated generalized geohydrological parameters for Cenozoic and Quaternary units (porosity, hydraulic conductivity or permeability):

De Rooij, R., 2000. A hydrogeological schematization of the Roer Valley Graben. MSc Thesis Centre of Hydrology Utrecht (ICHU), Utrecht University. TNO report NITG 00-200-A.

Wiers, J., 2001. A hydrogeological characterization and groundwater model of the Roer Valley Graben. Msc Thesis. Centre of Hydrology Utrecht (ICHU), Utrecht University and Netherlands Institute of Applied Geoscience TNO – National Geological Survey.

Wildenborg, A.F.B., Orlic, B., De Lange, G., De Leeuw, C.S., Zijl, W., Van Weert, F., Veling , E.J.M., De Cock, S., Thimus, J.F., Lehnen-de Rooij, C., Den Haan, E.J., 2000. Transport of Radionuclides disposed of in Clay of Tertiary Origin (TRACTOR). Netherlands Institute of Applied geoscience TNO – National Geological Survey. TNO report NITG 00-223-B, 223 p.

Appendix 4

Table 1: Lithological composition in sampled boreholes <2 µm.

Well Name	Top NMFRC mTVDss	Bottom NMFRC mTVDss	Sample no.	TVDss m	Gradistat Textural Group	Clay (< 2µm) %	Sand %	Porosity %	Permeability m2	Hydraulic conductivity m/s
NORTHERN AREA										
BUR-01	570.8	646.06								
			XV-1	576.1	sandy mud	6.6%	12.8%	25	1.9E-18	1.9E-11
			XV-2	641.6	mud	9.0%	4.9%	16	2.2E-19	2.2E-12
LWO-02	590.69	674.51	XI-1	597	mud	8.1%	6.1%	16	2.2E-19	2.2E-12
			XI-2	619	mud	8.9%	4.0%	17	2.3E-19	2.3E-12
			XI-3	637	mud	8.7%	1.9%	16	2.1E-19	2.1E-12
GRD-01	446.07	570.81	VIII-1	447.8	mud	9.5%	0.3%	18	4.5E-19	4.5E-12
			VIII-2	453.8	mud	8.8%	0.0%	18	4.0E-19	4.0E-12
			VIII-3	482.3	mud	9.4%	0.1%	18	3.8E-19	3.8E-12
			VIII-4	500.3	mud	9.3%	0.2%	18	3.6E-19	3.6E-12
			VIII-5	513.8	mud	9.4%	0.2%	18	3.4E-19	3.4E-12
			VIII-6	522.8	mud	8.5%	0.3%	17	3.0E-19	3.0E-12
			VIII-7	534.8	mud	7.4%	3.8%	16	2.5E-19	2.5E-12
			VIII-8	546.8	mud	8.2%	2.5%	17	2.7E-19	2.7E-12
			VIII-9	555.8	mud	7.8%	2.4%	16	2.4E-19	2.4E-12
			VIII-10	568.8	mud	4.3%	0.0%	14	1.3E-19	1.3E-12
ESG-01	602.75	689.96	XII-1	601.7	sandy mud	6.6%	13.7%	25	2.0E-18	2.0E-11
			XII-2	611.7	mud	8.1%	7.5%	16	2.1E-19	2.1E-12
			XII-3	621.7	mud	8.1%	8.3%	16	2.0E-19	2.0E-12
			XII-4	631.7	mud	7.8%	4.8%	16	1.9E-19	1.9E-12
			XII-5	641.7	mud	7.2%	2.2%	15	1.7E-19	1.7E-12
			XII-6	651.7	mud	7.4%	1.1%	16	1.7E-19	1.7E-12
			XII-7	661.7	mud	8.4%	0.1%	16	1.9E-19	1.9E-12
			XII-8	671.7	mud	6.7%	1.4%	15	1.4E-19	1.4E-12
EMO-01	604.72	668.27	XIV-1	611	mud	6.5%	6.3%	15	1.7E-19	1.7E-12
			XIV-2	623	mud	7.5%	5.9%	16	1.9E-19	1.9E-12
			XIV-3	636	mud	5.5%	4.1%	15	1.3E-19	1.3E-12
			XIV-4	658	mud	7.9%	0.5%	16	1.8E-19	1.8E-12
NNE-07	427.98	538.64	XIII-10	432	mud	10.1%	0.9%	19	5.0E-19	5.0E-12
			XIII-2	441.5	mud	8.4%	3.8%	18	4.0E-19	4.0E-12
			XIII-3	453	mud	7.7%	2.6%	17	3.5E-19	3.5E-12
			XIII-4	465	mud	11.6%	0.4%	19	5.0E-19	5.0E-12
			XIII-5	476.5	mud	11.8%	0.0%	19	4.9E-19	4.9E-12
			XIII-6	488.5	mud	9.1%	3.5%	18	3.6E-19	3.6E-12
			XIII-7	503.5	sandy mud	9.1%	11.9%	26	2.0E-18	2.0E-11
			XIII-8	513.5	sandy mud	9.5%	27.4%	25	1.5E-17	1.5E-10
			XIII-9	522.5	sandy mud	8.6%	33.3%	24	3.9E-17	3.9E-10
			XIII-10	537	mud	17.6%	0.5%	22	5.6E-19	5.6E-12
SOUTHWEST & SOUTHERN AREA										
B48G0159	20.01	43.09	IX-1	21	mud	10.7%	1.7%	31	2.3E-17	2.3E-10
			IX-2	23	mud	9.9%	1.7%	30	2.0E-17	2.0E-10
			IX-3	25	mud	11.4%	1.5%	31	2.1E-17	2.1E-10
			IX-4	27	mud	10.8%	5.2%	31	1.8E-17	1.8E-10
			IX-5	29	mud	17.1%	0.7%	35	2.4E-17	2.4E-10
			IX-6	31	mud	12.7%	1.5%	32	1.8E-17	1.8E-10
			IX-7	33	mud	9.0%	0.4%	28	1.3E-17	1.3E-10
			IX-8	35	sandy mud	6.0%	10.7%	52	1.2E-16	1.2E-09
			IX-9	37	sandy mud	5.2%	12.4%	52	1.8E-16	1.8E-09
			IX-10	39	sandy mud	4.6%	10.1%	52	1.2E-16	1.2E-09
			IX-11	41	sandy mud	4.1%	14.5%	51	2.2E-16	2.2E-09
			IX-12	43	sandy mud	7.2%	23.0%	50	7.8E-16	7.8E-09
B49G0191	79.12	84.37	X-1	79.9	sandy mud	5.9%	10.7%	48	6.4E-17	6.4E-10
			X-2	80.9	sandy mud	5.2%	14.6%	48	1.5E-16	1.5E-09
			X-3	81.9	mud	9.1%	9.9%	25	5.0E-18	5.0E-11
			X-4	82.9	sandy mud	9.5%	42.4%	45	2.5E-14	2.5E-07
			X-5	84.7	mud	7.5%	7.4%	24	4.2E-18	4.2E-11
B49G0959	73.54	174.5	VII-1	75.8	mud	5.5%	6.9%	22	3.8E-18	3.8E-11
			VII-2	87.8	mud	11.3%	3.0%	26	5.4E-18	5.4E-11
			VII-3	106.8	mud	9.6%	1.5%	24	3.8E-18	3.8E-11
			VII-4	113.3	mud	9.5%	2.5%	24	3.5E-18	3.5E-11
			VII-5	128.8	mud	11.6%	0.8%	25	3.5E-18	3.5E-11
			VII-6	155.3	sandy mud	6.0%	39.0%	38	1.5E-15	1.5E-08
			VII-7	162.8	sandy mud	4.2%	31.6%	38	4.4E-16	4.4E-09
			VII-8	170.3	sandy mud	5.4%	25.4%	38	1.6E-16	1.6E-09
B50H0373	319.49	472.02	III-1	324.7	sandy mud	6.4%	13.3%	31	5.8E-18	5.8E-11
			III-2	330.7	sandy mud	7.2%	23.6%	29	2.2E-17	2.2E-10
			III-3	348.2	mud	11.9%	5.2%	21	8.5E-19	8.5E-12
			III-4	365.7	mud	11.7%	2.7%	21	7.7E-19	7.7E-12
			III-5	382.2	mud	6.6%	0.0%	17	4.1E-19	4.1E-12
			III-6	394.2	mud	9.0%	1.6%	19	5.3E-19	5.3E-12
			III-7	407.2	mud	9.4%	1.6%	19	5.2E-19	5.2E-12
			III-8	424.2	mud	9.7%	1.7%	19	5.0E-19	5.0E-12
			III-9	442.2	mud	8.8%	4.0%	18	4.2E-19	4.2E-12
			III-10	455.7	sandy mud	6.2%	17.8%	27	6.4E-18	6.4E-11
			III-11	469.7	sandy mud	5.1%	32.3%	26	6.0E-17	6.0E-10

Table 1 continued:

EAST & SOUTHEASTERN AREA										
B41G0024	1.97	107.91	VI-1	6.75	sandy mud	5.0%	24.6%	52	1.1E-15	1.1E-08
			VI-2	14.75	sandy mud	6.1%	18.2%	52	4.9E-16	4.9E-09
			VI-3	22	sandy mud	9.4%	11.7%	53	1.7E-16	1.7E-09
			VI-4	29.5	sandy mud	4.7%	13.8%	52	2.1E-16	2.1E-09
			VI-5	37.25	sandy mud	6.4%	12.4%	51	1.4E-16	1.4E-09
			VI-6	46.25	sandy mud	10.1%	18.9%	49	3.2E-16	3.2E-09
			VI-7	56.75	mud	12.1%	3.7%	29	9.3E-18	9.3E-11
			VI-8	67.75	mud	13.0%	7.6%	29	8.1E-18	8.1E-11
			VI-9	78.25	mud	14.8%	1.9%	30	7.6E-18	7.6E-11
			VI-10	86.25	mud	11.8%	1.1%	27	5.7E-18	5.7E-11
			VI-11	96	mud	13.2%	3.8%	28	5.5E-18	5.5E-11
			VI-12	104.75	mud	8.3%	4.7%	23	3.5E-18	3.5E-11
B46C0478	132.69	345.61	V-1	135.3	sandy mud	7.2%	16.3%	42	5.8E-17	5.8E-10
			V-2	150.3	sandy mud	6.1%	16.8%	40	5.1E-17	5.1E-10
			V-3	165.3	sandy mud	4.8%	12.2%	40	2.4E-17	2.4E-10
			V-4	178.3	mud	7.8%	4.5%	21	1.6E-18	1.6E-11
			V-5	195.3	mud	8.4%	0.0%	21	1.5E-18	1.5E-11
			V-6	208.3	mud	14.6%	0.3%	25	2.2E-18	2.2E-11
			V-7	222.3	mud	12.1%	2.4%	23	1.7E-18	1.7E-11
			V-8	234.3	mud	9.6%	5.6%	21	1.3E-18	1.3E-11
			V-9	262.3	mud	7.8%	6.9%	20	8.9E-19	8.9E-12
			V-10	294.3	muddy sand	4.2%	76.3%	28	2.0E-13	2.0E-06
			V-11	312.3	sandy mud	5.5%	21.2%	30	2.0E-17	2.0E-10
B52E0114	364.7	526.7	II-1	380.95	sandy mud	7.5%	39.6%	27	2.1E-16	2.1E-09
			II-2	398.45	sandy mud	7.2%	38.6%	27	1.9E-16	1.9E-09
			II-3	418.45	mud	10.0%	9.7%	19	5.2E-19	5.2E-12
			II-4	436.2	mud	19.1%	0.0%	24	8.5E-19	8.5E-12
			II-5	443.7	mud	25.8%	0.0%	27	9.4E-19	9.4E-12
			II-6	460.35	sandy mud	13.5%	16.2%	28	4.6E-18	4.6E-11
			II-7	479.2	mud	15.2%	1.9%	21	6.1E-19	6.1E-12
			II-8	491.45	mud	18.5%	0.4%	23	6.8E-19	6.8E-12
			II-9	504.95	mud	8.7%	0.0%	17	3.3E-19	3.3E-12
			II-10	518.45	muddy sand	11.2%	56.9%	23	8.4E-16	8.4E-09
			II-11	523.7	muddy sand	3.9%	82.2%	23	4.6E-14	4.6E-07

TVDss: true vertical depth below surface
NMRFC: Rupel Clay Member

Table 2: Lithological composition in sampled boreholes clay to fine silt.

Well Name	Top NMFRC mTVDss	Bottom NMFRC mTVDss	Sample no.	TVDss m	Gradistat Textural Group	Clay (< 2µm) %	Clay to Fine Silt %	Sand %	Porosity %	Permeability m2	Hydraulic conductivity m/s
NORTHERN AREA											
BUR-01	570.8	646.06									
			XV-1	576.1	sandy mud	6.6%		12.8%	25	1.9E-18	1.9E-11
			XV-2	641.6	mud		46.1%	4.9%	34	3.4E-19	3.4E-12
LWO-02	590.69	674.51	XI-1	597	mud		38.5%	6.1%	32	4.9E-19	4.9E-12
			XI-2	619	mud		42.1%	4.0%	33	4.1E-19	4.1E-12
			XI-3	637	mud		40.0%	1.9%	32	4.2E-19	4.2E-12
GRD-01	446.07	570.81	VIII-1	447.8	mud		46.1%	0.3%	38	6.8E-19	6.8E-12
			VIII-2	453.8	mud		45.0%	0.0%	37	6.9E-19	6.9E-12
			VIII-3	482.3	mud		45.2%	0.1%	37	6.1E-19	6.1E-12
			VIII-4	500.3	mud		46.5%	0.2%	37	5.4E-19	5.4E-12
			VIII-5	513.8	mud		47.3%	0.2%	37	5.0E-19	5.0E-12
			VIII-6	522.8	mud		43.5%	0.3%	35	5.5E-19	5.5E-12
			VIII-7	534.8	mud		40.2%	3.8%	33	5.8E-19	5.8E-12
			VIII-8	546.8	mud		40.9%	2.5%	34	5.5E-19	5.5E-12
			VIII-9	555.8	mud		42.9%	2.4%	34	5.0E-19	5.0E-12
			VIII-10	568.8	mud		39.3%	0.0%	32	5.3E-19	5.3E-12
ESG-01	602.75	689.96	XII-1	601.7	sandy mud	6.6%		13.7%	25	2.0E-18	2.0E-11
			XII-2	611.7	mud		40.4%	7.5%	32	4.5E-19	4.5E-12
			XII-3	621.7	mud		36.7%	8.3%	30	4.7E-19	4.7E-12
			XII-4	631.7	mud		38.8%	4.8%	31	4.4E-19	4.4E-12
			XII-5	641.7	mud		37.7%	2.2%	31	4.3E-19	4.3E-12
			XII-6	651.7	mud		37.8%	1.1%	31	4.2E-19	4.2E-12
			XII-7	661.7	mud		42.1%	0.1%	32	3.6E-19	3.6E-12
			XII-8	671.7	mud		35.0%	1.4%	29	4.2E-19	4.2E-12
EMO-01	604.72	668.27	XIV-1	611	mud		31.9%	6.3%	28	5.3E-19	5.3E-12
			XIV-2	623	mud		36.1%	5.9%	30	4.8E-19	4.8E-12
			XIV-3	636	mud		33.6%	4.1%	29	4.8E-19	4.8E-12
			XIV-4	658	mud		40.4%	0.5%	32	3.9E-19	3.9E-12
NNE-07	427.98	538.64	XIII-10	432	mud		46.5%	0.9%	38	7.2E-19	7.2E-12
			XIII-2	441.5	mud		41.7%	3.8%	36	8.0E-19	8.0E-12
			XIII-3	453	mud		38.1%	2.6%	34	8.3E-19	8.3E-12
			XIII-4	466	mud		50.4%	0.4%	40	5.4E-19	5.4E-12
			XIII-5	476.5	mud		48.6%	0.0%	39	5.5E-19	5.5E-12
			XIII-6	488.5	mud		41.8%	3.5%	35	6.6E-19	6.6E-12
			XIII-7	503.5	sandy mud	9.1%		11.9%	26	2.0E-18	2.0E-11
			XIII-8	513.5	sandy mud	9.5%		27.4%	25	1.5E-17	1.5E-10
			XIII-9	522.5	sandy mud	8.6%		33.3%	24	3.9E-17	3.9E-10
			XIII-10	537	mud		56.1%	0.5%	41	3.1E-19	3.1E-12

Table 2 continued:

SOUTHWEST & SOUTHERN AREA											
B48G0159	20.01	43.09	IX-1	21	mud		51.8%	1.7%	60	7.7E-17	7.7E-10
			IX-2	23	mud		45.2%	1.7%	56	6.5E-17	6.5E-10
			IX-3	25	mud		50.6%	1.5%	59	6.1E-17	6.1E-10
			IX-4	27	mud		48.7%	5.2%	57	5.4E-17	5.4E-10
			IX-5	29	mud		53.4%	0.7%	60	4.8E-17	4.8E-10
			IX-6	31	mud		55.6%	1.5%	60	4.2E-17	4.2E-10
			IX-7	33	mud		44.6%	0.4%	54	4.1E-17	4.1E-10
			IX-8	35	sandy mud	6.0%		10.7%	52	1.2E-16	1.2E-09
			IX-9	37	sandy mud	5.2%		12.4%	52	1.8E-16	1.8E-09
			IX-10	39	sandy mud	4.6%		10.1%	52	1.2E-16	1.2E-09
			IX-11	41	sandy mud	4.1%		14.5%	51	2.2E-16	2.2E-09
			IX-12	43	sandy mud	7.2%		23.0%	50	7.8E-16	7.8E-09
B49G0191	79.12	84.37	X-1	79.9	sandy mud	5.9%		10.7%	48	6.4E-17	6.4E-10
			X-2	80.9	sandy mud	5.2%		14.6%	48	1.5E-16	1.5E-09
			X-3	81.9	mud		40.8%	9.9%	47	1.2E-17	1.2E-10
			X-4	82.9	sandy mud	9.5%		42.4%	45	2.5E-14	2.5E-07
			X-5	84.7	mud		34.3%	7.4%	43	1.1E-17	1.1E-10
B49G0959	73.54	174.5	VII-1	75.8	mud		16.8%	6.9%	31	8.6E-18	8.6E-11
			VII-2	87.8	mud		39.0%	3.0%	46	1.1E-17	1.1E-10
			VII-3	106.8	mud		32.3%	1.5%	40	8.0E-18	8.0E-11
			VII-4	113.3	mud		43.8%	2.5%	47	7.2E-18	7.2E-11
			VII-5	128.8	mud		46.1%	0.8%	47	5.8E-18	5.8E-11
			VII-6	155.3	sandy mud	6.0%		39.0%	38	1.5E-15	1.5E-08
			VII-7	162.8	sandy mud	4.2%		31.6%	38	4.4E-16	4.4E-09
			VII-8	170.3	sandy mud	5.4%		25.4%	38	1.6E-16	1.6E-09
B50H0373	319.49	472.02	III-1	324.7	sandy mud	6.4%		13.3%	31	5.8E-18	5.8E-11
			III-2	330.7	sandy mud	7.2%		23.6%	29	2.2E-17	2.2E-10
			III-3	348.2	mud		46.0%	5.2%	40	1.1E-18	1.1E-11
			III-4	365.7	mud		42.9%	2.7%	38	1.1E-18	1.1E-11
			III-5	382.2	mud		52.0%	0.0%	42	7.4E-19	7.4E-12
			III-6	394.2	mud		38.4%	1.6%	35	1.1E-18	1.1E-11
			III-7	407.2	mud		41.3%	1.6%	36	9.4E-19	9.4E-12
			III-8	424.2	mud		42.4%	1.7%	37	8.5E-19	8.5E-12
			III-9	442.2	mud		34.6%	4.0%	32	9.2E-19	9.2E-12
			III-10	455.7	sandy mud	6.2%		17.8%	27	6.4E-18	6.4E-11
			III-11	469.7	sandy mud	5.1%		32.3%	26	6.0E-17	6.0E-10
EAST SOUTHEASTERN AREA											
B41G0024	1.97	107.91	VI-1	6.75	sandy mud	5.0%		24.6%	52	1.1E-15	1.1E-08
			VI-2	14.75	sandy mud	6.1%		18.2%	52	4.9E-16	4.9E-09
			VI-3	22	sandy mud	9.4%		11.7%	53	1.7E-16	1.7E-09
			VI-4	29.5	sandy mud	4.7%		13.8%	52	2.1E-16	2.1E-09
			VI-5	37.25	sandy mud	6.4%		12.4%	51	1.4E-16	1.4E-09
			VI-6	46.25	sandy mud	10.1%		18.9%	49	3.2E-16	3.2E-09
			VI-7	56.75	mud		45.8%	3.7%	52	1.9E-17	1.9E-10
			VI-8	67.75	mud		36.6%	7.6%	46	1.5E-17	1.5E-10
			VI-9	78.25	mud		47.8%	1.9%	51	1.2E-17	1.2E-10
			VI-10	86.25	mud		49.0%	1.1%	51	1.0E-17	1.0E-10
			VI-11	96	mud		44.8%	3.8%	49	9.1E-18	9.1E-11
			VI-12	104.75	mud		38.0%	4.7%	44	8.4E-18	8.4E-11
B46C0478	132.69	345.61	V-1	135.3	sandy mud	7.2%		16.3%	42	5.8E-17	5.8E-10
			V-2	150.3	sandy mud	6.1%		16.8%	40	5.1E-17	5.1E-10
			V-3	165.3	sandy mud	4.8%		12.2%	40	2.4E-17	2.4E-10
			V-4	178.3	mud		37.0%	4.5%	40	3.9E-18	3.9E-11
			V-5	195.3	mud		47.2%	0.0%	45	2.9E-18	2.9E-11
			V-6	208.3	mud		55.3%	0.3%	49	2.0E-18	2.0E-11
			V-7	222.3	mud		46.6%	2.4%	44	2.4E-18	2.4E-11
			V-8	234.3	mud		40.6%	5.6%	40	2.5E-18	2.5E-11
			V-9	262.3	mud		39.9%	6.9%	39	2.1E-18	2.1E-11
			V-10	294.3	muddy sand	4.2%		76.3%	28	2.0E-13	2.0E-06
			V-11	312.3	sandy mud	5.5%		21.2%	30	2.0E-17	2.0E-10
B52E0114	364.7	526.7	II-1	380.95	sandy mud	7.5%		39.6%	27	2.1E-16	2.1E-09
			II-2	398.45	sandy mud	7.2%		38.6%	27	1.9E-16	1.9E-09
			II-3	418.45	mud		41.4%	9.7%	36	8.9E-19	8.9E-12
			II-4	436.2	mud		63.3%	0.0%	46	3.0E-19	3.0E-12
			II-5	443.7	mud		70.7%	0.0%	49	1.6E-19	1.6E-12
			II-6	460.35	sandy mud	13.5%		16.2%	28	4.6E-18	4.6E-11
			II-7	479.2	mud		49.9%	1.9%	39	5.2E-19	5.2E-12
			II-8	491.45	mud		60.5%	0.4%	44	2.9E-19	2.9E-12
			II-9	504.95	mud		47.8%	0.0%	38	5.1E-19	5.1E-12
			II-10	518.45	muddy sand	11.2%		56.9%	23	8.4E-16	8.4E-09
			II-11	523.7	muddy sand	3.9%		82.2%	23	4.6E-14	4.6E-07

TVDss: true vertical depth below surface
NMRFC: Rupel Clay Member

OPERA
Meer informatie:

Postadres
Postbus 202
4380 AE Vlissingen

T 0113-616 666
F 0113-616 650
E info@covra.nl

www.covra.nl